SEMMELWEIS EGYETEM

DOKTORI ISKOLA

Ph.D. értekezések

2985.

KATONA MIKLÓS TAMÁS

A gyógyszerészeti tudományok korszerű kutatási irányai
című program

Programvezető: Dr. Antal István, egyetemi tanár

Témavezetők: Dr. Takácsné Dr. Novák Krisztina, egyetemi tanár

IN VITRO METHOD DEVELOPMENTS FOR THE BETTER PREDICTION OF BIOAVAILABILITY

PhD thesis

Miklós Tamás Katona

Doctoral School of Pharmaceutical Sciences

Semmelweis University

Supervisor: Krisztina Takács-Novák, D.Sc., professor emerita

Official reviewers: Krisztina Ludányi, Ph.D., associate professor
Piroska Szabó-Révész, D.Sc., professor emerita

Head of the Complex Examination Committee:
Romána Zelkó, D.Sc., professor

Members of the Complex Examination Committee:
Rita Ambrus, Ph.D., associate professor
Márta Mazákné Kraszni, Ph.D., associate professor
Gergő Tóth, Ph.D., assistant professor

Budapest
2023

TABLE OF CONTENTS

LIST OF ABBREVIATIONS

ANVISA	-	Brazilian Health Regulatory Agency
API	-	Active Pharmaceutical Ingredient
ASA	-	Acetylsalicylic acid
ASD	-	Artificial stomach *duodenal* model
AUC	-	Area under the concentration *vs* time curve
BA	-	Bioavailability
BCS	-	Biopharmaceutical Classification System
BE	-	Bioequivalence
Caco-2	-	Human colorectal adenocarcinoma cells
C_{max}	-	Maximum plasma concentration or peak exposure
CSV	-	Chinese small volume apparatus
DGM	-	Dynamic Gastric Model
DR	-	Delayed-release
EC	-	Enteric-coated
EMA	-	European Medicines Agency
ER	-	Extended-release
f_2	-	Similarity factor
FaSSGF	-	Fasted State Simulated Gastric Fluid
FaSSIF	-	Fasted State Simulated Intestinal Fluid
FaSSIF-V2	-	Fasted State Simulated Intestinal Fluid version 2
FeSSIF	-	Fed State Simulated Intestinal Fluid
FeSSIF-V2	-	Fed State Simulated Intestinal Fluid version 2

FDA	-	United States Food and Drug Administration
GI	-	Gastrointestinal
GIS	-	Gastrointestinal Simulator
HGS	-	Human Gastric Simulator
HPLC	-	High performance liquid chromatography
IBU	-	ibuprofen
IR	-	Immediate-release
IVIVC	-	In vitro – in vivo correlation
LIWV	-	Large intestinal water volume
MMC	-	Migrating motor complex
MR	-	Modified-release
MRI	-	Magnetic resonance imaging
NCE	-	New Chemical Entity
PB-IVIVC	-	Physiologically-based IVIVC
PBPK	-	Physiologically-based pharmacokinetics
Ph. Eur.	-	European Pharmacopoeia
PK	-	Pharmacokinetics
RGE	-	Rapid gastric emptying
RTC	-	Radiotelemetry capsule
SBTT	-	Small bowel transit time
SGE	-	Slow gastric emptying
SIWV	-	Small intestinal water volume
SmPC	-	Summary of Product Characteristics

SUPAC	-	Scale-up and post-approval changes
TIM	-	TNO Gastro-Intestinal Model
t_{max}	-	Time to maximum plasma concentration
TXA2	-	Thromboxane A2
UIR	-	Unit impulse response
UPLC	-	Ultra high performance liquid chromatography
USP	-	United States Pharmacopeia
VAM	-	Value-added medicine

1 INTRODUCTION

1.1 Challenges in generic drug development

By definition, a generic medicine is a medicine that is developed to be the same as a medicine that has already been authorised. Its authorisation is based on efficacy and safety data from studies on the authorised medicine. A company can only market a generic medicine once the 10-year exclusivity period for the original medicine has expired (1). Generic pharmaceuticals can be divided into three subgroups: biosimilar, simple/commodity generics and super/value-added generics.

The annual report of the Food and Drug Administration's (FDA's) Office of Generic Drugs estimated that 91% of all prescriptions in the USA was filled as generic drugs in 2022. The approval of generics allows millions of patients to access the therapy they need more easily and reduces the risk of drug shortages by stabilizing the supply chains (2). According to "The Business Research Company", the current size of the global generic pharmaceuticals market is $358.5 billion in 2023 and is expected to grow to $453.2 billion in 2027 at a compound annual growth rate of 6.0%. The rising incidence of chronic diseases is one of the major drivers of the generic pharmaceutical market (3).

Competition with other generic manufacturers enables lower profit margin, thus cost and time efficiency of the development process is of key importance. In 2007, FDA released a document "Critical Path Opportunities for Generic Drugs" that identified some of the specific challenges in the development of generic drugs. According to the FDA, developing formulations that do not pass the bioequivalence study is a major risk, which results in repetition of formulation development. These failures are sometimes linked to the insufficiency of dissolution or lack of *in vitro – in vivo* correlation (IVIVC) to evaluate proposed formulations and processes during development. To accelerate the development and approval process, the FDA highlighted the importance of improving scientific understanding of the formulation by applying quality by design approach and improving the efficiency of current methods for assessment of bioequivalence (BE) (4).

Due to the emerging trends in combinatorial chemistry and high throughput screening, the properties of new chemical entities (NCEs) shifted towards higher molecular weight and increasing lipophilicity (5) (6). As a result, about 40% of drugs with market approval and nearly 90% of molecules in the discovery pipeline are poorly

water-soluble (7). In case of immediate-release generic drugs, the risk of bioinequivalence is significantly higher if the formulation contains a poorly soluble API. In a recent study Krajcar *et al.* performed a retrospective analysis of 198 Sandoz sponsored BE studies and found that 23% of poorly soluble drugs were non-BE compared to 0.1% of highly soluble drugs (8). A similar conclusion was reached by Ramirez *et al.*, who investigated the correlation between the Biopharmaceutical Classification System (BCS) classes and the probability of positive BE outcome by evaluating 124 BE studies. BCS Class 2 (poorly soluble, highly permeable) drugs had the worst success rate with 50% bioinequivalence outcome (9). Cristofoletti *et al.* compared 500 randomly selected studies from the database of the Brazilian Health Surveillance Agency (ANVISA) and found that the relative risk of obtaining a non-BE result was approximately 4 times higher for drugs in BCS Class 2 compared with highly soluble Class 1 and 3 drugs (10). With the number of poorly soluble drug candidates, the importance of applying predictive *in vitro* analytical methods is also increasing.

In the competitive environment of generic pharmaceutical industry, the development of value-added medicines (VAMs) may represent an opportunity to succeed. VAMs are based on known molecules and are further developed to address healthcare needs and deliver relevant improvement for patients, healthcare professionals and/or payers (11). By the reformulation of drugs, better route of delivery, better tolerability and/or better safety properties can be achieved (12). At the same time, influencing the pharmacokinetic properties of an existing drug product in the desired way with formulation techniques is a challenge for scientists in the field.

1.2 Bioequivalence studies

In applications for generic medicinal products the concept of bioequivalence is fundamental. The purpose of establishing bioequivalence is to demonstrate equivalence in biopharmaceutics quality between the generic medicinal product and a reference medicinal product in order to allow bridging of preclinical tests and of clinical trials associated with the reference medicinal product. In bioequivalence studies, the plasma concentration *vs* time curve is generally used to assess the rate and extent of absorption. Selected pharmacokinetic parameters and preset acceptance limits allow the final decision on bioequivalence of the tested products. AUC, the area under the concentration *vs* time

curve, reflects the extent of exposure. C_{max}, the maximum plasma concentration or peak exposure, and the time to maximum plasma concentration, t_{max}, are parameters that are influenced by absorption rate. The test conditions should be standardised in order to minimise the variability of all factors involved except that of the products being tested. Therefore, it is recommended to standardise diet, fluid intake and exercise. According to the European Medicines Agency's (EMA's) guideline, in general, a BE study should be conducted under fasting conditions, as this is considered to be the most sensitive condition to detect a potential difference between formulations (13). In order to prove bioequivalence, performing a study in fasted state is prescribed by the FDA as well (14). In general, subjects are fasting for 8 h prior to administration, then test and reference products are administered with a standardized amount of water (at least 150 mL). No food intake is allowed for at least 4 h post-dose. For products where the Summary of Product Characteristics (SmPC) recommends intake of the reference medicinal product only in fed state, the bioequivalence study should generally be conducted under fed conditions. If no specific recommendation is given in the originator SmPC, the meal should be a high-fat (approximately 50 percent of total caloric content of the meal) and high-calorie (approximately 800 to 1000 kcal) meal. As prescribed by the EMA, the sampling schedule of a bioequivalence study should include frequent sampling around the predicted t_{max} to provide a reliable estimation of peak exposure (13).

1.3 Characteristics of the GI system

Modelling the absorption of an oral formulation requires first an understanding of the interaction between the drug and the surrounding physiological environment. Consequently, the appropriate characterization of the medium compositions, volumes, pH conditions and the residence times in each relevant part of the gastrointestinal system is essential.

1.3.1 pH values in the GI system

A large percentage of drug substances contain one or more functional group(s) that are ionisable in the physiological range. The change in the ionization state affects the solubility of the molecules, and therefore also their absorption. The evaluation of the gastrointestinal pH conditions using radiotelemetry capsules (RTC) dates back to the late 1980s. Evans *et al.* used a pH sensitive RTC passing freely through the gastrointestinal

tract and recorded the signals with a portable solid-state receiver and recording system to measure the pH in 66 volunteers. The gastric pH was highly acidic (1.0-2.5) in all subjects, while the mean pHs in the proximal small intestine and terminal *ileum* were 6.6 (±0.5) and 7.5 (±0.4) respectively. After leaving the *ileocaecal* junction the pH fell sharply to a mean of 6.4 (±0.4), which then rose to a final mean value of 7.0 (±0.7) in the colon (15). Similarly, the pH of the gut lumen was investigated in 39 healthy subjects by Fallingborg *et al.* to provide a better basis for prediction of the release of pH-dependent sustained-release oral formulations. The results correlated well with the values reported by Evans *et al*: The pH rose from 6.4 in the *duodenum* to 7.3 in the distal small intestine, then it was 5.7 in the *caecum* and rose to 6.6 in the *rectum* (16). Ibekwe *et al.* studied the correlations between *in situ* gastrointestinal pH, transit time or feed status and the disintegration of Eudragit S coated tablets designed to dissolve above pH 7. Eight healthy subjects were tested in a three-way crossover study under fasted, pre-feed and fed conditions. In case of fasted and pre-feed administration, the tablets were co-administered with pH monitoring Bravo® capsule to measure the pH throughout the gastrointestinal tract of man. The observed mean pHs of the fasted arm of the study were 1.4 (±0.4) in the stomach, 6.5 (±0.3) in the proximal small bowel, 6.8 (±0.3) in the mid small bowel, 7.2 (±0.4) in the distal small bowel and 6.5 (±0.8) in the ascending colon (17). In 2013, van der Schaar *et al.* published the first human study of the IntelliCap®, an electronic drug delivery and monitoring device. The system includes an electronic capsule comprising drug reservoir, a pH and temperature sensor, a microprocessor and transceiver, a stepper motor, and batteries. The device was developed for targeted delivery of substances by expelling the content of the drug reservoir to well-defined areas of the GI tract. To determine the location of the capsule, temperature and pH data are monitored real-time (18). The use of IntelliCap® enabled a precise characterization of the physiological conditions in fasted state BE studies (19). Based on similar principle, Schneider *et al.* compared the pH conditions of fasted and fed state and also gained valuable information of the pressure activity within the GI tract using the SmartPill® device (20).

1.3.2 Transition times of drugs in the GI system

Physiologically, the gastric emptying is related to the migrating motor complex (MMC) of the stomach, which is a ~2 h long cycle that consists of four phases. Phase I is a period of motor quiescence lasting 40–60% of the cycle. Phase II, accounting for 20–

30% of the cycle, exhibits irregular phasic contractions. Phase III is a 5- to 10 min period of luminally occlusive, rhythmic contractions occurring at the slow-wave frequency. Phase IV is a transitional period of irregular contractions between phase III and phase I (21). Non-disintegrating solid dosage forms administered in the fasted state are mainly emptied during the intense contractions of phase III, also known as the 'housekeeper wave' (22) (23). The transition through the small intestine is governed by the activity of the smooth muscle, the contractions (or pressure waves) of which are determined by intrinsic myogenic activity, intrinsic and extrinsic nervous control and hormonal action (24).

Traditionally, the GI transition times were studied using gamma scintigraphy technique. In this method, the administered formulations were labelled with gamma emitting radionuclides (e.g., technetium-99m or indium-111), so that their transit through the GI tract could be followed by the detection of radiation (25) (26) (27) (28) (29). Davies *et al.* brought together data from 201 investigations in human subjects (representing 23 studies on solutions, 82 on pellets and 96 on single units) and studied the gastric emptying and transit in the small intestine. They found that the gastric emptying of different physical forms varied according to the feeding conditions. Solutions and small pellets (<2 mm) emptied rapidly (<1 h) and were less affected by food intake. Single units also often emptied rapidly in the fasted state, however even a light breakfast had a significant delaying effect, which was greater when heavy breakfast was administered. On the other hand, the small intestinal transit time (~3-4 h) was independent from the physical form. Surprisingly, the difference between the mean intestinal transit times of fasted and fed subjects was not statistically significant (30). Nowadays, the advance of radiotelemetry capsules provides a suitable alternative for the GI transition investigation as well. Gastric emptying and transition through the small intestine can be inferred indirectly through pH monitoring: as the RTC passes the pylorus and leaves the strongly acidic fasted stomach (pH 1.0-2.5), the pH rises sharply by at least 3 pH units. Similarly, the passage through the *ileocaecal* valve is indicated by a rapid drop of >0.8 pH units at least 1h after the pylorus to pH ≤6.5. The results of a study conducted by Maurer *et al.* showed that the gastric residence time varied between 0:15 and 3:14 h with a median of 1:30 h, while the median of the small bowel transit time (SBTT) was 4:01 h (31). Koziolek *et al.* reached a similar result by testing 20 healthy subjects under fasting bioequivalence conditions

with the Intellicap® system. The gastric emptying time was observed after 0:07-3:22 h (median: 0:30 h), and the median SBTT was 4:07 h (19).

1.3.3 GI liquid volumes

If the active substance of an orally administered drug has low aqueous solubility, the liquid volume of GI has major effect on absorption. Provided the formulation does not contribute to a dissolution-limited condition and permeability is rapid, any impact on solubility factors directly influences the fraction absorbed. Using GastroPlus, Sutton performed simulations of the mean plasma concentrations of four solubility-limited compounds. In his models he applied different literature small- and large intestinal water volumes (SIWV and LIWV). He found that the most accurate predictions compared to observed plasma concentrations in the fasted state were reached, when the SIWV averaged about 130 mL and the average LIWV was about 10 mL (32). Mudie *et al.* conducted a clinical study on 12 volunteers to quantify the total volume and distribution of liquid in the stomach and small intestine under conditions representing fasting BA/BE studies. The subjects after an overnight fast ingested a glass of water (240 mL), then they underwent upper and lower abdominal magnetic resonance imaging (MRI) scans at intervals for 2 h. According to the results, the initial fluid volume in the fasted stomach was 35 ± 7 mL, which rose to 242 ± 9 mL after liquid intake, then declined rapidly with a half emptying time of 13 ± 1 min and returned back to the baseline 45 min after the drink. Initially, the fasted small intestine contained 43 ± 14 mL fluid and reached a maximum volume of 94 ± 24 mL 12 min after water intake (33). The results also confirmed the presence of small intestinal fluid in small pockets (~6 mL), which phenomenon was first suggested by Schiller *et al*. (34). Based on the cited studies, for the development of physiologically relevant methods, it is likely to reduce the volume of the dissolution medium compared to pharmacopoeial methods.

1.3.4 Composition of GI fluids

In addition to food and beverages, various fluids are secreted by the GI tract, including hydrochloric acid, bicarbonate, enzymes, surfactants, electrolytes, mucus and water. As a result, the composition of GI fluids surrounding the drug varies widely with position in the GI tract and with timing of administration in relation to meal intake.

The gastric fluid is basically a hydrochloric acid solution, however it contains several other components as well. The primary enzyme in gastric juice is pepsin, which,

as one of the main digestive enzymes, is responsible for breaking down proteins into smaller peptides. It is secreted by the stomach as an inactive precursor, pepsinogen. The basal output is reported to be ~0.8 mg/mL (35), which is diluted by about tenfold at the time of drug administration with the ingestion of a glass of water (200-250 mL). According to the measurements in eight subjects by Efentakis and Dressman, the surface tension of the gastric fluid is 35-45 mN/m (36), which is significantly lower than that of water and suggests that surfactants are present in this region as well. Rhodes *et al.* investigated the bile salt levels in the stomach by radiolabelling technique and found an average concentration of 80 μM total bile salts in fasted conditions, as a result of reflux through the pylorus (37).

After emptying from the stomach, the acidic fluid entering the small intestine is neutralized with bicarbonate ions secreted by the pancreas. The emerging buffer capacity plays an important role in determining the microclimate pH of drug substances (38). The secretion of bile results in substantial concentrations of bile salts and lecithin, which form mixed micelles even in fasted state. Fasting bile salt concentrations in the proximal small intestine are reported to be 3-5 mM (39) (40) (41) (42). The average concentration values are similar in the *duodenum* and *jejunum* and falling rapidly in the *ileum* thanks to the absorption by an active transport mechanism. In response to meal ingestion, lipase, amylase and protease enzymes are secreted into the small intestine responsible for the bulk of nutrient digestion (43).

1.4 Rate limiting factors of GI absorption

1.4.1 Immediate-release dosage forms

When focusing on immediate-release formulations, the Biopharmaceutics Classification System (BCS) is widely accepted today in the academic, industrial and regulatory world (44). The BCS is a scientific framework for classifying a drug substance based on its aqueous solubility and intestinal permeability. When combined with the *in vitro* dissolution characteristics of the drug product, the BCS considers three major factors: solubility, dissolution rate and intestinal permeability, all of which govern the rate and extent of oral absorption from IR solid oral-dosage forms (45). According to the system, drug substances are classified into four groups, summarized in Figure 1.

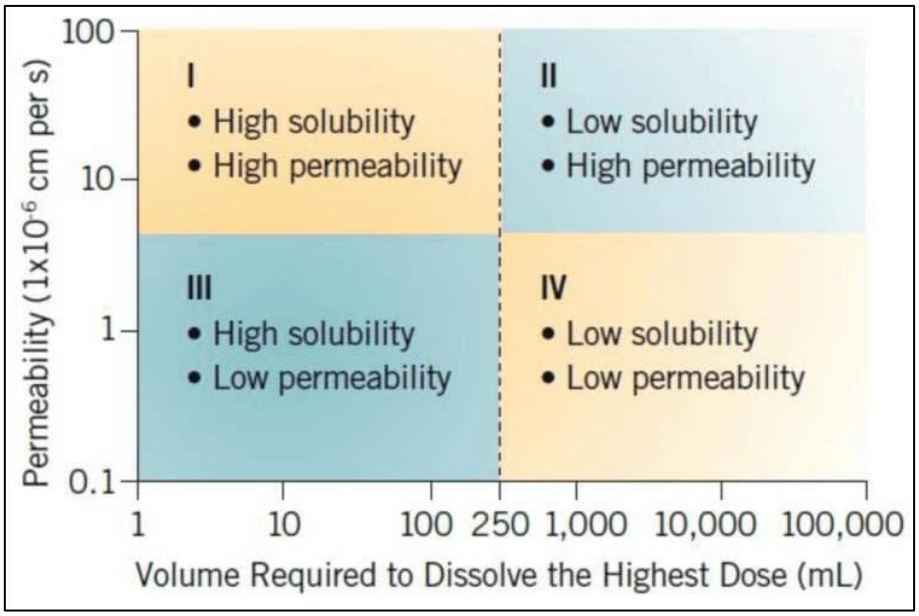

Figure 1. Classification of drug substances according to the BCS system.

A drug substance is classified as highly soluble if the highest single therapeutic dose is completely soluble in 250 ml or less of aqueous media over the pH range of 1.2–6.8 at 37±1°C. The assessment of permeability should preferentially be based on the extent of absorption derived from human pharmacokinetic studies, e.g., absolute bioavailability or mass balance. High permeability can be concluded when the absolute bioavailability is ≥85%. High permeability can also be concluded if ≥85% of the administered dose is recovered in urine as unchanged (parent drug), or as the sum of parent drug, Phase 1 oxidative and Phase 2 conjugative metabolites. Permeability can be also assessed by validated and standardized *in vitro* methods using Caco-2 cells (46).

Class I drugs are typically well-absorbed and the rate limiting step to drug absorption is drug dissolution or gastric emptying if dissolution is very rapid. Thus, correlation between absorption and dissolution rate is expected if dissolution is slower than gastric emptying rate. Class II is the class of drugs for which drug dissolution *in vivo* is the rate controlling step in drug absorption. Dissolution media and methods that reflect the *in vivo* controlling process are particularly important in this case if good *in vitro – in vivo* correlations are to be obtained. For Class III drugs, permeability is the rate controlling step in drug absorption. In this case, limited or no IVIVC is expected. Class IV drugs present significant problems for oral drug delivery. To decide whether IVIV correlation is expected or not, a case-by-case evaluation may be necessary (47).

BCS Class II and IV drug product dissolution *in vivo* and *in vitro* is highly dependent on the acidic or basic nature of the drug, the drug solubility and formulation factors, in addition to the *in vivo* luminal environment. To support the development of *in vivo* predictive dissolution methodology, Tsume *et al.* proposed a sub-classification of the BCS with a, b and c subclasses dependent on the acidic (a), basic (b), or neutral (c) characteristics of the drug in the physiological pH range (~pH <7.5). BCS Class IIa drugs are typically carboxylic acids with a pK_a in the range of 4 to 5, are insoluble at typical, gastric pHs but soluble at intestinal pHs. Alternatively, BCS Class IIb weak bases exhibit high solubility and (likely) dissolution rates at acidic pH in the stomach and may precipitate (in a very complex poorly understood manner) in the small intestine. The intestinal precipitation of a Class IIb drug depends on numerous formulation and GI physiological factors (luminal composition) and environment at the time of dosing. While BCS Class II weak acids and bases demonstrate complimentary solubility profiles due to the pH variation of the GI tract, the solubility of BCS Class IIc drugs would not be affected by the *in vivo* pH change. However, for BCS Class IIc drug products, the *in vivo* environment e.g., surfactants and lipids, play a significant, but difficultly predictable role in drug dissolution (48).

1.4.2 Modified-release dosage forms

Modified-release (MR) drugs, by definition, are formulated to alter the timing and/or the rate of release of the drug substance. In this way, the formulation properties of the drug product strongly influence the *in vivo* absorption (49). An MR dosage form that allows at least twofold reduction in dosage frequency as compared to that drug presented as an IR dosage form is called an extended-release (ER) product. Examples of extended-release dosage forms include controlled-release, sustained-release, and long-acting drug products. Due to their prolonged, formulation-controlled dissolution, these dosage forms are the most likely to show good correlation between the *in vitro* dissolution and *in vivo* absorption. Manufacturers are also encouraged by the FDA to develop IVIVCs for ER products in the expectation that the information will permit certain formulation and manufacturing changes without an *in vivo* BE study (50) (51). In this case, several published studies highlight the importance of modelling the mechanical stress resulting from gastrointestinal contractions in order to simulate the degradation of the formulation (e.g.: hydrophilic matrix tablets) and to achieve good predictability (52) (53) (54).

Enteric-coated (EC) formulations are designed to delay the release of the drug substance until it is emptied from the stomach, in order to protect it from the highly acidic gastric fluid. In general, enteric coatings are weakly acidic polymers that are insoluble at gastric pH but ionize and dissolve under intestinal conditions (55). Thereafter, the site of drug release is affected by several factors, such as the structure of the employed film former, the thickness of the applied film, and the nature and quantities of the additives used together with it (56). Although the *in vivo* dissolution of these products is highly formulation dependent, in this case the lack of predictive *in vitro* dissolution method is particularly common (55).

1.5 Pharmacopoeial dissolution

The *in vitro* dissolution testing is an important tool for characterizing the biopharmaceutical properties of a drug product at different stages throughout its life cycle. Compliance with the dissolution requirements ensures that the finished drug product is consistent with the release rates of the active pharmaceutical ingredient (API) as determined in bioavailability studies during the clinical trials (57). The results obtained need to be independent of the testing laboratory, therefore, reproducible methods and standardized equipment are to be used. The generally used apparatus types are specified in USP chapter <711> (58), which is harmonized with the corresponding texts of the European Pharmacopoeia (Ph. Eur.) (59) and the Japanese Pharmacopoeia (60).

1.5.1 Dissolution Apparatus

Apparatus I (Basket Apparatus) consists of the following: a vessel, which is typically made of glass; a motor; a metallic drive shaft; and a cylindrical basket. The vessel has a nominal capacity of 1 L and is partially immersed in a suitable water bath which holds the temperature inside the vessel at 37 ± 0.5 °C. A speed-regulating device is used that allows the shaft rotation speed to be selected and maintained at the specified rate ±4 %. The dosage unit is placed in a dry basket at the beginning of each test. Apparatus II (Paddle Apparatus) is identical to the assembly from Apparatus I, except that a paddle formed from a blade and a shaft is used as the stirring element. Apparatus III (Reciprocating cylinder) consists of a set of cylindrical, flat-bottomed glass vessels; a set of glass reciprocating cylinders; and a motor and drive assembly to reciprocate the cylinders vertically inside the vessels and, if desired, index the reciprocating cylinders

horizontally to a different row of vessels. The vessels are partially immersed in a suitable water bath of any convenient size that permits holding the temperature at 37 ± 0.5 °C. Apparatus IV (Flow-Through Cell) consists of a reservoir and a pump for the dissolution medium; a flow-through cell; and a water bath that maintains the dissolution medium at 37 ± 0.5 °C. The pump forces the dissolution medium upwards through the flow-through cell. The pump has a delivery range between 240 and 960 mL/h with standard flow rates of 4, 8, and 16 mL per minute. The flow-through cell is mounted vertically with a filter system that prevents escape of undissolved particles from the top of the cell. The USP Apparatus I-IV. are shown on Figure 2 (58).

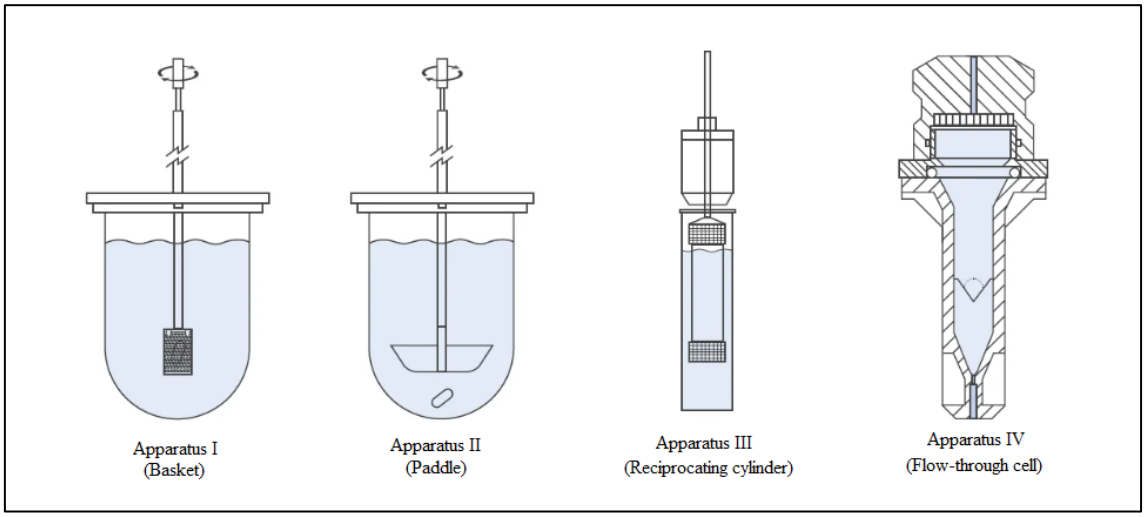

Figure 2. Dissolution Apparatus I-IV. according to USP chapter <711> (58).

Among the listed equipment, Apparatus I and II are the most common in the pharmaceutical industry, especially in the case of immediate-release formulations. Due to its design, Apparatus III is limited to non-disintegrating dosage forms. The device may be useful when it is desirable to study the effect of changing medium composition through the GI system. Moreover, the reciprocating motion models the mechanical stress resulting from gastrointestinal contractions relatively well, so that, for example, the degradation of hydrophilic matrix tablets can be simulated. Apparatus IV provides an environment in which the drug product is always surrounded by fresh dissolution medium by means of continuous flow. Thus, it is suitable for testing formulations whose absorption is dissolution rate controlled (typically ER formulations or occasionally IR formulations containing BCS Class II API). Similar to Apparatus III, in Apparatus IV the effect of pH change through the GI tracts can be simulated effectively.

The Chinese Pharmacopoeia describes a small volume paddle apparatus (CSV). In this case, the vessel is cylindrical with a hemispherical bottom, and a nominal capacity of 250 mL (internal diameter 62 ± 3 mm, height 126 ± 6 mm). The CSV better reflects the gastric liquid volume after the intake of drug product with a glass of water. This may play an important role when studying poorly soluble compounds (61).

1.5.2 Dissolution media

In general, an aqueous dissolution medium is used. The composition of the medium is chosen on the basis of the physico-chemical characteristics of the active substance(s) and excipient(s) within the range of conditions to which the dosage form is likely to be exposed after its administration. This applies in particular to the pH and ionic strength of the dissolution medium. The pH of the dissolution medium is usually set between pH 1 and pH 8. For the lower pH values in the acidic range, 0.1 M hydrochloric acid is normally used. The Ph. Eur. recommended dissolution media are listed in Table 1 (62).

Table 1. Ph. Eur. recommended dissolution media (62).

pH	Dissolution media
pH 1.0	HCl
pH 1.2	NaCl, HCl
pH 1.5	NaCl, HCl
pH 4.5	Phosphate or acetate buffer
pH 5.5 and 5.8	Phosphate or acetate buffer
pH 6.8	Phosphate buffer
pH 7.2 and pH 7.5	Phosphate buffer

For the testing of formulations containing poorly soluble active substances, modification of the medium may be necessary. In such circumstances, a low concentration of surfactant is recommended. The use of the basket and the paddle apparatus and the reciprocating cylinder apparatus is generally based on the principle of operating under sink conditions, i.e., in such a manner that the material already in solution does not exert a significant modifying effect on the rate of dissolution of the remainder.

Sink conditions normally occur in a volume of dissolution medium that is at least 3-10 times the saturation volume (62).

1.5.3 Acceptance criteria of quality control tests

A given batch of an immediate-release dosage form meets the dissolution requirements, if the quantities of active ingredient dissolved from the dosage units tested conform to the three-stage acceptance criteria. The testing should be continued through the three stages unless the results conform at either S_1 or S_2. The quantity, Q, is the amount of dissolved active ingredient (specified in the individual monograph), expressed as a percentage of the labelled content of the dosage unit. The acceptance criteria for immediate-release dosage forms are summarized in Table 2 (58).

Table 2. Acceptance criteria for immediate-release dosage forms (58).

Stage	**Number tested**	**Acceptance criteria**
S_1	6	Each unit is not less than Q + 5%.
S_2	6	Average of 12 units (S_1 + S_2) is equal or greater than Q, and no unit is less than Q – 15 %.
S_3	12	Average of 24 units (S_1 + S_2 + S_3) is equal to or greater than Q, and not more than 2 units are less than Q – 15 %, and no unit is less than Q – 25 %.

Extended-release dosage forms must also meet three-stage acceptance criteria. Generally, three test-time points are defined, the value of the first two of which must be within a specified range and the value at the final test time must be not less than a specified amount.

Delayed-release dosage forms are tested in a two-stage dissolution method, 2 hours of acid stage in 0.1 M hydrochloric acid is followed by a buffer stage at pH 6.8 ± 0.05 using phosphate buffer solution. In the acid stage the dissolution of the dosage form must not exceed 10 %, while in the buffer stage, three-stage acceptance criteria equivalent to the IR dosage forms must be met. The value of Q is 75 % dissolved unless otherwise specified in the individual monograph (58).

1.5.4 Comparative dissolution studies

When applying BCS based biowaiver approach (46) or justifying dose proportionality (13) (or in some cases of post-approval changes) comparative *in vitro* dissolution tests should be conducted. The conditions to be employed to characterize the dissolution profile of the product are listed in Table 3 (46).

Table 3. Conditions to be employed in comparative dissolution studies (46).

Parameter	**Condition to be used**
Apparatus	paddle or basket
Volume of dissolution medium	900 mL or less
Temperature of dissolution medium	37 ± 1 °C
Agitation	paddle – 50 rpm/ basket – 100 rpm
Units of the dosage form to be tested	at least 12
Buffers	pH 1.2, pH 4.5, and pH 6.8

The comparison of dissolution profiles is generally made by estimation of the similarity factor (f_2) using the following formula:

$$f_2 = 50 \bullet \log \{[1 + (1/n) \Sigma_{t=1}^{n} (R_t - T_t)^2]^{-0.5} \bullet 100\} \quad (1)$$

Where, 'n' is the number of time points, 'R_t' is the mean percent reference drug dissolved at time 't' after initiation of the study and 'T_t' is the mean percent test drug dissolved at time 't' after initiation of the study.

Two dissolution profiles are considered similar when the f_2 value is ≥50. When both test and reference products demonstrate that ≥85% of the labelled amount of the drug is dissolved in 15 minutes, comparison with an f_2 test is unnecessary and the dissolution profiles are considered similar. The evaluation of f_2 should be based on a minimum of three time points which are the same for the two products and not more than one mean value exceeds 85 % dissolved for either of the products (46).

1.6 Biorelevant dissolution

The appearance of the BCS and its implementation in the regulatory thinking highlighted the importance of dissolution in the regulation of post-approval changes and

introduced the possibility of substituting dissolution tests for clinical studies in some cases. As a result, the need for the development of such dissolution tests that better predict the *in vivo* performance has increased (43). From the early 2000s, intensive research began on the development of both physiologically relevant media and advanced dissolution systems.

1.6.1 Biorelevant media

In 2005, Vertzoni *et al.* proposed a dissolution medium for the simulation of fasting gastric environment. In their study, attention was paid to eliminate the shortcomings of the previously used gastric media, such as the absence or non-relevant concentration of physiological substances that may affect dissolution characteristics (e.g.: pepsin and bile salts) and the use of non-relevant substances (e.g.: artificial surfactants). The medium is a pH 1.6 hydrochloric acid solution containing 34.3 mM NaCl with a surface tension of 42.6 mN/m and an osmolality of ~120.7 mOsm/kg. To simulate the content of biomolecules in the gastric juice, the solution contains 0.1 mg/mL pepsin, 80 μM sodium taurocholate and 20 μM lecithin. Using the developed dissolution medium, the absorption of a lipophilic, weakly basic model compound was assessed and advanced predictability was demonstrated. The authors named the medium "Fasted State Simulated Gastric Fluid (FaSSGF)" and nowadays it is the generally accepted medium in the pharmaceutical industry for modelling fasting gastric conditions (63). Later, Jantratid *et al* proposed a composition for the "Fed State Simulated Gastric Fluid (FeSSGF)" as well, which consists of UHT-milk and an acetate buffer mixed in equal volumes. The pH of the mixture is 5.0 with a buffer capacity of 25 mM/L and an osmolality of 400 mOsm/kg (64).

Fluids simulating conditions in the proximal small intestine in the fasted state (FaSSIF) and fed state (FeSSIF) were introduced by Galia *et al.* (65). The composition of the two media relies heavily on the pH values summarized by Dressman *et al.* (43) and the bile salt concentrations by Bakatselou *et al.* (66). Vertzoni *et al.* also took a big step towards the daily routine use of simulated intestinal fluids by the simplification of FaSSIF and FeSSIF media using pure sodium-taurocholate and egg phosphatidylcholine (67). However, the most widespread intestinal media (FaSSIF-V2 and FeSSIF-V2) were published by Jantratid *et al.* after fine-tuning the composition of existing biorelevant

media according to physiological conditions (64). The properties of FaSSIF-V2 and FeSSIF-V2 are summarized in Table 4.

Table 4. Composition of the media simulating fasted and fed state small intestine.

Composition/medium	**FaSSIF-V2**	**FeSSIF-V2**
Sodium taurocholate (mM)	3	10
Lecithin (mM)	0.2	2
Glyceryl monooleate (mM)	-	5
Sodium oleate (mM)	-	0.8
Maleic acid (mM)	19.12	55.02
Sodium hydroxide (mM)	34.8	81.65
Sodium chloride (mM)	68.62	125.5
pH	6.5	5.8
Osmolality (mOsm/kg)	180±10	390±10
Buffer capacity (mmol/(L*ΔpH))	10	25

Nowadays, thanks to the appearance of instant powder mixtures containing the necessary components, the preparation of biorelevant media has become simple and robust. To support laboratory workers, an online media preparation tool is also available, which automatically calculates the recipe for the desired type and volume of dissolution medium (68). At the same time, the application of biorelevant media to predict the absorption of drugs has been integrated into the everyday practice of generic drug development.

1.6.2 Dynamic multi-compartmental dissolution systems

In order to achieve better predictivity, pharmaceutical scientists made great efforts to develop advanced *in vitro* biopharmaceutics models (69). An artificial stomach model was published by Vatier *et al.,* in which the ‘gastric reservoir’ was supplemented with two elements simulating the secretory flux and gastric emptying. Both flows were driven by a peristaltic pump (70). Later, the artificial stomach was further developed by adding a ‘*duodenal* reservoir’ to receive the gastric emptying flux and simulated bicarbonate secretion. The two-compartmental system was named ‘artificial stomach *duodenal*

model' (ASD) and supported the evaluation of the effect of antacids (71). The ASD has also been used to aid formulation development and crystal form selection (72) (73). To date, several more complex systems have been reported in the literature, such as TNO Gastro-Intestinal Model (TIM) (74), Dynamic Gastric Model (DGM) (75), and Human Gastric Simulator (HGS) (76). Based on the ASD system, Takeuchi *et al*. developed the Gastrointestinal Simulator (GIS), which is a three compartmental model consisting of a gastric, a *duodenal*, and a *jejunal* chamber connected by peristaltic pumps. The transfer rates (representing the gastric-emptying rate) were determined using propranolol and metoprolol model compounds by comparing the dissolution results with clinical data (77). The schematic diagram of the GIS system is shown in Figure 3.

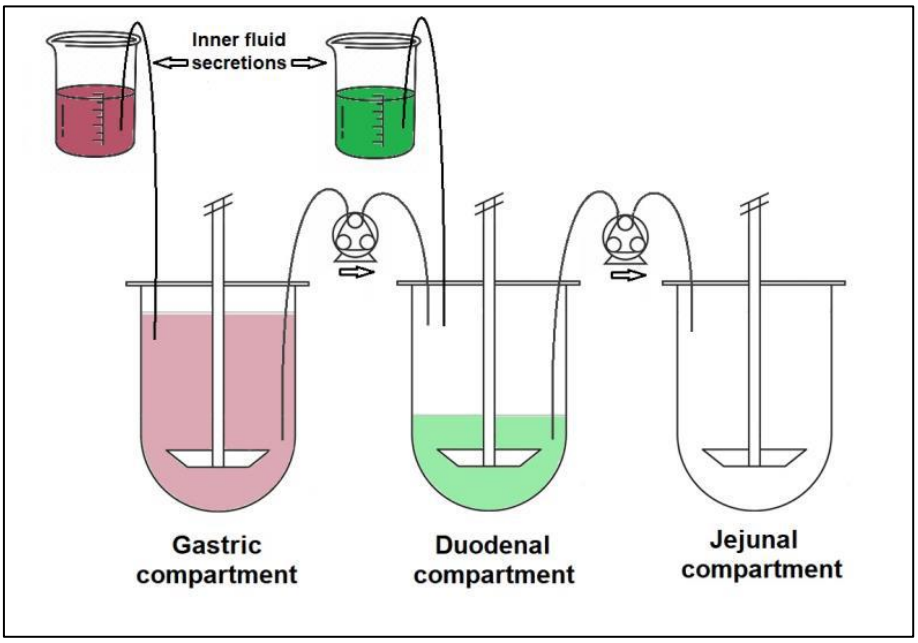

Figure 3. Gastrointestinal Simulator.

The GIS was successfully applied in several studies to predict the *in vivo* performance of drugs, investigate the supersaturation phenomena, or evaluate the possible drug-drug interaction with acid-reducing agents (78) (79) (80) (81) (82). In order to achieve better IVIVC, some of the models are combined with *in silico* simulations. The published studies focused primarily on BCS Class IIb (and BCS Class IIc) compounds. Despite the promising results achieved with the GIS system, to the best of our knowledge, poorly soluble acidic drugs (BCS Class IIa) have not yet been studied.

1.6.3 *In silico* methods

IVIVC is a predictive mathematical model describing the relationship between an *in vitro* property and a relevant *in vivo* response. The aim of developing and evaluating an IVIVC is to establish the dissolution test as a surrogate for human bioequivalence studies. In the case of ER products, in certain scale-up and post approval changes specified by the FDA's SUPAC-MR guideline (51), an IVIVC may serve as a waiver of *in vivo* study. While in the case of IR dosage forms, the main objective of an IVIVC is to reduce the risk of BE studies via supporting the optimization of the drug formulation. The correlation has four levels from A to D. Level A correlation is generally linear and represents a point-to-point relationship between *in vitro* dissolution and the *in vivo* input rate (e.g., the *in vivo* dissolution of the drug from the dosage form). A model of this level should be able to predict the entire *in vivo* time course (e.g., plasma drug concentration or amount of drug absorbed) from the *in vitro* data. A Level B IVIVC compares the mean *in vitro* dissolution time either to the mean residence time or to the mean *in vivo* dissolution time. The model uses all the *in vitro* and *in vivo* data but is not considered to be a point-to-point correlation. A Level C model establishes a single point relationship between a dissolution parameter, for example, $t_{50\%}$, percent dissolved in 4 hours and a pharmacokinetic parameter (e.g., 50% AUC, C_{max}, T_{max}). A Level C correlation does not reflect the complete shape of the plasma concentration *vs*. time curve, which is the critical factor that defines the performance of ER products. A Level D (or multiple Level C) correlation relates one or several pharmacokinetic parameters of interest to the amount of drug dissolved at several time points of the dissolution profile.

A Level A IVIVC is usually established by a two-stage procedure: *in vivo* absorption is estimated using an appropriate deconvolution technique (e.g., Wagner-Nelson, Loo-Riegelman, numerical deconvolution) followed by the comparison of drug absorbed to the fraction of drug dissolved. In a linear correlation, the *in vitro* dissolution and *in vivo* input curves may be directly superimposable or may be made to be superimposable by the use of a scaling factor. Even though the deconvolution method is often applied for regulatory submission, the method is limited to linear pharmacokinetics (PK) regimen (50).

Alternatively, the mechanistic deconvolution using the physiologically based pharmacokinetic (PBPK) modelling popularly known as physiologically based IVIVC

(PB-IVIVC) is nowadays extensively utilized for biopharmaceutics modelling (83) (84). Besides its applicability to the nonlinear PK, the PBPK model also considers the different factors governing the drug release and absorption such as particle size of the API, food effect, pH-dependent solubility profile, precipitation, gastric emptying time, drug degradation, drug solubilization in the presence of excess bile acids and permeation across the intestinal membranes (85) (86) (87) (88).

2 OBJECTIVES

The purpose of my work was to develop advanced *in vitro* dissolution methods and mathematical models to support generic/value-added generic drug formulation development by a better prediction of *in vivo* bioavailability.

- Development of an *in vitro* dissolution method for enteric-coated formulations using acetylsalicylic acid (ASA) model compound.
  - Determination of the pH conditions, residence times and fluid volumes of the fasted stomach and small intestine based on the collection of literature data. Experimental implementation of the determined pH profile and volume changes.
  - Investigation of the dissolution of enteric coated ASA formulations using the developed method. Comparison with USP dissolution method.
  - Analysis of the coating and the composition of the formulations. Evaluation of the relationship with *in vitro* and *in vivo* performance.
- Investigation of multi-compartmental dissolution method for enhanced bioavailability immediate-release formulations containing BCS Class IIa drugs.
  - Measurement of the pH-dependent equilibrium solubility of ibuprofen in aqueous buffers and biorelevant media using the saturation shake-flask method.
  - Investigation of the dissolution of conventional and rapid-release ibuprofen formulations in the GIS. Comparison with the USP method.
  - Establishment of a Level A IVIVC model to simulate the absorption of the investigated formulations and to justify the predictivity of the GIS method.
- Prediction of the effect of food on the absorption of Rivaroxaban 20 mg IR formulations.
  - Establishment of a Level A IVIVC model relying on a biorelevant USP IV dissolution method and published clinical data in fasted state.
  - Simulation of the plasma concentration *vs.* time in fed state, based on USP IV dissolution data in fed media.
  - Evaluation of the predicted food effect in relation to literature data.

3 METHODS

3.1 Materials

3.1.1 Biorelevant multi-stage pH shift dissolution study

Six commercially available enteric-coated ASA-containing products were tested: Walgreens Aspirin 81 mg (LNK, USA), Aspirin Protect 100 mg (Bayer AG, Germany), Asatrin-Teva Protect 100 mg (Teva Pharmaceutical Industries Zrt., Hungary), ASA Krka 100 mg (KRKA, Slovenia), Asactal 100 mg (Actavis Group PTCehf., Iceland) and ASA Protect Pharmavit 100 mg (PharmaSwiss Ceska Republika, Czech Republic). Walgreens Aspirin was purchased in the USA, while other products were purchased from pharmacies in Hungary. All formulations were white coloured, round, cylindrical biconvex tablets with slight differences in the sizes: the height and the diameter of the formulations varied between 3 and 4 mm and 6.5–8 mm.

3.1.2 Multi-compartmental dissolution study

Four commercially available immediate release ibuprofen-containing products were investigated: Advil 200 mg coated tablets, Advil 256 mg film-coated tablets, Advil ULTRA 200 mg soft-gelatine capsules (Pfizer Consumer Healthcare, Madison, NJ, USA) and Dolowill RAPID 342 mg film-coated tablets (Goodwill Pharma, Szeged, Hungary). Advil 256 mg film-coated tablets were purchased in the USA, others three formulations were bought in Hungarian pharmacies. Ibuprofen drug substance was purchased from Sigma–Aldrich (Burlington, VT, USA). All chemicals used were of analytical grade.

3.2 Methods

3.2.1 Equilibrium solubility determination of ibuprofen

The standardized saturation shake–flask method was used to determine the equilibrium solubility of the API (89) (90). The measurements were carried out at 37 ± 0.1 °C. Because of its simplicity UV spectroscopy was used for concentration measurement. In each medium, the solubility experiments were performed in triplicate. The pH dependence of solubility was determined in Britton-Robinson (BR) buffers in the pH range 2–8 (pH = 2.0; 4.0; 6.0; 7.0; 8.0) and in 1 M NaOH (pH = 14). The equilibrium solubility was also investigated in biorelevant media modelling gastric and small intestinal fluid in a fasted and fed state with and without solubilizing agents (pepsin or

lecithin and bile acid salts). The tested biorelevant media were Blank FaSSGF, FaSSGF, Blank FaSSIF, FaSSIF, FeSSGF-acetate (without milk), Blank FeSSIF, and FeSSIF. The solutions were prepared according to the media preparation tool of biorelevant.com (68).

3.2.2 Dissolution testing

The dissolution tests were carried out using an Agilent 708 DS dissolution apparatus (Agilent Technologies, Inc., Santa Clara, CA, USA). The media were thermostated at 37 ± 0.5 C. Each formulation in each method was tested on six parallel samples.

3.2.2.1 Dissolution of ASA formulations using USP method (91)

The samples were first placed into USP I baskets and stirred at 100 rpm in 1000 mL of 0.1 M HCl solution for 120 min, then the medium was replaced by 900 mL of pH 6.8 ± 0.5 phosphate buffer and the test was continued for an additional 60 min at constant stirring rate. The buffer solution was prepared by mixing 0.1 M HCl with 0.2 M tribasic sodium phosphate (3:1). In case it was necessary, the pH was adjusted with 2M hydrochloric acid or 2 M sodium hydroxide. Samples at each sampling time point were taken into HPLC vials via autosampling. The sampling cannulas were equipped with 10 μm PVDF, full-flow filter tips (Agilent Technologies, Inc., Santa Clara, California, USA). The applied sampling schedule is shown in Table 5.

Table 5. Sampling time points of USP method for ASA formulations.

Medium	**Sampling time (min)**
0.1 M HCl	60, 120
pH 6.8 phosphate buffer	5, 15, 30, 45, 60

3.2.2.2 Dissolution of ibuprofen formulations using USP method (92)

The tests were performed in a USP II (paddle) apparatus. The dissolution medium was pH 7.2 ± 0.5 phosphate buffer solution prepared by dissolving 6.89 g $NaH_2PO_4 \cdot H_2O$ in 1 L distilled water, and the pH was adjusted with 3 M NaOH solution. The samples were placed into a 900 mL medium and stirred at 50 rpm. Samples at 5, 15, 30, 45, and 60 min were taken into HPLC vials via autosampling. The volume of each sample was ~1.2 mL. The sampling cannulas were equipped with 10 μm PVDF full-flow filter tips (Agilent Technologies, Inc., Santa Clara, CA, USA).

3.2.2.3 Dissolution of ASA formulations using biorelevant multi-stage pH shift method

The dissolution apparatus was equipped with 250 mL small volume vessels and rotating paddles according to the Chinese Pharmacopoeia (61). The media were stirred at 50 rpm. The initial dissolution medium was 160 mL of 0.01 M HCl solution, which was modified in three steps through the addition of different amounts of Na_2HPO_4 buffer in order to simulate the conditions of the stomach and different parts of the small intestine. The addition of the buffer solution was performed using Cole Parmer 74,900 infusion pumps (Cole Parmer, Vernon Hills, Illinois, USA), the pH of the media was measured by an Inolab-type pH meter (WTW GmbH, Weilheim, Germany). Due to the highly variable *in vivo* residence times in the stomach, two variants of the method simulating rapid gastric emptying (RGE) and slow gastric emptying (SGE) were applied. The two variants differed only in the length of the acidic treatment (20 and 120 min, respectively). Samples at each time point were taken manually using equivalent filtration to that of the USP method. The volume of the samples was 1 mL in all cases. Table 6 shows the sampling schedule of the biorelevant methods.

Table 6. Sampling time points of biorelevant methods.

Method	Sampling time (min)
RGE	20, 30, 60, 70, 80, 90, 100, 110, 120, 135, 150, 160, 175, 190, 205
SGE	120, 130, 160, 170, 180, 190, 200, 210, 220, 235, 250, 260, 275, 290, 305

Onset of the dissolution was determined by 5% of dissolved drug substance. The f_2 statistic was calculated based on the EMA guideline on the Investigation of Bioequivalence (13).

3.2.2.4 Dissolution of ibuprofen formulations using multi-compartmental GIS method

The GIS was implemented in a dissolution apparatus equipped with 250 mL small volume vessels, according to the Chinese Pharmacopoeia (61). The system consisted of three main compartments (250 mL vessels) modelling the stomach, *duodenum*, and *jejunum*. The vessels were connected to each other by Gilson Minipuls 3-type peristaltic pumps (Gilson Inc., Middleton, WI, USA). At the beginning of the test, 50 mL pH 1.6 gastric fluid and 250 mL water were poured into the stomach, 50 mL pH 6.5 intestinal fluid into the *duodenum*, and the *jejunal* chamber was left empty. Two additional vessels

were used to model the inner fluid secretion into the stomach (pH 1.6 gastric fluid) and the *duodenum* (pH 6.5 intestinal fluid concentrate), both the stomach and *duodenum* had a flow rate of 1 mL/min. The biorelevant dissolution media were prepared, and the tests were conducted with and without biomolecules (pepsin, SIF powder). The composition of the applied buffer solutions is summarized in Table 7.

Table 7. Preparation of 1 L buffer solutions for GIS dissolution.

	Blank Biorelevant Media			**Biorelevant Media**		
	Blank FaSSGF	**Blank FaSSIF**	**Blank FaSSIF conc.**	**Full FaSSGF**	**Full FaSSIF**	**Full FaSSIF conc.**
NaCl	2.00 g	6.19 g	40.24 g	2.00 g	6.19 g	40.24 g
NaOH	-	0.40 g	2.60 g	-	0.40 g	2.60 g
$NaH_2PO_4.H_2O$	-	3.96 g	25.74 g	-	3.96 g	25.74 g
SIF powder	-	-	-	0.06 g	2.25 g	14.63 g
Pepsin	-	-	-	0.10 g	-	-
pH adjustment	cc. HCl:purified water = 1:1	1M NaOH	-	cc. HCl:purified water = 1:1	1M NaOH	-

The tested formulation was dropped into the gastric chamber, and the media were stirred at 50 rpm using rotating paddles. The applied flow rates were 5.5 mL/min from the gastric to the *duodenal* and 6.5 mL/min from the *duodenal* to the *jejunal* chamber, as suggested by Takeuchi *et al*. (77). Samples from the compartments were taken manually every 5 min during the 45-min duration of the tests. The duration was limited by the initial fluid volume and the gastric emptying rate. Each sample was filtered through Acrodisc® syringe filters (d = 13mm) with 0.45 μm GHP membrane (Pall Co., Port Washington, NY, USA). The volume of each sample was ~0.5 mL

3.2.3 Determination of dissolved ASA content by High Performance Liquid Chromatography (HPLC)

Waters Acquity UPLC device (Waters, Milford, Massachusetts, USA) was used to determine the amount of dissolved drug in the solutions. For this purpose, YMC-Pack

Pro C18 RS S-5 μm, 8 nm 150 × 4.6 mm I.D type HPLC column was used. The mobile phase was ACN:H_2O:cc.H_3PO_4 = 400:600:1 and the flow rate was 1.0 mL/min. The mode of separation was isocratic. External calibration was applied by five consecutive injections of the standard solution containing the concentration of API corresponding to the approximated concentration of 100% dissolution. The calibration was controlled by the injection of the standard control solution containing the same nominal concentration, then followed by the injection of the sample solutions. The absorbance was detected at 237 nm. For standard preparations, accurate measurements were achieved using a Mettler Toledo XP26 microanalytical balance (Mettler Toledo, Columbus, Ohio, USA). The sample concentrations in mg/L were calculated using the dilution of the standard solution and the sample solution and the peak areas of the sample solutions. The chromatographic conditions for each test preparation were the same as well as the column used for the measurement.

3.2.4 Determination of dissolved ibuprofen content by Ultra High Performance Liquid Chromatography (UPLC)

Waters Acquity type UPLC device (Waters, Milford, Massachusetts, USA) with Waters Acquity BEH C18 1.7 μm (2.1 x 50 mm) type UPLC column was equipped to measure the amount of dissolved drug in the solutions. Isocratic separation was applied with ACN:H_2O:cc.H_3PO_4 = 450:550:1 mobile phase and 0.7 mL/min flow rate. External calibration was prepared by five consecutive injections of standard solution containing the concentration of API corresponding to the approximated concentration of 100 % dissolution. The calibration was controlled by the injection of control standard solution containing the same nominal concentration, then followed by the injection of the sample solutions. The detection wavelength was 214 nm. The solid standards were weighed using a Mettler Toledo XP 26 microanalytical balance (Mettler Toledo, Columbus, Ohio, USA). The sample concentrations in mg/L were calculated using the dilution factor of the standard and the sample solutions and the peak areas of the sample solutions. The chromatographic conditions for each test preparation were the same as well as the column used for the measurement.

3.2.5 Examination of enteric coating by scanning electron microscopy (SEM)

Before the test, the samples were fixed with double-sided carbon glue to copper stumps, then gilded with a JEOL 1200 type device (JEOL, Akishima, Tokyo, Japan).

Images were taken from the samples in tablet form using a JEOL JSM- 6380LA scanning electron microscope (JEOL, Akishima, Tokyo, Japan) applying 15 kV accelerating voltage and 10 mm sample distance under high vacuum.

3.2.6 IVIVC model for ibuprofen formulations

A Level A IVIVC model was developed using the IVIVC Toolkit 8.3. of Phoenix Win-Nonlin 8.3.4.295 for Windows (Certara, St. Louis, MO, USA). *In vivo* data were obtained by digitizing the mean plasma concentration profiles of four different ibuprofen formulations from a fasted state crossover pharmacokinetic study published by Legg *et al*. (93). The administered formulations were identical to that of Table 6, except for IBU-Lys. In the case of IBU-Lys, Nurofen Express 342 mg caplets (Reckitt Benckiser, Slough, Berkshire, UK) were administered, the manufacturer of which differed from the formulation used in the *in vitro* studies. However, the salt form of the active ingredient was the same. A two-compartmental PK model (model 14 of PK tab) was then fitted to the *in vivo* data of each formulation. The gained parameters of Advil 200 mg tablets were implemented to the unit impulse response (UIR) function, and the fitted plasma concentration curve was deconvolved, resulting in the calculated fraction absorbed profile. The cumulative dissolution data of the *duodenal* and *jejunal* compartments of the GIS measured in blank biorelevant media were fitted with the Weibull equation.

The *in vitro* fraction dissolved, and *in vivo* fraction absorbed of Advil 200 mg tablets were correlated using the Levy plot. Based on the calculated correlation and UIR function, the plasma concentration profile of each formulation was simulated from the fitted dissolution profiles. Finally, the plasma concentrations predicted from the model and the observed data were compared.

3.2.7 IVIVC model for rivaroxaban formulations

The IVIVC was established to predict the PK profile after oral administration of formulation in the fed state using IVIVC Toolkit 8.0 of Phoenix WinNonlin 8.2.0.4383 for Windows (Certara, St. Louis, MO, USA). The IVIVC model was developed and internally validated using the *in vitro* dissolution and *in vivo* profile of 20 mg strength of Xarelto IR tablet in fasted conditions. The *in vitro* profiles were obtained by dissolving the formulation in fasted and fed biorelevant media using USP IV flow-through cell apparatus. In case of the *in vivo* data, results published in the literature were used (94) (95).

IVIVC was based on a two-step deconvolution method. Initially, the Weibull function was fitted to the *in vitro* data. Thereafter, the UIR function was calculated using the *in vivo* data of the 10 mg oral solution published by Kubitza *et al* (94) (95). The fasted *in vivo* data of Xarelto 20 mg IR tablet were then deconvolved and a correlation was built between the *in vitro* drug release and *in vivo* drug absorption. As the final step, the internal validation of the IVIVC model was performed by comparing the predicted and observed PK data of Xarelto 20 mg tablet in the fasted condition.

Using the established IVIVC, the PK profile of the Xarelto 20 mg IR tablet in fed condition was predicted from the *in vitro* dissolution of the formulation in fed biorelevant media. At the end, the predicted PK profile and the observed (literature) data were compared.

4 RESULTS

4.1 Dissolution method for delayed-release dosage forms (ASA model compound)

The lack of *in vitro* dissolution methods that adequately predict the *in vivo* performance of delayed-release dosage forms is clear from the literature. The pharmacopoeial methods of such formulations focus on examining the resistance of the applied enteric-coating to gastric acid, and the immediate-release nature after emptying from the stomach. These methods are robust and simple to implement, however GI conditions are not properly modelled. The aim of our development was to provide an *in vitro* dissolution method that better reflects the physiological characteristics (especially pH, residence times and volumes) of the upper GI tract, thus expected to show better *in vivo* predictivity for delayed-release drug products.

The performance of the new method was tested using enteric-coated acetylsalicylic acid (ASA) formulations as model drugs. The examined products, the inactive ingredients of the tablet cores and the applied coating materials are summarized in Table 8.

Table 8. Dose and qualitative ingredients of the tested products.

Product	Dose (mg)	Tablet core	Coating
Aspirin Protect	100	Microcrystalline cellulose, corn starch	Methacrylic acid− ethyl acrylate 1:1 copolymer, polysorbate 80, sodium lauryl sulphate, triethyl citrate, talc
Asatrin – Teva Protect	100	Microcrystalline cellulose, potato starch, silica colloidal anhydrous, lactose monohydrate	Methacrylic acid− ethyl acrylate 1:1 copolymer, triacetin, talc
ASA Krka	100	Microcrystalline cellulose, potato starch, silica colloidal anhydrous, lactose monohydrate	Methacrylic acid− ethyl acrylate 1:1 copolymer, polysorbate80, sodium lauryl sulphate, triacetin, talc
Asactal	100	Microcrystalline cellulose, corn starch, silica colloidal anhydrous, stearic acid	Methacrylic acid− ethyl acrylate 1:1 copolymer, polysorbate 80, sodium lauryl sulphate, triethyl citrate, talc
ASA Protect Pharmavit	100	Microcrystalline cellulose, potato starch, silica colloidal anhydrous, lactose monohydrate	Methacrylic acid− ethyl acrylate 1:1 copolymer, triacetin, talc
Walgreens Aspirin	81	Microcrystalline cellulose, corn starch, silica colloidal anhydrous, polydextrose, sodium bicarbonate	Hypromellose, methacrylic acid, shellac wax, sodium lauryl sulphate, polyethylene glycol, simethicone, triacetin, triethyl citrate, talc, titanium dioxide

ASA is a nonsteroidal anti-inflammatory drug (NSAID) which is commonly used to reduce pain, fever or inflammation (96). It irreversibly inhibits platelet aggregation by inhibiting thromboxane A2 (TxA2) synthesis, therefore in 100 mg dose, it is recommended in single and dual antiplatelet therapy as well. In order to reduce the irritating effect on the gastric mucosa, ASA is usually prescribed as enteric-coated tablet. The difficulty of developing such type of generic drugs is well illustrated by the fact that among the five tested generic formulations only the manufacturer of ASA Krka and Asactal submitted BE study results to support the application for marketing authorization (97) (98). However, both failed to demonstrate bioequivalence. Other applicants, such as Teva, referred to the well-established clinical use and provided only an overview of literature references (99).

4.1.1 Development of the biorelevant dissolution method

The development of the new method was focused on modelling the gastrointestinal conditions in fasted state. The applied pH conditions and residence times were determined based on published experimental results of ingestible pH monitoring capsules (15) (16) (17) (19) (31) (20) (30) (100). According to the published data, the mean pH of the stomach was found to be around 2.0, which is resulted by the dilution of the initial gastric acid with the liquid intake following the administration of the drug product. The residence time in the stomach is reported to be typically between 20 and 120 min with high variability. Since the time spent in the acidic medium may affect the physicochemical properties of the weakly acidic film formers, instead of specifying the average residence time, two versions of the method were tested. One with 20 min and one with 120 min acidic treatment, to model both rapid and slow gastric emptying (RGE and SGE). The pH conditions modelling the small intestinal tracts were set to pH 6.5 (*proximal* phase), pH 6.8 (middle phase) and pH 7.2 (*distal* phase), respectively. The time spent at each pH was 30 min (*proximal* phase), 70 min (middle phase), and 45 min (*distal* phase), excluding the time of the pH changes. Initially, the gastric solution was 0.01 M HCl, while the appropriate pH changes were achieved by the addition of different amounts of Na_2HPO_4 solutions with different molarities. The molarities of the phosphate-based buffer solutions were set based on the results of Al-Gousous *et al.*, who elaborated a simplified alternative to unstable bicarbonate buffer systems (101). The volume of the dissolution media varied from 160 mL to 210 mL, which better suits the amount of fluid

in the stomach after the intake of drugs with a glass of water. Considering the amount of dissolution media, the dissolution apparatus was equipped with 250 mL small volume vessels and rotating paddles according to the Chinese Pharmacopoeia (61) and the media were stirred at 50 rpm. The applied conditions of the new method are summarized in Table 9.

Table 9. Applied conditions of dissolution method with RGE and SGE.

			Method with RGE	**Method with SGE**
	Medium	**pH**	**Residence time (min)**	
Gastric phase	160 mL, 0.01M HCl solution	2.0	**20**	**120**
pH change 1.	*Addition of 20 mL, 135 mM Na_2HPO_4 buffer*		*10*	*10*
Duodenal phase	180 mL, 15 mM phosphate buffer	6.5	30	30
pH change 2.	*Addition of 10 mL, 100 mM Na_2HPO_4 buffer*		*20*	*20*
Jejunal phase	190 mL, 19.5 mM phosphate buffer	6.8	70	70
pH change 3.	*Addition of 20 mL, 100 mM Na_2HPO_4 buffer*		*10*	*10*
Ileal phase	210 mL, 27.1 mM phosphate buffer	7.2	45	45

According to the results of radiotelemetry capsules, the pH change between each tract is rather gradual than momentary (102). To model this phenomenon, the buffer solutions were administered using an infusion pump. The experimental pH *vs.* time profile of the developed method with rapid gastric emptying is shown in Figure 4.

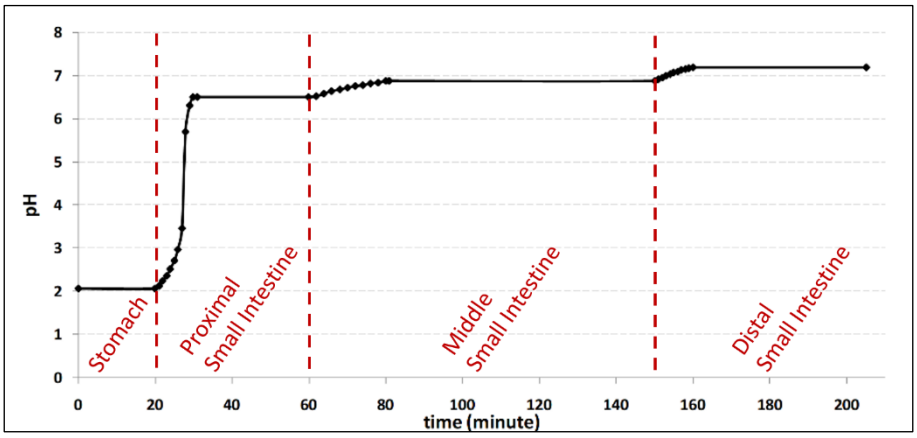

Figure 4. Experimental pH profile of biorelevant dissolution method with RGE.

4.1.2 Dissolution results obtained by USP method

In order to evaluate the advantages of the developed method compared to the pharmacopoeial approach, the formulations were first dissolved according to the USP method described in the individual monograph of Aspirin delayed-release tablets (91). The dissolution results of the six selected ASA formulations are depicted on Figure 5.

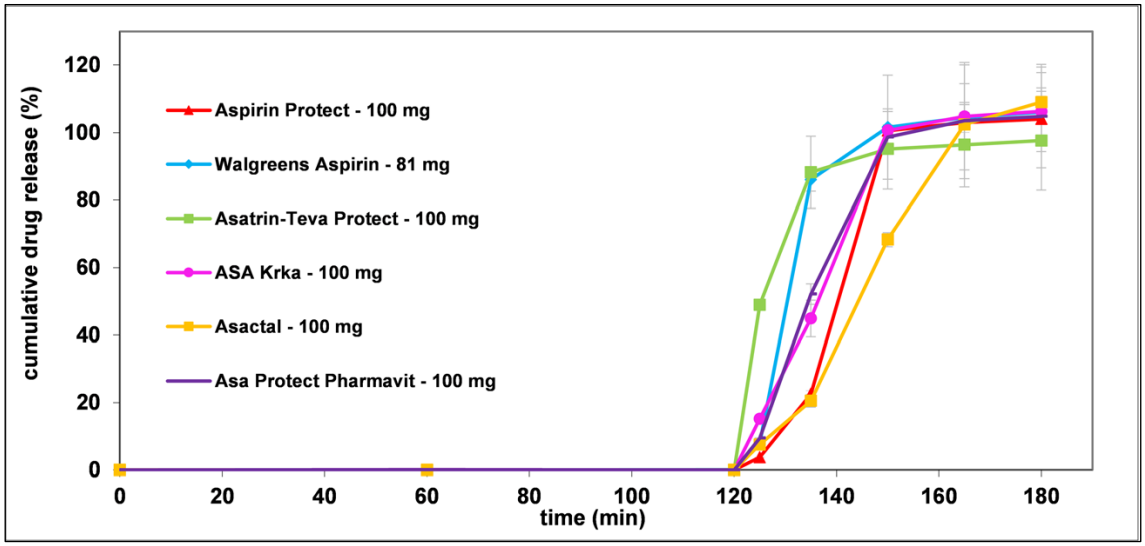

Figure 5. Dissolution results obtained by USP method.

As evident from Figure 5, no dissolution was observed during the 2-h treatment in 0.1M HCl solution. After the replacement of the dissolution medium by pH 6.8 phosphate buffer, each formulation started to dissolve immediately, and a measurable concentration of ASA was observed at the 5-min sampling point in all cases. The post-acidic dissolution of all formulations except Asactal was rapid (≥85% for the mean percent dissolved in ≤30 min). Walgreens Aspirin and Asatrin Teva Protect even met the criterion of very rapid dissolution (≥85% for the mean percent dissolved in ≤15 min) in this medium (46). The dissolution rate of Asactal was significantly lower as its mean dissolution exceeded 85% only after 45 min residence in pH 6.8 buffer. However, the USP acceptance criteria (not more than 10% dissolved in the acidic stage, and the dissolution must exceed 75% in the buffer stage after 45 min) were met in all cases regardless of the formulation.

4.1.3 Dissolution results obtained by Biorelevant method with RGE

After the USP dissolution, the performance of the formulations was tested using the new biorelevant method with rapid (20 min) gastric emptying. The resulting dissolution profiles are compared on Figure 6.

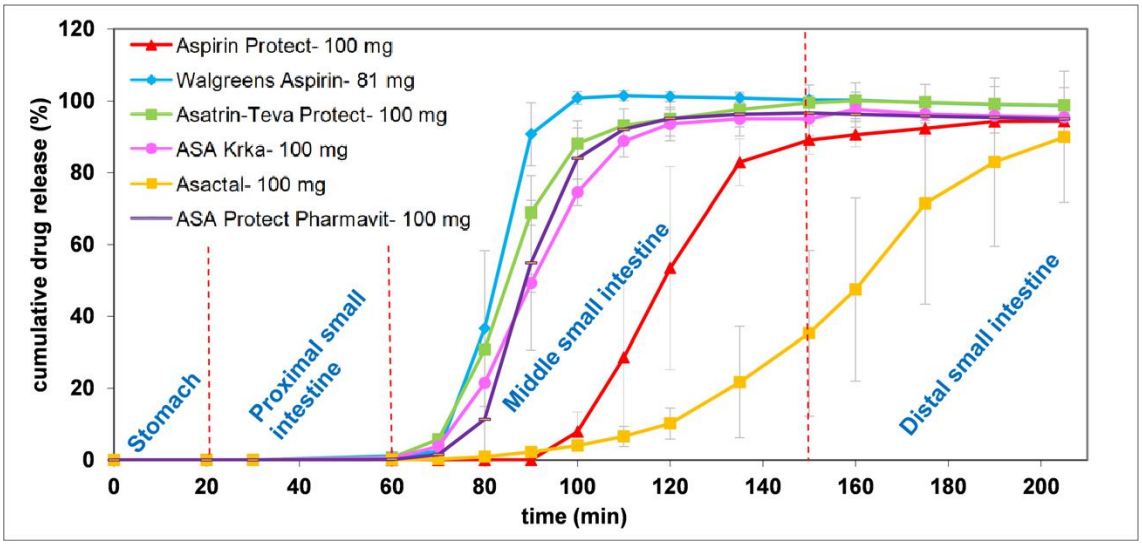

Figure 6. Dissolution results obtained by biorelevant method with RGE.

According to the results none of the products released the API in the gastric or proximal small intestinal phase (0–60 min). In case of Walgreens Aspirin, Asatrin-Teva Protect, ASA Krka and ASA Protect Pharmavit the mean onset of dissolution ranged from 78.3 ± 4.1 to 80.0 ± 6.3 min, which belongs to the pH change between the proximal and middle small intestinal phase. The dissolution profiles of the latter formulations except Walgreens Aspirin were found to be similar to each other, as the calculated similarity factors (f_2) were ≥ 50 ($f_{2,\text{Asatrin-Teva Protect vs. ASA Protect Pharmavit}}$ = 50; $f_{2,\text{ASA Krka vs. ASA Protect Pharmavit}}$ = 58). Aspirin Protect and Asactal started to dissolve at the pH of the middle small intestinal phase (pH 6.8; 80–150 min), however, the dissolution rate of Asactal is significantly slower compared to Aspirin Protect (f_2 = 21). The dissolution of the products except Asactal is completed or almost completed in the 80–150-min interval, while Asactal releases its API mostly in the distal small intestine.

4.1.4 Dissolution results obtained by Biorelevant method with SGE

To investigate the possible effect of a longer acidic treatment on the post-gastric behaviour of enteric coatings, the new method with slow (120 min) gastric emptying was also tested. The comparative dissolution profiles are shown in Figure 7.

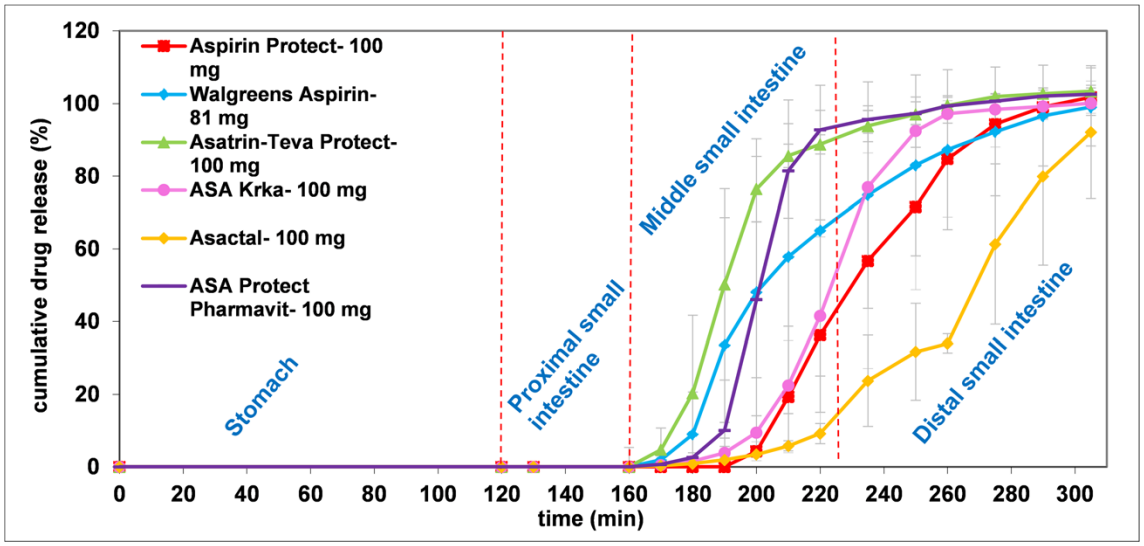

Figure 7. Dissolution results obtained by biorelevant method with SGE.

Dissolution in the gastric and proximal small intestinal periods (from 0 to 160 min on Figure 7) was not observed with this method either. The dissolution of the formulations except Asatrin Teva Protect and Walgreens Aspirin started at the pH 6.8 period (180–250 min). In case of Asatrin Teva Protect and Walgreens Aspirin, a certain amount of API has already been released at the pH change between the proximal and middle small intestinal phases (160–180 min), however it was also less than in case of short gastric residence. Similar to the RGE method, Asatrin Teva Protect and ASA Protect Pharmavit dissolved faster, while Asactal dissolved more slowly than the reference Asprin Protect. On the other hand, as a result of longer acidic treatment the shape of Walgreens Aspirin dissolution profile changed to a greater extent and the onset of dissolution of ASA Krka was more shifted.

4.1.5 Scanning electron microscopic images

In order to characterize the structure and thickness of the coatings surrounding the tablet cores, the different tablets were examined using scanning electron microscopy. The microscopic images can be seen in Figure 8.

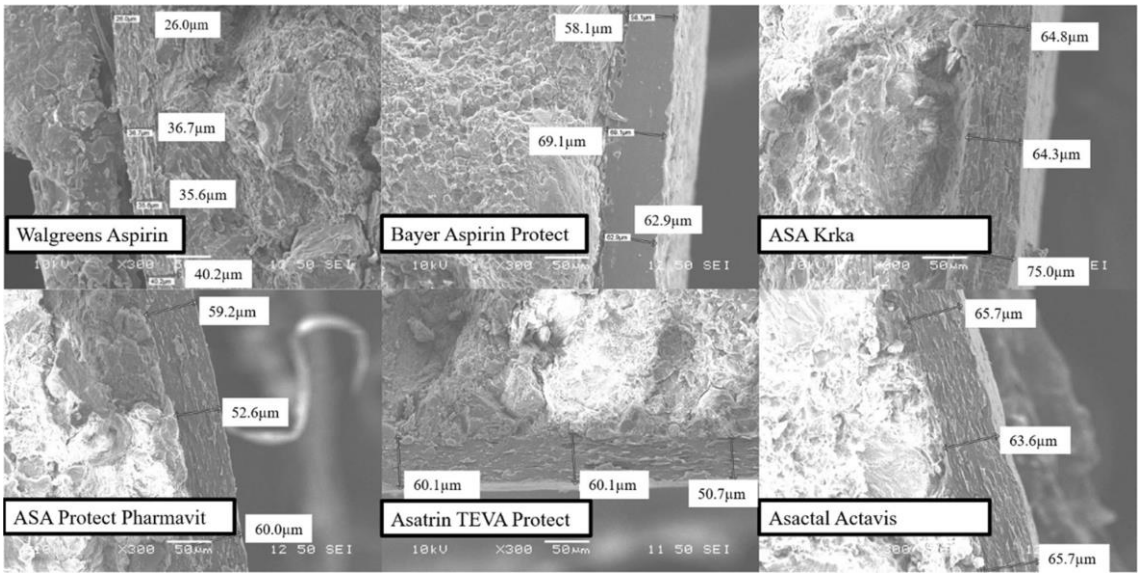

Figure 8. SEM pictures of enteric coated ASA formulations.

The coatings were found to be evenly distributed around the cores in all cases. Comparing the structure of methacrylic acid-ethyl acrylate coated formulations and Walgreens Aspirin, it can be said that methacrylic acid-ethyl acrylate is more concise, especially in the case of Bayer Aspirin Protect.

The measured thickness of the coatings is summarized in Table 10.

Table 10. Thickness of the coating of ASA formulations.

Formulation	Thickness of the coating (µm)
Walgreens Aspirin	26.0 – 40.2
ASA Protect Pharmavit	52.6 – 60.0
Bayer Aspirin Protect	58.1 – 69.1
Asatrin Teva Protect	50.7 – 60.1
ASA Krka	64.3 – 75.0
Asactal Actavis	63.6 – 65.7

Based on Table 10, the coating of Walgreens Aspirin was found to be thinner than methacrylic acid-ethyl acrylate coated formulations, the coating thicknesses of which can be considered similar to each other.

4.2 Multi-compartmental dissolution of immediate-release BCS IIa drugs (ibuprofen model compound)

The aim of this study was to investigate the applicability of multi-compartmental dissolution methods to predict the *in vivo* performance of BCS Class IIa compounds. For this purpose, different conventional and rapid-dissolving ibuprofen 200 mg formulations were tested using the GIS system with biorelevant dissolution media. The investigated formulations and the forms of the active substances used in them are listed in Table 11.

Table 11. Dosage form and active ingredients of the tested products.

Product	Manufacturer	API Form	Abbreviation
Advil 200 mg coated tablets	Pfizer Consumer Healthcare, Madison, NJ, USA	ibuprofen free acid	IBU
Advil 256 mg film-coated tablets	Pfizer Consumer Healthcare, Madison, NJ, USA	ibuprofen sodium	IBU-Na
Dolowill RAPID 342 mg film-coated tablets	Goodwill Pharma, Szeged, Hungary	ibuprofen lysinate	IBU-Lys
Advil ULTRA 200 mg soft-gelatine capsules	Pfizer Consumer Healthcare, Madison, NJ, USA	ibuprofen in solution	IBU-lq

Ibuprofen is one of the most common analgesic/antipyretic agents. It is available in over-the-counter (OTC) strengths (100 mg and 200 mg) and prescription strengths (400 mg, 600 mg and 800 mg) as well. In case of OTC dosing, adults and children, over 12 years old are advised to take 1 to 2 tablets (i.e., 200 mg to 400 mg) by mouth every 4 to 6 h while symptoms last (104). In addition to the conventional tablet form, ibuprofen is marketed as different rapid-dissolving formulations (e.g., soft-gelatin capsules and tablets containing sodium or lysinate salts of the API). The rapid onset of the analgesic effect as well as the higher absorption rate of rapid-dissolving formulations is discussed by several *in vivo* studies (105) (106) (107).

4.2.1 Thermodynamic equilibrium solubility measurements

As a basis for the better understanding of the dissolution mechanism, the pH-dependent equilibrium solubility of the API as well as the equilibrium solubility in biorelevant media were determined using the saturation shake-flask method.

4.2.1.1 pH-dependent solubility

The pH-dependent solubility (S_{pH}) of ibuprofen was tested at 5 different pH values in the pH 2–8 range using BR buffer solutions. Additionally, the solubility of the fully ionized form was determined in 1M NaOH solution. The obtained results are summarized in Table 12, and the solubility/pH profile is shown in Figure 9.

Table 12. The pH-dependent equilibrium solubility of ibuprofen at 37 °C.

pH	**S_{pH} ± SD (µg/mL)[1]**	**logS_{pH} (mol/L)**
1.92	70.8 ± 3.0	-3.46
3.96	124 ± 13	-3.22
5.95	1910 ± 70	-2.03
7.17	32,033 ± 4135	-0.81
8.02	300,000 ± 6500	0.16
14	734,000 ± 30,500	0.55

[1] the results at each pH are the mean of 3 parallel measurements.

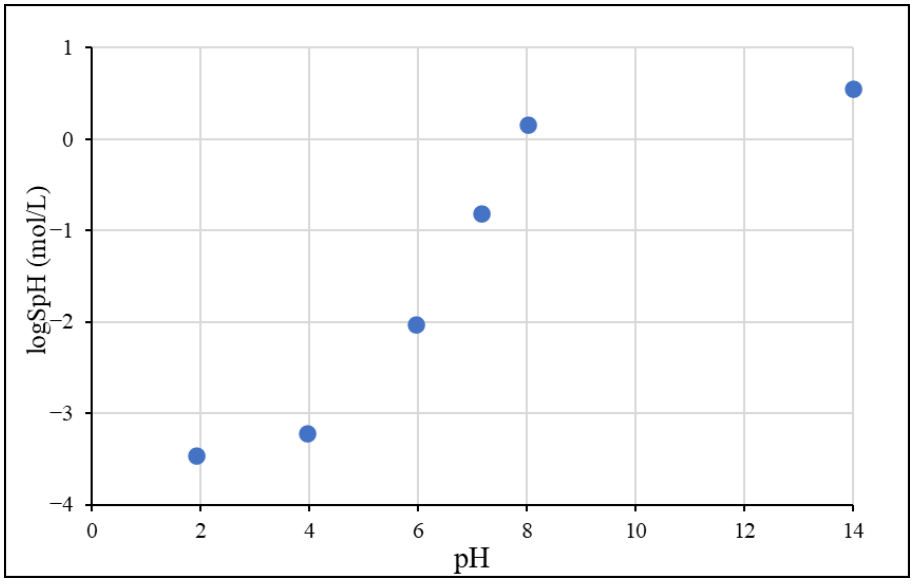

Figure 9. The solubility-pH profile of ibuprofen in Britton–Robinson buffers.

As expected from a weak acid compound with pK_a: 4.45, the solubility of ibuprofen is increasing according to the Henderson–Hasselbalch relationship in the pH 2–8 range and reaches a plateau at a higher pH due to the salt formation (108).

4.2.1.2 Solubility in biorelevant media

The equilibrium solubility values in biorelevant media are listed in Table 13.

Table 13. Equilibrium solubility of ibuprofen in biorelevant media at 37 °C.

Solvent	**S_{pH} ± SD (µg/mL)[1]**
FaSSGF blank, pH 1.6	56.3 ± 0.6
FaSSGF, pH 1.6	56.0 ± 0.5
FeSSGF-acetate, pH 4.5	194 ± 2
FeSSIF blank, pH 5.0	416 ± 12
FeSSIF, pH 5.0	2103 ± 56
FaSSIF blank, pH 6.5	2513 ± 15
FaSSIF, pH 6.5	3160 ± 31

[1] the results at each pH are the mean of 3 parallel measurements.

Solubility data in biorelevant media are in accordance with results measured in BR buffers, showing that the pH significantly affects the solubility of ibuprofen. Changing the pH from 1.6 to 4.5, 5.0, and 6.5 results in a 3.4-fold, 7.4-fold, and 44.6-fold increase in solubility, respectively. Pepsin has no effect on solubility at gastric pH. However, the solubilizing effect of natural surfactants of the small intestine further increases the solubility: FaSSIF/FaSSIF blank 1.3-fold; and FeSSIF/FeSSIF blank 5-fold. In the case of FeSSIF, a greater solubilizing effect was observed, which can be explained by the higher concentration of taurocholate and lecithin.

4.2.2 Dissolution results obtained by the USP method

The USP individual monograph of ibuprofen tablets suggests the dissolution of the formulations at pH 7.2 using USP II (Paddle) apparatus with 50 rpm (92). The average dissolution profiles of each formulation (1 × 200 mg dosage unit per vessel) are presented in Figure 10.

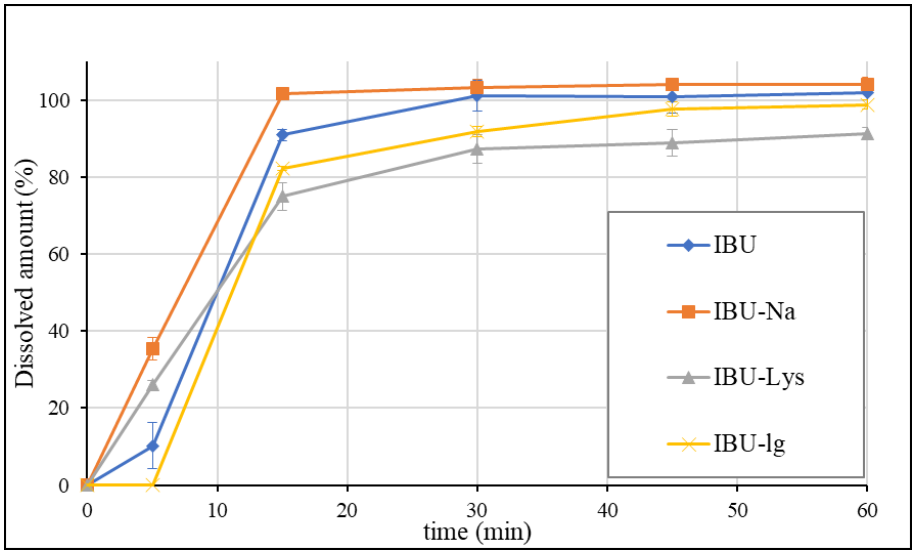

Figure 10. Dissolution results of ibuprofen formulations obtained by USP method.

According to the USP method, IBU and IBU-Na dissolved rapidly, as more than 85% of the drug substance dissolved in 15 min. The mean dissolved amount of IBU-lq was less than 85% in 15 min, however, its dissolution profile can be considered similar to IBU based on the calculated similarity factor (f_2 = 55). The dissolution rate of IBU-Lys was found to be significantly slower than that of IBU (f_2 = 37).

4.2.3 Dissolution results obtained by GIS method

Since it is advised to take 1 to 2 tablets of the 200 mg dose strength formulations, and 400 mg dose equivalents were administered in the published pharmacokinetic study, the *in vitro* dissolution of IBU 1 × 200 mg tablets *vs*. 2 × 200 mg tablets was compared in blank biorelevant media. The average dissolution profiles in each compartment are presented in Figure 11.

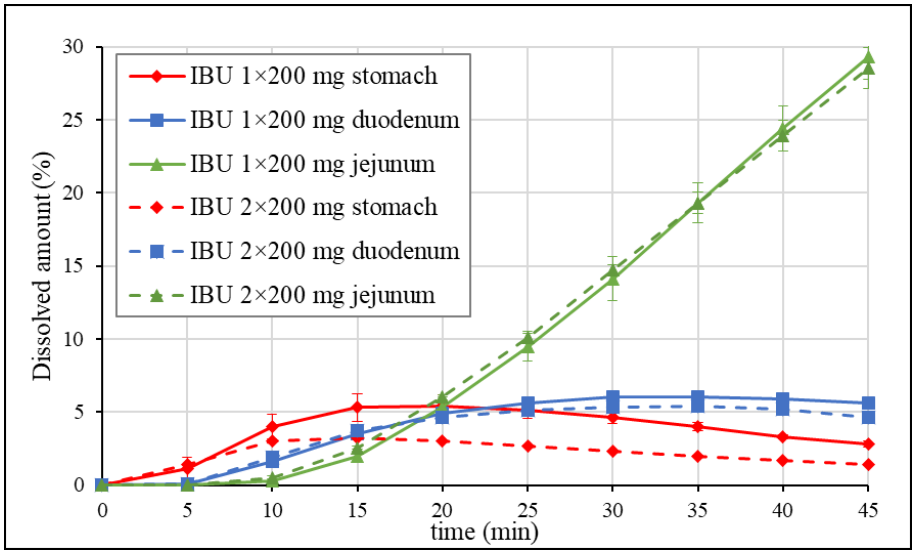

Figure 11. GIS dissolution of 1 *vs.* 2 tablets of IBU in blank biorelevant media.

Figure 11 shows that only a small amount of the API was dissolved in the stomach. Both dissolution profiles reached a maximum after 15 min, then a slow decrease was observed. The maximum of the curve represents the time when the gastric emptying rate of the API equals the dissolution rate. The difference in the percentage dissolved in the later stage of the test can be explained by reaching the equilibrium solubility limit (the different percentages belong to similar concentrations). The dissolution in the *duodenum* is determined by the composition of the suspension (dissolved API and suspended solid particles) entering the gastric chamber. Due to the higher equilibrium solubility in pH 6.5 blank FaSSIF (~2.5 mg/mL), the transferred solid particles are expected to dissolve. A dose-proportional dissolution profile was observed in this compartment and the *jejunum* as well. Since most of the absorption takes place in the upper small intestine, linear pharmacokinetics may be assumed based on the dissolution results.

The GIS dissolutions in blank biorelevant media were also performed with the other formulations. Figure 12 shows the obtained concentration profiles of 1 × 200 mg tablets in the gastric compartment.

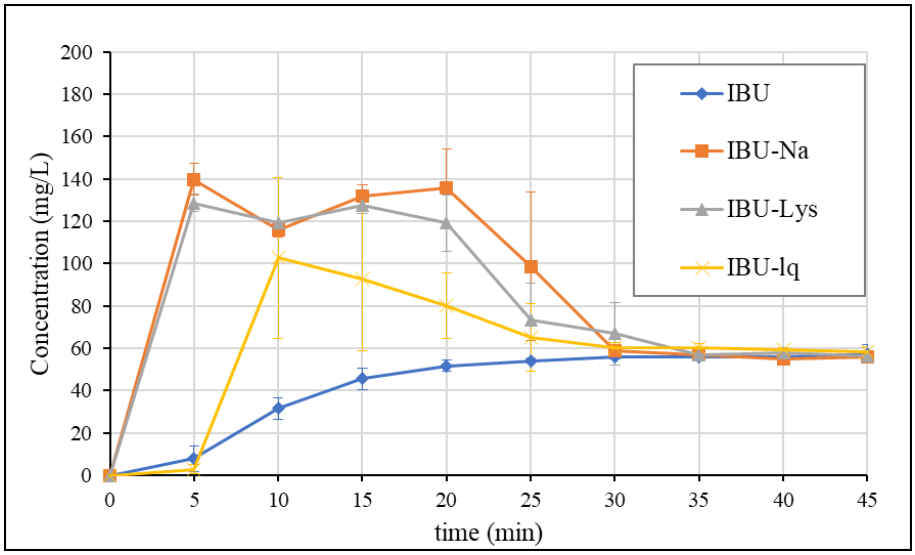

Figure 12. Gastric concentration of ibuprofen formulations in blank media.

The results show that rapid-release products form supersaturated solutions that precipitate over time. By the end of the measurement, the concentration of the API approaches the equilibrium solubility ($S_{BlankFaSSGF}$ = 56.3 mg/L) for all formulations. The degree of supersaturation is similar in the case of salt forms (IBU-Na: ~2.5× and IBU-Lys: ~2.3×) and somewhat less in the case of soft-gelatin capsules (IBU-lq: ~1.8×). The onset of release is delayed by ~5 min for IBU-lq, which is due to the disintegration of the capsule shell based on visual observation. The lack of supersaturation of IBU (free acid) suggests that the obtained result of rapid-release products is a consequence of the applied formulation techniques (salt formation or pre-dissolved API).

Figure 13 shows the dissolution curves in the *duodenal* chamber (a) compared to the first 45 min of the published clinical results (b) (93).

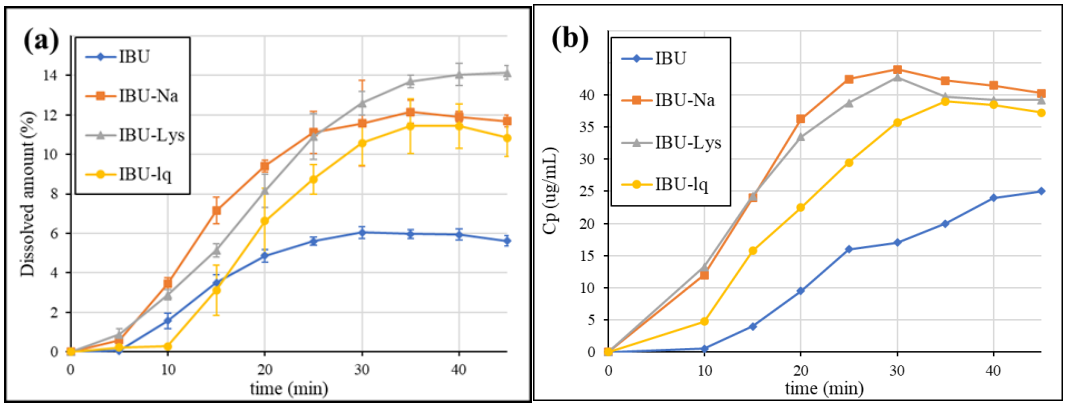

Figure 13. GIS *duodenal* dissolution in blank media (**a**) *vs.* fasting BA study results (**b**) (93).

Based on the dissolution profiles of Figure 13a, all three rapid-release products reach a higher maximum concentration compared to the standard IBU formulation, which is consistent with the *in vivo* results. The plateau of IBU-Lys is slightly higher than that of IBU-Na and IBU-lq, which, however, was not experienced *in vivo*. It should be noted, though, that the formulations containing ibuprofen-lysinate salt tested in the *in vitro* and *in vivo* studies came from different manufacturers. In the case of IBU-lq, the delay in the onset of dissolution experienced in the gastric chamber persists in the *duodenum* and also appears *in vivo*.

The absorption of the API is expected in the entire upper small intestine, therefore, the sum of dissolution in the *duodenum* and *jejunum* compartments may correlate with the *in vivo* performance of the formulations. Thus, the results were also evaluated in this way. In addition to the GIS dissolutions in blank biorelevant media, the tests were also carried out in biorelevant media containing biomolecules. The obtained results are compared in Figure 14.

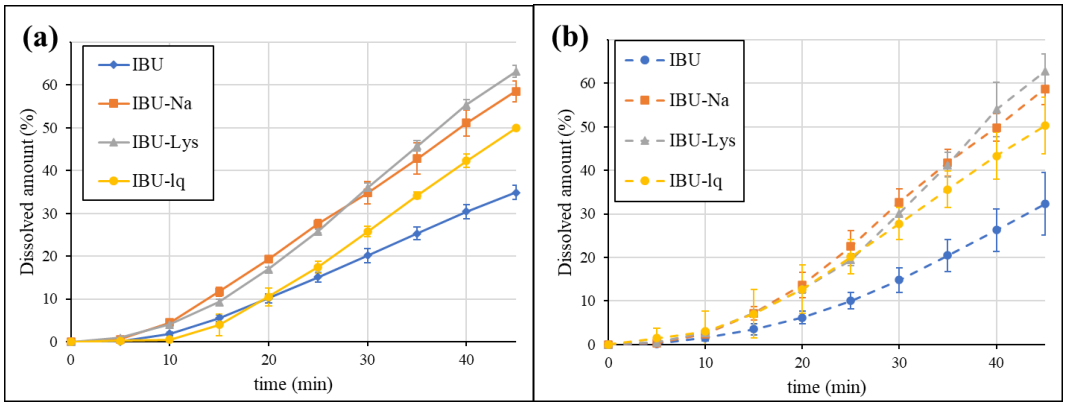

Figure 14. GIS sum of the amount dissolved in the *duodenum* and *jejunum* in blank biorelevant media (**a**) and biorelevant media (**b**).

According to Figure 14, regardless of the addition of biomolecules, the dissolution rate of rapid-release formulations is higher than that of IBU (conventional tablet). The applied natural surfactants have only a small effect on the dissolution, which indicates that the increase in solubility (owing to the ionization caused by the pH shift between the stomach and the *duodenum*) is sufficient to dissolve the entering suspension.

4.2.4 Establishment of the IVIVC model

A Level A IVIVC model was established to justify the predictivity of the GIS method. The correlation was built on the *in vitro* and *in vivo* data of IBU (internal batch),

and then the plasma profiles of the other formulations were simulated based on the dissolution results (external batches).

4.2.4.1 Analysis of *in vivo* data

The mean plasma concentrations of the fasting crossover pharmacokinetic study published by Legg *et al*. (93). were first digitized and then fitted using the PK module (Model 14: two-compartmental PK model) of the WinNonLin IVIVC Toolkit. The *in vivo* profiles are presented in Figure 15.

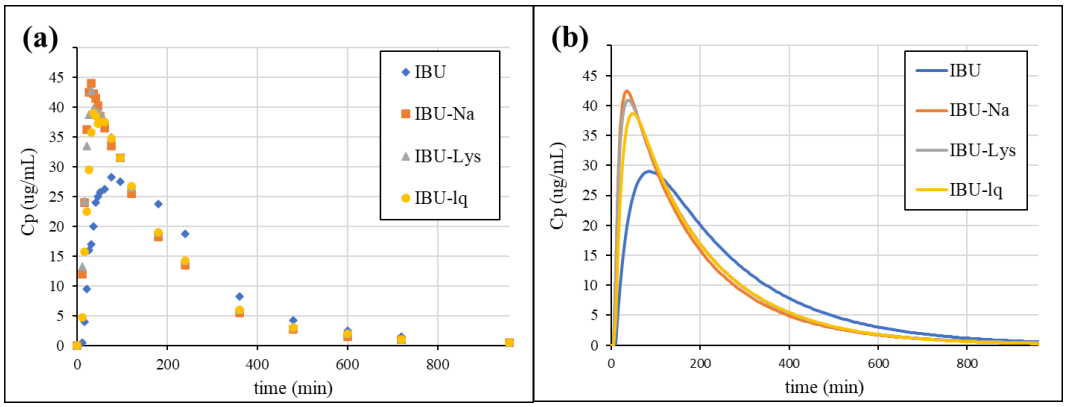

Figure 15. Published plasma concentration profiles (**a**) (93) vs. fitted curves (**b**).

The estimated parameters of the model describing the plasma profile of IBU were applied as input parameters to calculate the UIR function. The UIR function enabled the deconvolution of plasma concentration profiles, resulting in the fraction absorbed curves, which are shown in Figure 16.

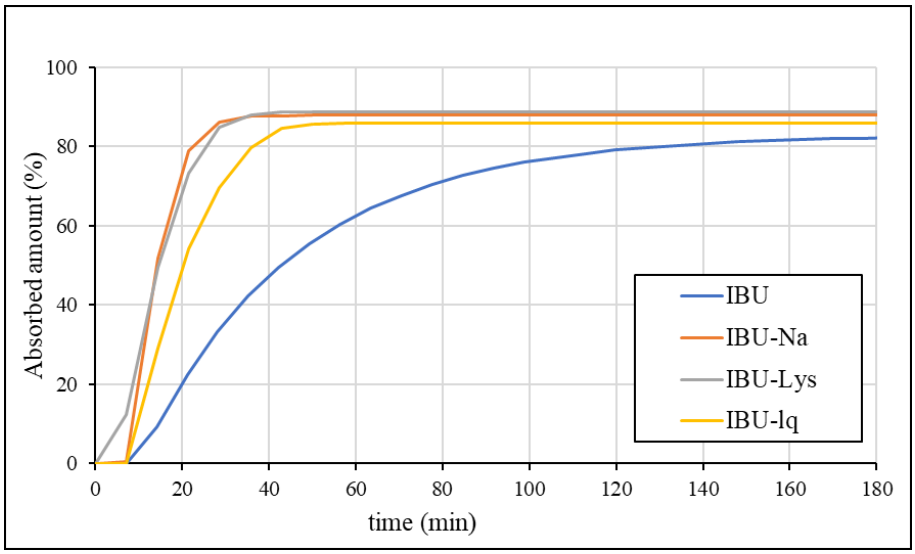

Figure 16. Absorption profiles obtained by deconvolution of clinical data (93).

4.2.4.2 Fitting of *in vitro* dissolution data

The sum of the amount dissolved curves in the *duodenum* and *jejunum* chambers of the GIS using blank biorelevant media was fitted with the Weibull function. The calculated dissolution profiles fitted to the average data are shown in Figure 17.

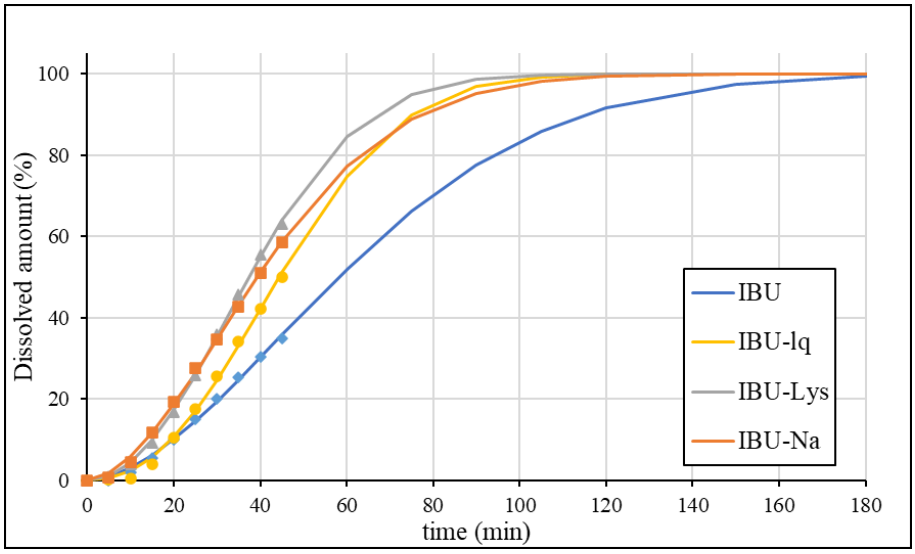

Figure 17. Fitted dissolution data using the Weibull function.

Based on Figure 17, the calculated curves fit the experimental data well, however, extrapolation is required to describe the whole dissolution profile. Therefore, this phase of the profiles has a greater uncertainty. Comparing the *in vitro* (Figure 17) and the *in vivo* (Figure 16) data, it appears that there is a slightly greater difference in the absorption rate between IBU and the rapid-release formulations than in the observed dissolution rate.

4.2.4.3 Correlation

The *in vitro* dissolution (from Weibull fitting) and the *in vivo* absorption (from deconvolution) of IBU were correlated using the Levy plot. The times corresponding to nominally the same dissolution (t_{Vitro}) and absorption (t_{Vivo}) were plotted, and the relationship was estimated using linear regression. The Levy plot is presented in Figure 18.

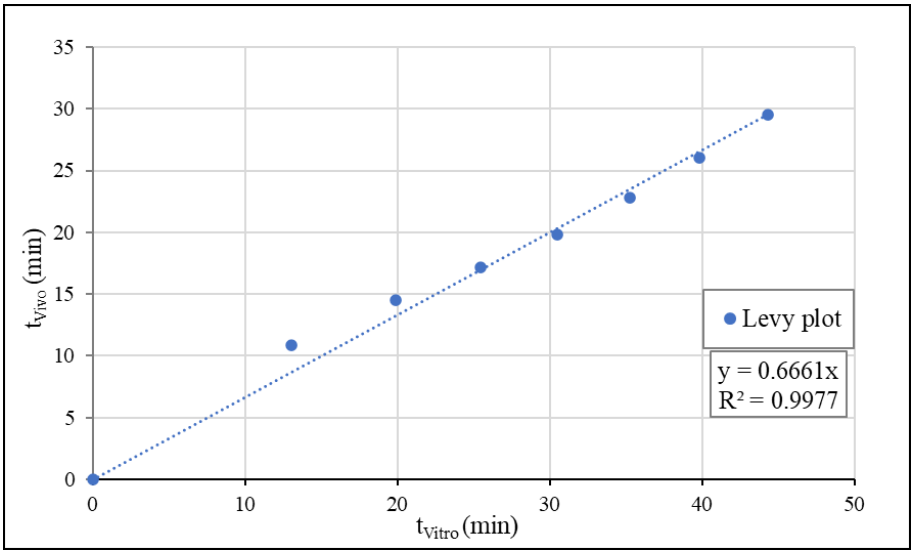

Figure 18. The Levy plot of IBU.

4.2.4.4 Simulation of plasma concentration profiles

Based on the estimated correlation, we calculated the absorption curves from the dissolution of the formulations and then convolved using the UIR function, which resulted in the plasma concentration profiles. The simulated profiles are shown in Figure 19.

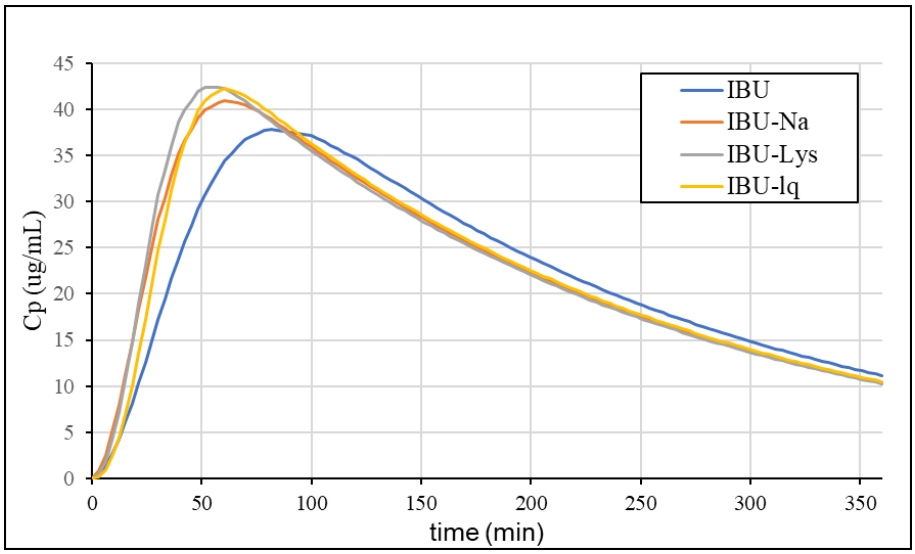

Figure 19. The simulated plasma concentration profiles of ibuprofen formulations.

The C_{max} values and their ratio compared to IBU from the statistical analysis of the individual plasma concentration profiles, the mean curves, and the IVIVC prediction are summarized in Table 14.

Table 14. Observed (93) *vs* predicted pharmacokinetic data of ibuprofen formulations.

	Clinical Data Statistical Analysis of Individual Profiles			Clinical Data Mean Plasma conc. Profiles		IVIVC Prediction from GIS Dissolution		
Formulation	**C_{max}**	**Ratio**	**t_{max}**	**C_{max}**	**Ratio**	**C_{max}**	**Ratio**	**t_{max}**
IBU	37.70	N/A	82.1	28.25	N/A	37.80	N/A	81.7
IBU-Na	47.00	1.25	35.2	44.00	1.56	41.00	1.09	60.5
IBU-Lys	49.90	1.32	35.1	42.75	1.51	42.40	1.12	61.4
IBU-lq	46.80	1.24	40.0	39.00	1.38	42.20	1.12	60.5

According to the summarized C_{max} values, the ratios predicted based on IVIVC correlate more with the statistical analysis of the individual profiles than with the ratio of the mean profiles. The statistical output of a clinical study provides the most relevant description of the differences between the formulations of interest, however, mean profiles are usually used for modelling purposes in the absence of published individual data. The simulation of the plasma concentration profiles using the established IVIVC model was able to predict the enhanced absorption rate of the rapid-dissolving ibuprofen formulations. Higher C_{max} and lower t_{max} values were obtained compared to IBU. For both parameters, the differences were slightly underestimated. The rapid-release formulations were found to be similar to each other, which is also consistent with the *in vivo* data.

4.3 Food effect prediction of Rivaroxaban 20 mg IR tablets

Rivaroxaban is a BCS Class II anti-coagulant drug, which is marketed as immediate release tablets. The reference formulation (Xarelto) is reported to exhibit dose-dependent food effects. More precisely, while the lower dose (10 mg) can be taken with or without food, the highest dose strength tablet (20 mg) should be taken with food to attain the positive food effect for oral absorption and systemic availability (109).

As a participant of an international collaborative research project that investigated the effect of food on the absorption of rivaroxaban, I was responsible for the establishment of a mathematical IVIVC model that predicts the plasma concentration profile of Xarelto

20 mg tablets in both fasted and fed conditions. The simulations were based on the results of a biorelevant USP IV flow-through cell dissolution method, which was developed previously in the project. The dissolution profiles obtained with the method modelling both fasted and fed conditions are included in the results to the extent necessary, however, the development and detailed description of the *in vitro* method was omitted due to industrial property protection reasons.

4.3.1 *In vitro* release profile of rivaroxaban in fasted and fed conditions

Figure 20 demonstrates the *in vitro* release profiles of the Xarelto 20 mg tablet in fasted and fed conditions using the USP IV flow-through cell dissolution method. After 30 min, *in vitro* release of Xarelto IR tablet in the fed state and fasted simulated gastric fluids were found to be 27.7 and 11.0%.

Thereafter, the fed and fasted simulated gastric fluid was replaced via simulated intestinal fluids without removing the Xarelto IR tablets. The *in vitro* release, and the time to 80% drug release was found to be the 360 and 210 min in case of fasted and fed state conditions, respectively. Furthermore, the f_2 (similarity factor) was also calculated and found to be 38. Thus, the release profile in the case of the fed condition was found to be significantly faster as compared to the fasted condition.

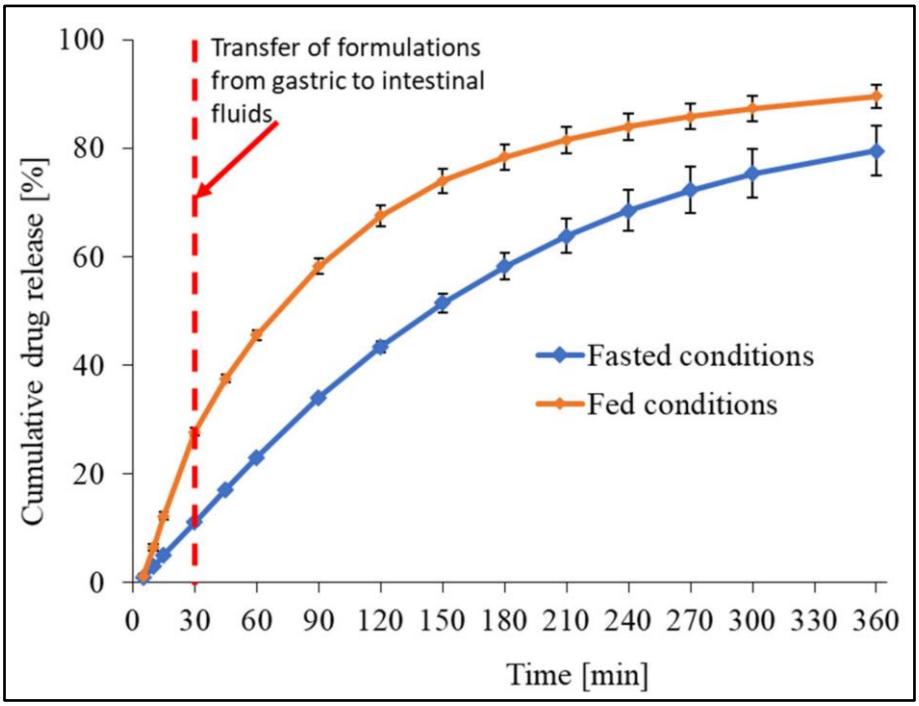

Figure 20. *In-vitro* release profile of rivaroxaban from Xarelto 20 mg IR tablet using USP IV apparatus.

4.3.2 Establishment of the IVIVC model

A Level A IVIVC model was established to predict the effect of food on the absorption of Xarelto 20 mg tablets. The correlation was built on the *in vitro* and *in vivo* data in the fasted state, and then the plasma profiles of the formulation were simulated based on the dissolution modelling fed conditions.

4.3.2.1 Dissolution curve fitting

The fasted state *in vitro* release profile of the Xarelto 20 mg tablet was fitted with the Weibull function. As evident from Figure 21, the predicted *in vitro* release or, more precisely, the fraction of API dissolved was found to be overlapping with the observed *in vitro* release data as a function of time, suggesting that the Weibull function was suitable to fit the dissolution data.

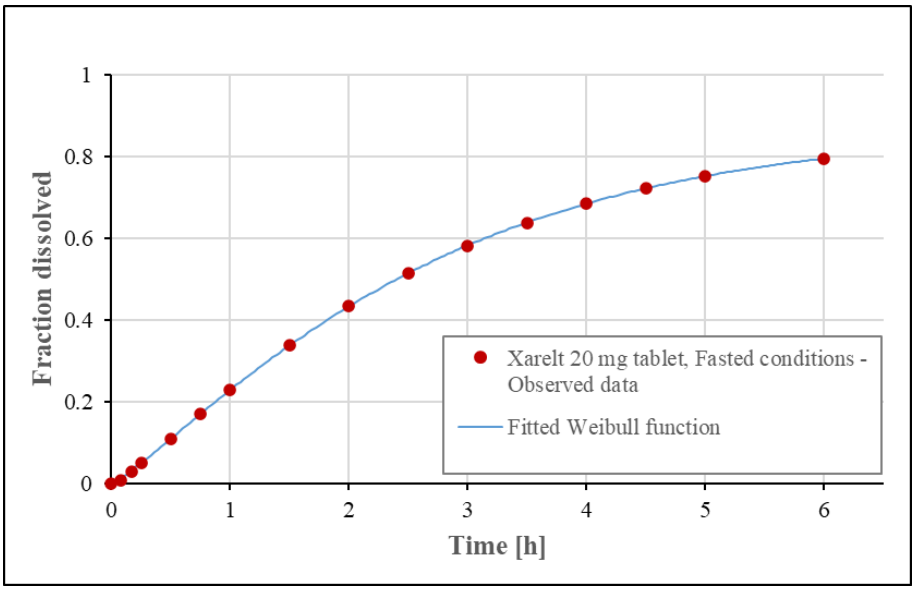

Figure 21. Observed *in vitro* profile *vs*. fitted curve of the Xarelto 20 mg tablet.

4.3.2.2 Analysis of *in vivo* data

The *in vivo* data of rivaroxaban 10 mg oral solution in the fasted condition were obtained by literature published by Kubitza *et al.* (94) (95) . The PK profile was fitted using the UIR function. The UIR function obtained was then used to deconvolve the *in vivo* PK profile of Xarelto 20 mg tablets in fasted condition, for the assessment of the *in vivo* absorption curve. The resulting fraction absorbed profile is presented in Figure 22.

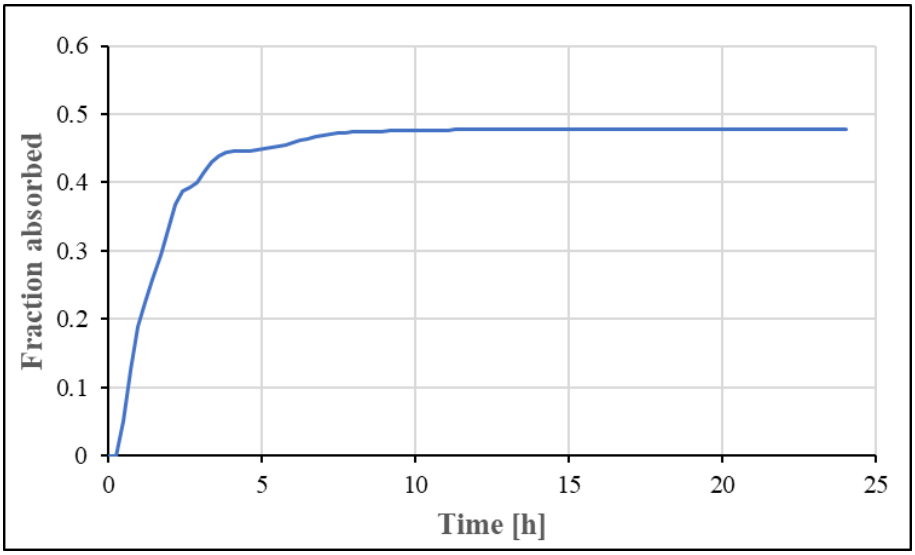

Figure 22. Fraction absorbed *vs* time profile of Xarelto 20 mg tablet (deconvolved from *in vivo*)

4.3.2.3 Correlation

The dissolved API fraction (obtained from the fitting of *in vitro* release profile) was then related with the absorbed *in vivo* fraction (obtained from the deconvolution of plasma concentration). As evident from Figure 23, the relationship was found to be linear.

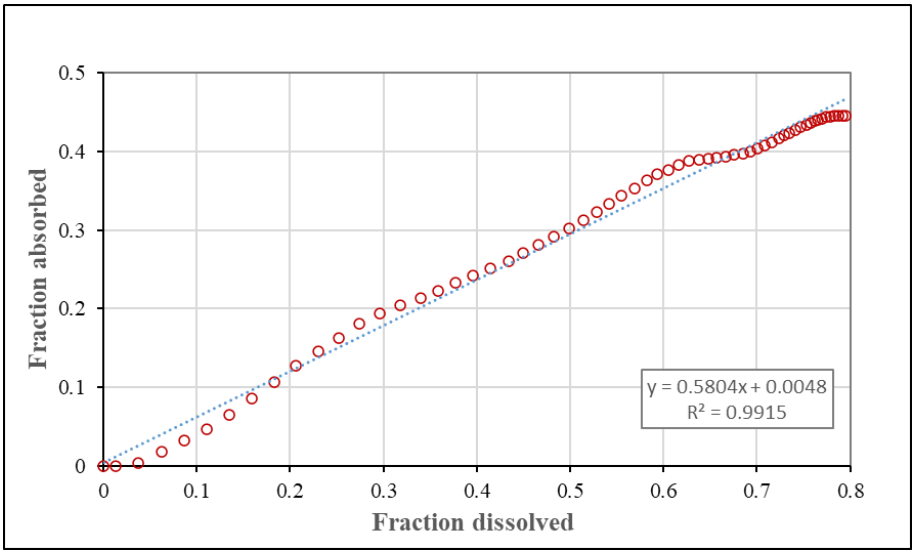

Figure 23. Fraction absorbed *vs* Fraction dissolved correlation of Xarelto 20 mg tablet.

4.3.2.4 Internal validation of the IVIVC method and prediction of food effect

In order to justify the validity of the established IVIVC model, the *in vivo* profile of the Xarelto 20 mg tablet in fasted conditions was simulated and compared to the

observed clinical data. Thereafter, the plasma concentration profile in fed state was also simulated and the expected effect of food on C_{max} and AUC values were evaluated. The resulting plasma profiles are presented in Figure 24 and the PK parameters are summarized in Table 15.

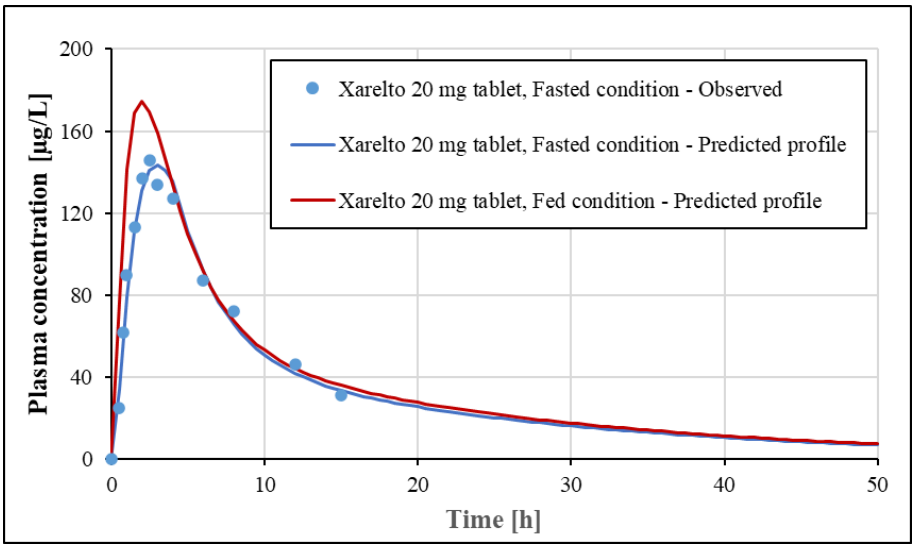

Figure 24. Predicted mean *in vivo* profiles of Xarelto 20 mg tablet using IVIVC model.

Table 15. Observed and predicted PK parameter values of Xarelto 20 mg tablet.

Formulation	**Parameter**	**Predicted**	**Observed***	**%Predicted Error**
Xarelto 20 mg tablet	AUC (µg*h/L)	1381.9	1361.1	1.5 %
Fasted condition	C_{max} (µg/L)	143.6	146.0	-1.7 %
Xarelto 20 mg tablet	AUC (µg*h/L)	1543.1	1750.2	13.4 %
Fed condition	C_{max} (µg/L)	174.6	241.0	38.1 %

**Literature data* (94) (95)

According to Table 15, the PK parameters of the internal batch could be predicted with a very low prediction error (≤ 2%) for both parameters, based on which the mathematical model can be considered correct. The predicted fed/fasted ratio of the of C_{max} (1.22) and AUC values (1.12) suggests a positive food effect, which, however, is less than expected based on the literature (1.65 for C_{max} and 1.29 for AUC).

5 DISCUSSION

5.1 Dissolution method for delayed-release dosage forms (ASA model compound)

5.1.1 USP method

The results (see Figure 5) are in agreement with the expectation for delayed-release formulations designed to release the active substance after the dosage form has reached the small intestine, therefore do not dissolve in acidic media. As the dosage form is placed in the higher-pH environment, the polymer coating dissolves, and the tablet core behaves similarly to immediate-release formulations. Based on the results of the acid phase, the gastro resistance of the enteric coating of each formulation was found to be appropriate. As the pH 6.8 used after the pH change is typical for the *jejunum* in fasted state, the formulations are expected to dissolve in this intestinal tract at the latest. However, in the absence of a medium modelling the *duodenal* pH, the results do not provide information about the exact site of the onset of the drug release. Although all formulations met the acceptance criteria, the *in vivo* studies performed did not demonstrate bioequivalence for either ASA Krka or Asactal tablets (97) (98). The latter also points out the importance of an appropriate biorelevant dissolution method during generic formulation development phase.

5.1.2 Dissolution results obtained by Biorelevant method with RGE

The examined products except Walgreens Aspirin are coated with methacrylic acid − ethyl acrylate 1:1 copolymer, with a dissolution pH threshold of 5.5, which is considered to target the onset of release to the *duodenum* (55). Interestingly, the results showed that the release of the drug substance is more typical in the later small intestinal phases (Figure 6). The dissolution profiles of the generic formulations were different (f_2 < 50) from that of the reference Aspirin Protect despite the same coating material, which indicated that other coating properties or the composition of the tablet core may also affect the release of the drug substance.

5.1.3 Dissolution results obtained by Biorelevant method with SGE

Compared to the RGE method, the disintegration of all formulations was found to be delayed, which is most probably due to the additional accumulation of protons on the

surface of enteric coatings during the longer acidic treatment. The results (Figure 7) suggest that the coating material of Walgreens Aspirin is more sensitive for the longer gastric residence than methacrylic acid−ethyl acrylate 1:1 copolymer. However, the unexpected performance of ASA Krka compared to other formulations with the same coating material requires further investigation.

5.1.4 Scanning electron microscopic images

Based on the thinner coating of Walgreens Aspirin compared to other formulations faster dissolution can be assumed, which correlates well with the results of the RGE method (Figure 6), where Walgreens Aspirin showed the highest dissolution rate. In case of all five methacrylic acid-ethyl acrylate coated formulations, the thickness of coating is between 50 and 75 μm which indicates that the differences in their dissolution profiles are most probably due to other factors that cannot be identified microscopically.

5.1.5 Relationship between the composition and *in vitro/in vivo* performance

A summary of the available clinical results provided by Krka and Actavis is presented in Table 16.

Table 16. *In vivo* results of available clinical studies in fasting conditions.

Test formulation	Reference formulation	Study ID	PK parameter	Test/ref ratio
ASA Krka 100 mg	Aspirin Protect 100 mg	091B13	C_{max}	1.16 (CI 0.92-1.48)
			AUC	1.16
Asactal 100 mg	Aspirin Protect 100 mg	1267/07	C_{max}	1.22 (CI 1.03-1.43)
			AUC	1.18 (CI 1.05-1.33)
		1321/07	C_{max}	0.76 (CI 0.65-0.89)
			AUC	0.98 (CI 0.88-1.10)
		1747/08	C_{max}	1.24 (CI 1.04-1.47)
			AUC	1.12 (CI 0.97-1.29)

Actavis has performed three *in vivo* studies in fasted state to compare Asactal and Aspirin Protect, each of which failed to demonstrate bioequivalence (98). Differences of C_{max} and AUC values were observed in both directions, most probably due to the high variability of the *in vivo* results. Comparing the *in vitro* dissolutions, Asactal dissolved

more slowly than all other formulations, which can be seen also with the USP method (Figure 5), but even more typical with the two alternatives of the new method (Figure 6 and 7). In case of both RGE and SGE, the onset of dissolution was similar to that of the reference Aspirin Protect formulation, which meets the expectations based on the qualitatively equivalent composition (see Table 8.) and similar thickness (see Table 10.) of the coatings. The slower rate of dissolution may be explained by the different performance of the tablet cores. As evident from Table 8, Asactal contains hydrophobic stearic acid, which may reduce the wettability of the tablet core compared to other formulations. Overall, based on the *in vitro* results, a lower bioavailability compared to the reference product is expected.

In case of ASA Krka, bioequivalence could not be demonstrated in the fasted state (97). The study showed 16% increase for both AUC and C_{max} compared to the reference product which is consistent with the results of the RGE method. RGE predicts an earlier release of the ASA Krka formulation compared to Aspirin Protect. The onset of release of ASA Krka in the SGE method is similar to that of Aspirin Protect. However, the slope of its dissolution curve is slightly higher, which generally predicts a higher C_{max} value as well. Based on Table 8, the applied plasticizer in the coating of this formulation is triacetin, while the reference product is formulated with triethyl citrate, which may explain the different onset of drug release observed with the RGE method. The slightly higher dissolution rate is probably related to the hydrophilic lactose monohydrate in the tablet core.

In case of Asatrin Teva Protect and ASA Protect Pharmavit there were no clinical data available, thus it was not possible to make *in vitro – in vivo* comparisons. The qualitative compositions of these formulations are equivalent to that of ASA Krka. Accordingly, their dissolution profiles were also similar with the RGE method. Interestingly, the onset of their drug release was less affected by the longer acidic pretreatment used in the SGE method. Based on this, both formulations are expected to have higher bioavailability compared to the reference product.

The dissolution of ASA Krka, Asatrin Teva Protect and ASA Protect Pharmavit demonstrate the importance of the plasticizer type in the onset of release and the wettability of the tablet core in the rate of dissolution of the tested formulations.

Walgreens Aspirin differs from other tested formulations in the type and thickness of coating, composition of the tablet core, and even in the labelled drug content. This difference occurs especially in case of the SGE method, which indicates that the applied coating material is more sensitive for the longer acidic treatment compared to methacrylic acid−ethyl acrylate 1:1 copolymer. The experienced reduction in the dissolution may be a risk of lower bioavailability in case of subjects with longer gastric residence times.

5.2 Multi-compartmental dissolution of immediate-release BCS IIa drugs (ibuprofen model compound)

5.2.1 Thermodynamic equilibrium solubility measurements

5.2.1.1 pH-dependent solubility

The measured equilibrium solubility in pH 2.0 BR buffer (logS = -3.46 mol/L) (Table 12) is consistent with the literature intrinsic solubility data ($logS_0$ = -3.62) (110). The small difference might be explained by the fact that the literature data were measured at 25 °C and that at pH 2.0, the molecules are mostly—but not totally—unionized; thus, a slightly higher value is expected compared to the intrinsic solubility. Below pH 5, the solubility is low, therefore, it can be assumed that from the formulations, the API can only partially dissolve in acidic gastric media.

5.2.1.2 Solubility in biorelevant media

Similar to the solubility results measured in BR buffers, low solubility is observed in fasted state gastric fluids (Table 13). Regardless of the presence of pepsin, ~7% of the 200 mg dose is expected to dissolve in a volume of 250 mL medium ($S_{FaSSGF\ blank}$ = 56,3 µg/mL, S_{FaSSGF} = 56.0 µg/mL). However, after emptying from the stomach, the solubility ($S_{FaSSIF\ blank}$ = 2513 µg/mL, S_{FaSSIF} = 3160 µg/mL) is sufficient to dissolve the entire quantity of drug substance, even when 2 × 200 mg tablets are administered together. The results indicate that in the case of ibuprofen (or BCS Class IIa drug substances in general), enhancement of the solubility in the fasted stomach may be crucial to achieve faster absorption. In fed conditions, the intestinal solubility (S_{FeSSIF} = 2103 µg/mL) is lower than the fasting results despite the higher surfactant concentration, due to the effect of pH, which is greater than that of surfactants. These results may explain the lower absorption rate (higher t_{max} and lower C_{max}) observed in the fed state during clinical trials (93).

5.2.2 Dissolution results obtained by the USP method

Since, based on the solubility of the API, the dissolution of the formulation is expected mostly in the small intestine, the USP method requires the use of pH 7.2 phosphate buffer. In this medium, sink condition criterium is fulfilled, thus no difference appeared in the dissolution of the different forms of the drug substance. The only statistically different profile was that of IBU-Lys, which is probably more related to the formulation technology than to the properties of the active ingredient. This difference is expected to be irrelevant *in vivo* due to disintegration of the tablet in the stomach. The observation does not correlate with the clinical results either, as significantly faster absorption was measured compared to the standard IBU. Overall, the USP method was unable to discriminate between rapid-release and standard ibuprofen formulations (Figure 10).

5.2.3 Dissolution results obtained by the GIS method

As a first step of the GIS measurements, the dissolution profiles of 1 × 200 mg *vs.* 2 × 200 mg IBU tablets were compared (Figure 11). This was necessary because 2 × 200 mg tablets were administered during the published clinical trials, however, the simultaneous dissolution of two tablets, especially in small volume causes several difficulties (such as cone formation or clogging of the peristaltic pump) in the *in vitro* measurement. Since a dose-proportional drug release was observed in the *duodenal* and *jejunal* compartments (relevant for absorption), further experiments were performed by dissolving one tablet at a time.

During the measurement in blank biorelevant media, significant supersaturation of the rapid-release formulations was observed in the gastric compartment (Figure 12). Although absorption is not expected in the stomach, differences in the gastric dissolution may impact the processes taking place in the small intestine. As expected, the supersaturation resulted in advanced dissolution in the *duodenum* and *jejunum* as well. The visual similarity between *duodenal* dissolution profiles and plasma concentrations (shown in Figure 13) suggests that the experienced phenomenon is biologically relevant and may be crucial for the predictivity of the method. At the same time, it clearly shows the advantage of the multi-compartmental design.

In order to study the effect of natural surfactants, the formulations were dissolved in full biorelevant media as well. The results showed a good agreement with those

observed in blank biorelevant media (Figure 14). This indicates that the small intestinal dissolution of ibuprofen (and BCS Class IIa drugs in general) in fasted conditions is much more influenced by the pH change (i.e., ionization) than by the presence of biomolecules (solubilizing effect). These findings are in agreement with previous study results (111). The simplification of biorelevant buffers by omitting the addition of biomolecules may be a cost-effective way of the GIS analysis without affecting the predictivity of the method.

5.2.4 Establishment of the IVIVC model

Direct comparison of the dissolution curves is a frequently used, simple approach to compare the developed formulation with the reference product. However, when the goal is to achieve enhanced bioavailability, the simulation of the plasma concentration profile may be more informative. The IVIVC model was developed using the *in vivo* data of the conventional IBU tablets, which had been the reference for the development of rapid-release formulations before. The limited amount of published *in vivo* data is a common difficulty, however, the mean plasma profile of the reference product is in many cases available without conducting clinical trials. Despite the slight underestimation of the *in vivo* differences, the model using the sum of *duodenal* and *jejunal* dissolution was able to predict the enhanced bioavailability of rapid-release formulation. The simulation served as a useful additional tool for dissolution studies.

5.3 Food effect prediction of Rivaroxaban 20 mg IR tablets

Comparing the biorelevant USP IV dissolution of Xarelto 20 mg tablets in fasted and fed state, an enhanced dissolution rate was observed in fed conditions, which is probably due to the higher solubility of the BCS Class II rivaroxaban in fed media (containing a higher concentration of surfactants). Based on the calculated similarity factor (f_2 =38), the difference is statistically significant, i.e., the *in vitro* method was able to predict the presence of food interaction. To evaluate the effect of different dissolution rates on *in vivo* absorption, a Level A IVIVC model was developed, and the plasma concentration profiles were simulated.

According to Table 15, the developed IVIVC model relying on the fasted *in vitro* dissolution profiles was able to predict the *in vivo* performance of the internal batch (Xarelto 20 mg tablet in fasted conditions) with a very low prediction error (< 2% for

both C_{max} and AUC). The latter confirms the validity of the established model. The predicted C_{max} and AUC values suggested 22% and 12% increase in the fed state which was less than that of the literature data (65% for C_{max} and 29% for AUC). The difference between the predicted food effect compared to the reported data may be a result of slight underestimation of dissolution differences. At the same time, minor changes in the formulation may have occurred in the time between the published clinical trials and the *in vitro* study of the commercially available product, which may explain the observed difference.

6 CONCLUSIONS

The *in vitro* dissolution is the primary method to assess the *in vivo* performance of both generic and value-added generic formulations. In case of drug products with dissolution-controlled absorption, the existence of a predictive biorelevant dissolution method is essential during the formulation development phase. Supplementing the *in vitro* method with an appropriate IVIVC model significantly reduces the risk of bioequivalence studies.

My first objective was to provide a dissolution method for a better understanding of the *in vivo* performance of delayed-release formulations. Two alternatives of a biorelevant dissolution method – differing in the length of acidic treatment – were successfully developed, modelling the conditions of the stomach and the small intestine in fasted state. Biorelevant molarity and volume of dissolution medium as well as gradual pH change between each tract, were also considered. Six commercially available low-dose enteric coated ASA formulations were tested with the USP method and the two versions of the novel dissolution method. Despite of the difficulties of demonstrating bioequivalence, all formulations met the acceptance criteria specified in the individual USP monograph of Aspirin Delayed-Release Tablets, which pointed out the importance of an appropriate biorelevant dissolution method. Comparing the compositions of the formulations with the *in vitro* results, the new method, especially with rapid gastric emptying proved to be discriminative. The different plasticizers applied in the coating process appeared to affect the onset of dissolution, while the hydrophilicity of the inactive ingredients affected the dissolution rate by altering the wettability of the tablet cores. Based on the increased discriminating power of the new dissolution method, and the comparison of the *in vitro* and the limited available bioequivalence data, an enhanced *in vivo* predictivity can also be assumed. Consequently, the new method can be a good alternative for reaching a better understanding of the post gastric behaviour of enteric-coated formulations which is essential to get appropriate information on intestinal release and bioavailability.

The advanced *in vivo* predictivity of the GIS dissolution system for BCS Class IIb and Class IIc compounds has previously been studied in the literature. In the second part of my study, the better *in vivo* predictivity of the method was also demonstrated for immediate release formulations containing BCS Class IIa compounds, to which less

attention was paid before. The key factors resulting in the superiority of the GIS compared to the USP method were the multi-compartmental design, the biorelevant fluid volumes and the pH change, which enabled the modelling of the complex mechanism behind the advanced absorption of rapid dissolving ibuprofen formulations. It was found that pre-dissolving or salt formation of poorly soluble acidic compounds leads to temporary supersaturation in an acidic medium, which, thanks to the continuous gastric emptying, affects the resulting concentration in the upper small intestine as well. Both dissolution and solubility results indicated that the role of gastrointestinal pH conditions in the *in vivo* dissolution of poorly soluble, acidic drug substances is more significant compared to the solubilizing effect of biomolecules. In conclusion, the multi-compartmental GIS model using blank biorelevant media was found efficient in predicting the *in vivo* performance of ibuprofen formulations. Predicting the *in vivo* behaviour and providing a better understanding of the absorption process can both contribute to the successful development of enhanced bioavailability formulations containing BCS Class IIa drugs.

The last part of my study focused on the establishment of a Level A IVIVC method, that models the effect of food on absorption of Rivaroxaban 20 mg IR tablets, relying on the biorelevant *in vitro* dissolution in fasted and fed media using USP IV apparatus. The model successfully demonstrated a significant food effect increasing the C_{max} and AUC of rivaroxaban, which could be due to higher solubility in fed conditions. The developed model can contribute to the development and optimization of the formulation parameters, mainly in the early-stage development phase, reducing preclinical and clinical time and cost.

7 SUMMARY

A novel *in vitro* dissolution method was developed with the aim of enabling a better understanding of the post-gastric behaviour of enteric-coated formulations, and thus better prediction of *in vivo* bioavailability. First, the physiological conditions at each tract of the gastrointestinal system in fasted state were determined on the basis of literature data. Then, the theoretical (time-varying) conditions were successfully modelled by adding different phosphate buffer solutions to the initial 0.01M HCl in a "Chinese small volume" apparatus using a multistep procedure. Because of the high variability of gastric residence time, two versions of the method (RGE and SGE) were tested, differing in the length of acid treatment (20 min *vs* 120 min). The improved discriminatory power of the new method compared to the USP method was demonstrated by investigating six commercially available low-dose ASA formulations. The results pointed out the influence of the plasticizer used in the coating on the onset of drug release, while the rate of dissolution was determined by the wettability of the excipients used in the tablet cores. The observations may explain the negative bioequivalence outcome of ASA Krka and Asactal formulations i.e. advanced predictivity of the new method may also be assumed.

The multi-compartmental Gastrointestinal Simulator was implemented to test its applicability to BCS Class IIa compounds. The method using blank biorelevant media was able to differentiate between rapid-release and conventional-release formulations. The study showed that either the salt formation or pre-dissolving the API in a lipid-based solution resulted in temporary supersaturation in the stomach, which affected the dissolution in the later compartments as well. Moreover, a Level A IVIVC model was developed, and the plasma concentrations were simulated based on the *in vitro* dissolution in the *duodenum* and *jejunum* compartments. Similar to the literature, significant increases in C_{max} values were observed.

An IVIVC model was also established to predict the effect of food on Rivaroxaban 20 mg formulations. The correlation was built between the published *in vivo* fasting clinical results and the measured *in vitro* dissolution in fasted biorelevant media using USP IV apparatus. Then, the fed plasma concentration profile was predicted based on the *in vitro* dissolution using the same apparatus with fed biorelevant media. The predicted food-effect, especially for C_{max} was significant but below the reported literature results.

8 REFERENCES

1. EMA. ema.europa.eu. [Online].; 2023. Available from: https://www.ema.europa.eu/en/glossary/generic-medicine.

2. FDA. Office of Generic Drugs 2022 Annual Report. ; 2023.

3. The Business Research Company. Generic Pharmaceuticals Global Market Report. 2023.

4. Lionberger RA. FDA Critical Path Initiatives: Opportunities for Generic Drug Development. AAPS J. 2008; 10: 103-109.

5. Stegemann S, Leveiller F, Franchi D, de Jong H, Lindén H. When poor solubility becomes an issue: From early stage to prrof of concept. Eur J Pharm Sci. 2007; 31(5): 249-261.

6. Lipinski CA. Drug-like properties and the causes of poor solubility and poor permeability. J Pharmacol Toxicol Methods. 2000; 44(1): 235-249.

7. Kalepu S, Nekkanti V. Insoluble drug delivery strategies: review of recent advances and business aspects. Acta Pharmaceutica Sinica B. 2015; 5(5): 442-453.

8. Krajcar D, Grabnar I, Jereb R, Legen I, Opara J. Predictive Potential of BCS and Pharmacokinetic Parameters on Study Outcome: Analysis of 198 In Vivo Bioequivalence Studies. Eur J Drug Metab Pharmacokinet. 2023; 48(3): 241-255.

9. Ramirez E, Laosa O, Guerra P, Duque B, Mosquera B, Borobia AM, et al. Acceptability and characteristics of 124 human bioequivalence studies with active substances classified according to the Biopharmaceutic Classification System. Br J Clin Pharmacol. 2010; 70(5): 694-702.

10. Cristofoletti R, Chiann C, Dressman JB, Storpiritis S. A comparative analysis of BCS and BDDCS: A cross-section survey with 500 mioequivalence studies. J Pharm Sci. 2013; 102(9): 3136-44.

11. Petykó Z, Kaló Z, Espin J, Podrazilová K, Tesaf T, Maniadakis N, et al. Development of a core evaluation framework of value-added medicines: report 1 on methodology and findings. Cost Effectiveness and Resource Allocation. 2021; 19(1): 57.

12. Stoller C, Krahenbuhl S, Voiculescu EM. Value-added medicines: how repurposed medicines bring value to patients and pharmacists. Generics and Biosimilars Initiative Journal. 2017; 6(3): 141-146.

13. Committee for Medicinal Products for Human use. Guideline on the investigation of bioequivalence. European Medicines Agency. 2010.

14. FDA. Bioequivalence studies with pharmacokinetic endpoints for drugs submitted under ANDA. U.S. Food and Drug Administration. 2013.

15. Evans DF, Pye G, Bramley R, Clark AG, Dyson TJ, Hardcastle JD. Measurement of gastrointestinal pH profiles in normal ambulant human subjects. Gut. 1988; 29(8): 1035-41.

16. Fallingborg J, Christensen LA, Ingeman-Nielsen M, Jacobsen BA, Abildgaard K, Rasmussen HH. pH-profile and regional transit times of the normal gut measured by a raditelemetry device. Aliment. Pharmacol. Therap. 1989; 3(6): 605-613.

17. Ibekve VC, Fadda HM, McConnell EL, Khela MK, Evans DF, Basit AW. Interplay between intestinal pH, transit time and feed status on the in vivo performance of pH responsive Ileo-colonic release systems. Pharm Res. 2008; 25(8): 1828-35.

18. van der Schaar P, Dijksman J, Broekhuinzen-de Gast H, Shimizu J, van Lelyveld N, Zou H, et al. A novel ingestible electronic drug delivery and monitoring device. Gastointest Endosc. 2013; 78(3): 520-8.

19. Koziolek M, Grimm M, Becker D, Iordanov V, Zou H, Shimizu J, et al. Investigation of pH and temperature profiles in the GI tract of fasted human subjects using the Intellicap System. J Pharm Sci. 2015; 104(9): 2855-63.

20. Schneider F, Grimm M, Koziolek M, Modess C, Dokter A, Roustom T, et al. Resolving the physiological conditions in bioavailability and bioequivalence studies: comparison of fasted and fed state. European Journal of Pharmaceutics and Biopharmaceutics. 2016; 108: 214-219.

21. Hasler W. Duodenal motility. In Encyclopedia of Gastroenterology.: Academic Press; 2003. p. 636-641.

22. Locatelli I, Nagelj Kovai N, Mrhar A, Bogataj M. Gastric emptying of non-disintegrating solid drug delivery systems in fasted state: relevance to drug dissolution. Expert Opin Drug Deliv. 2010; 7: 967-76.

23. Minami M, McCallum R. The physiology and pathophysiology of gastric emptying in humans. Gastroenterology. 1984; 86(6): 1592-610.

24. Scratchered T, Grundy D. The physiology of intestinal motility and secretion. Br J Anaesth. 1984; 56: 3.

25. Caride VJ, Troncale FJ, Buddoura W, Winchenbach K, McCallum RW. Scintigraphic determination of small intestinal transit time: comparison with the hydrogen breath technique. Gastroenterology. 1984; 86(4): 714-20.

26. Read NW. Small bowel transit of food in man: measurement regulation and possible importance. Scand J Gastroenterol. 1984; 96: 77-85.

27. Read NW, Cammack J, Edwards C, Holgate AM, Cann PA, Brown C. Is the transit time of a meal through the small intestine related to the rate at which it leaves the stomach? Gut. 1982; 23(10): 824-8.

28. Jian R, Najean Y, Bernier JJ. Measurement of intestinal progression of a meal and its residues in normal subjects and patients with functional diarrhoea by a dual isotope technique. Gut. 1984; 25(7): 728-31.

29. Malagelada JR, Robertson JS, Brown ML, Remington M, Duenes JA, Thomforde GM. Intestinal transit of solid and liquid components of a meal in health. Gastroenterology. 1984; 87(6): 1255-63.

30. Davis SS, Hardy JG, Fara JW. Transit of pharmaceutical dosage forms through the small intestine. Gut. 1986; 27(8): 886-892.

31. Maurer JM, Schellekens RCA, van Rieke HM, Wanke C, Iordanov V, Stellaard F, et al. Gastrointestinal pH and transit time profiling in healthy volunteers using the Intellicap system confirms ileo-colonic release of colopulse tablets. Plos One. 2015; 10(7).

32. Sutton SC. Role of physiological intestinal water in oral absorption. AAPS J. 2009; 11(2): 277-285.

33. Mudie D, Murray K, Hoad C, Pritchard S, Garnett M, Amidon G, et al. Quantification of gastrointestinal liquid volumes and distribution following a 240mL dose of water in the fasted state. Mol Pharm. 2014; 11(9): 3039-47.

34. Schiller C, Fröhlich CP, Giessmann T, Siegmund W, Mönnikes H, Hosten N, et al. Intestinal fluid volumes and transit of dosage forms as assessed by magnetic resonance imaging. Aliment Pharmacol Ther. 2005; 22(10): 971-979.

35. Lambert R, Martin F, Vagne M. Relationship between hydrogen ion and pepsin concentration in human gastric secretion. Digestion. 1968; 1(2): 65-77.

36. Efentakis M, Dressman JB. Gastric juice as a dissolution medium: surface tension and pH. Eur. J. Drug Metab. Pharmacokin. 1998; 23: 97-102.

37. Rhodes J, Barnardo D, Phillips S, Rovelstad R, Hofmann A. Increased reflux of bile into the stomach in patients with gastric ulcer. Gastroenterology. 1969; 57(3): 241-252.

38. Ozturk SS, Palsson BO, Dressman JB. Dissolution of ionizable drugs in buffered and unbuffered solutions. Pharm Res. 1988; 5(5): 550-565.

39. van Berge Henegouwen GP, Hofmann AF. Nocturnal gallbladder storage and emptying in gallstone patients and healthy subjects. Gastroenterology. 1978; 75(5): 879-885.

40. Tangerman A, vanSchalk A, van der Hoek EW. Analysis of conjugated and unconjugated bile acids in serum and jejunal fluid of normal subjects. Clin. Chim. Acta. 1986; 159(2): 123-132.

41. Peeters TL, Vantrappen G, Janssens J. Bile acid output and theinterdigestive migrating motor complex in normals and in cholecystectomy patients. Gastroenterology. 1980; 79(4): 678-681.

42. Marzio L, Neri M, Capone F, Di Felice F, De Angelis C, Mezzeti A, et al. Gallbladder contraction and its relationship to interdigestive duodenal motor activity in normal human subjects. Dig. Dis. Sci. 1988; 33(5): 540-544.

43. Dressman JB, Amidon GL, Reppas C, Shah VP. Dissolution testing as a prognostic tool for oral drug absorption: Immediate release dosage forms. Pharmaceutical Research. 1998; 15(1): 11-22.

44. Shah V, Amidon G. G.L. Amidon, H. Lennernas, V.P. Shah, and J.R. Crison. A Theoretical Basis for a Biopharmaceutic Drug Classification: The Correlation of In Vitro Drug Product Dissolution and In Vivo Bioavailability, Pharm Res 12, 413–420, 1995—Backstory of BCS. The AAPS Journal. 2014; 16: 894-898.

45. Yang Y, Zhao Y, Yu A, Sun D, Yu L. Oral drug absorption: Evaluation and prediction. In Developing solid oral dosage forms.: Elsevier; 2017. p. 331-354.

46. ICH M9 guideline on biopharmaceutics classification system-based biowaivers. European Medicines Agency. 2020.

47. Amidon G, Lennernas H, Shah V, Crison J. A theoretical basis for a biopharmaceutic drug classification: The correlation of in vitro drug product dissolution and bioavailability. Pharm Res. 1995; 12(3): 413-420.

48. Tsume Y, Mudie DM, Langguth P, Amidon GE, Amidon GL. The Biopharmaceutics Classification System: Subclasses for In Vivo Predictive Dissolution (IPD) Methodology and IVIVC. Eur J Pharm Sci. 2014; 57: 152-63.

49. Shargel L, Wu-Pong S, Yu AC. Modified-Release Drug Products. In Applied Biopharmaceutics & Pharmacokinetics.: McGraw Hill; 2012. p. Chapter 17.

50. FDA. GFI, Extended release dosage forms: Development, evaluation and application of in vitro/in vivo correlations. In. U.S. Department of Health and Human Services: Center for Drug Evaluation and Research (CDER); 1997.

51. FDA. SUPAC-MR: Modified Release Solid Oral Dosage Forms Scale-Up and Postapproval Changes: Chemistry, Manufacturing, and Controls; In Vitro Dissolution Testing and In Vivo Bioequivalence Documentation. In. U.S. Department of Health and Human Services: Center for Drug Evaluation and Research (CDER); 1997.

52. Gao Z, Ngo C, Ye W, Rodriguez JD, Keire D, Sun D, et al. Effects of Dissolution Medium pH and Simulated Gastrointestinal Contraction on Drug Release From Nifedipine Extended-Release Tablets. J Pharm Sci. 2019; 108(3): 1189-1194.

53. Mohylyuk V, Goldoozian S, Andrews GP, Dashevskiy A. IVIVC for Extended Release Hydrophilic Matrix Tablets in Consideration of Biorelevant Mechanical Stress. Pharmaceutical Research. 2020; 37(11): 227.

54. Gao Z, Cao LNY, Liu X, Tian L, Rodriguez JD. An In Vitro Dissolution Method for Testing Extended Release Tablets Under Mechanical Compression and Sample Friction. J Pharm Sci. 2022; 111(6): 1652-1658.

55. Al-Gousous J, Tsume Y, Fu M, Salem I, Langguth P. Unpredictable performance of pH-dependent coatings accentuates the need for improved predictive in vitro test systems. Mol Pharm. 2017; 14(12): 4209-19.

56. Agyilirah G, Banker G. Polymers for enteric coating applications. In Polymers for controlled drug delivery. Boca Raton: CRC Press; 1991. p. 39-66.

57. Agilent Dissolution Seminar Series. [Online]. [cited 2023 january 10. Available from: https://www.agilent.com/cs/library/flyers/Public/Dissolution_Seminar_Series.pdf.

58. USP. Chapter 711 - Dissolution. The United States Pharmacopoeial Convention. 2011.

59. Ph. Eur. 2.9.3 Dissolution test for solid oral dosage forms. European Pharmacopoeia 10.0. 2016.

60. JP. 6.10 Dissolution Test. Japansese Pharmacopoeia 17th Edition. 2016.

61. ChP. Appendix X - Dissolution Test. Chinese Pharmacopoeia. 2010.

62. Ph. Eur. 5.17.1 Recommendations on dissolution testing. European Pharmacopoeia 10.0. 2016.

63. Vertzoni M, Dressman JB, Butler J, Hempenstall J, Reppas C. Simulation of fasting gastric conditions and its importance for the in vivo dissolution of lpophilic compounds. European Journal of Pharmaceutics and Biopharmaceutics. 2005; 60: 413-417.

64. Jantarid E, Janssen N, Reppas C, Dressman JB. Dissolution media simulating conditions in the proximal human gastrointestinal tract: An update. Pharm Res. 2008; 25(7): 1663-1676.

65. Galia E, Nicolaides E, Hörter D, Löbenberg R, Reppas C, Dressman JB. Evaluation of various dissolution media for predicting in vivo performance of class i and ii drugs. Pharm Res. 1998; 15: 698-705.

66. Mithani SD, Bakatselou V, TenHoor CN, Dressman JB. Estimation of the increase in solubility of drugs as a function of bile salt concentration. Pharm Res. 1996; 13: 163-167.

67. Vertzoni M, Fotaki N., Kostewicz E, Stippler E, Leuner C, Nicolaides E, et al. Dissolution media simulating the intralumenal composition of the small intestine: physiological issues and practical aspects. J Pharm Pharmacol. 2004; 56(4): 453-462.

68. Biorelevant.com. [Online]. [cited 2023 January 15. Available from: https://biorelevant.com/#media_prep_tool_tab.

69. Kostewicz ES, Abrahamsson B, Brewster M, Brouwers J, Butler J, Carlert S, et al. In vitro models for the prediction of in vivo performance oral dosage forms. Eur. J. Pharm. Sci. 2014; 57: 342-366.

70. Vatier J, Lionnet F, Vitré MT, Mignon M. A model of an 'artificial stomach' for assessing the characteristics of an antacid. Aliment. Pharmacol. Therap. 1988; 2: 461-470.

71. Vatier J, Malikova-Sekera E, Vitre M, Mignon M. An artificial stomach-duodenum model for the in-vitro evaluation of antacids. Aliment. Pharmacol. Ther. 1992; 6: 447-458.

72. Carino SR, Sperry DC, Hawley M. Relative bioavailability estimation of carbamazepine crystal forms using an artificial stomach-duodenum model. J. Pharm. Sci. 2006; 95: 116-125.

73. Bhattachar SN, Perkins EJ, Tan JS, Burns LJ. Utilization of an artificial stomach and duodenum dissolution model and GastroPlus simulations to predict absorption. J. Pharm. Sci. 2011; 100: 4756-4765.

74. Minekus M, Smeets-Peters M, Havenaar R, Bernalier A, Fonty G, Marol-Bonnin S, et al. A computer-controlled system to simulate conditions of the large intestine with peristaltic mixing, water absorption and absorption of fermentation products. Appl. Microbiol. Biotechnol. 1999; 53: 108-114.

75. Wickham MJS, Faulks RM, Mann J, Mandalari G. The design, operation, and application of a dynamic gastric model. Dissolution Technol. 2012; 19: 15-22.

76. Kong F, Singh RP. A Human Gastric Simulator (HGS) to Study Food Digestion in Human Stomach. J. Food. Sci. 2010; 75(9): E627-E635.

77. Takeuchi S, Tsume Y, Amidon GE, Amidon GL. Evaluation of a three compartment in vitro gastrointestinal simulator dissolution apparatus to predict in vivo dissolution. J. Pharm. Sci. 2014; 103: 3416-3422.

78. Tsume Y, Takeuchi S, Matsui K, Amidon GE, Amidon GL. In vitro dissolution methodology, mini-Gastrointestinal Simulator (mGIS), predicts better in vivo dissolution of a weak base drug, dasatinib. Eur. J. Pharm. Sci. 2015; 76: 203-212.

79. Tsume Y, Matsui K, Searls AL, Takeuchi S, Amidon GE, Sun D, et al. The impact of supersaturation level for oral absorption of BCS class IIb drugs, dipyridamole and ketoconazole, using in vivo predictive dissolution system: Gastrointestinal Simulator (GIS). Eur. J. Pharm. Sci. 2017; 102: 126-139.

80. Tsume Y, Igawa N, Drelich AJ, Amidon GE, Amidon GL. The combination of GIS and Biphasic to better predict in vivo dissolution of BCS Class IIb drugs, Ketoconazole and Raloxifene. J. Pharm. Sci. 2018; 107: 307-316.

81. Tsume Y, Igawa N, Drelich AJ, Ruan H, Amidon GE, Amidon GL. The in vivo predictive dissolution for immediate release dosage of donepezil and danazol, BCS class IIc drugs, with the GIS and the USP II with biphasic dissolution apparatus. J. Drug Deliv. Sci. Technol. 2020; 56: 1-9.

82. Hens B, Bermejo M, Tsume Y, Gonzalez-Alvarez I, Ruan H, Matsui K, et al. Evaluation and optimized selection of supersaturating drug delivery systems of posaconazole (BCS class 2b) in the gastrointestinal simulator (GIS): An in vitro-in silico approach. Eur. J. Pharm. Sci. 2018; 115: 258-269.

83. Stillhart C, Pepin X, Tistaert C, Good D, Bergh A, Van Den Parrott N, et al. PBPK Absorption Modeling: Establishing the In vitro-In vivo Link - Industry Perspective. AAPS J. 2019; 21: 1-13.

84. Kesisoglou F, Xia B, Agrawal NGB. Comparison of Deconvolution-Based and Absorption Modeling IVIVC for Extended Release Formulations of a BCS III Drug Development Candidate. AAPS J. 2015; 17: 1492-1500.

85. Kaur N, Narang A, Bansal AK. Use of biorelevant dissolution and PBPK modeling to predict oral drug absorption. Eur. J. Pharm. Biopharm. 2018; 129: 222-246.

86. Pepin XJH, Flanagan TR, Holt DJ, Eidelman A, Treacy D, Rowlings CE. Justification of drug product dissolution rate and drug substance particle size specifications based on absorption PBPK modeling for lesinurad immediate release tablets. Mol. Pharm. 2016; 13: 3256-3269.

87. Willmann S, Thelen K, Becker C, Dressman JB, Lippert J. Mechanism-based prediction of particle size-dependent dissolution and absorption: Cilostazol pharmacokinetics in dogs. Eur. J. Pharm. Biopharm. 2010; 76: 83-94.

88. Pepin XJH, Huckle JE, Alluri RV, Basu S, Doss S, Parrott N, et al. Understanding Mechanisms of Food Effect and Developing Reliable PBPK Models Using a Middle-out Approach. AAPS J. 2021; 23: 1-14.

89. Baka E, Comer JEA, Takács-Novák K. Study of equilibrium solubility measurement by saturation shakeflask method using hydrochlorothiazide as model compound. J. Pharm. Biomed. Anal. 2008; 46: 335-341.

90. Avdeef A, Fuguet E, Llinas A, Rafols C, Bosch E, Völgyi G, et al. Equilibrium solubility measurement of ionizable drugs - Consensus recommendations for improving data quality. ADMET DMPK. 2016; 4: 117-178.

91. USP. Chapter 724 - Drug release - delayed-release (enteric-coated) articles - general drug release standard. 2012.

92. USP Monograph-Ibuprofen Tablets. [Online]. [cited 2023 01 15. Available from: http://www.pharmacopeia.cn/v29240/usp29nf24s0_m39890.html.

93. Legg TJ, Laurent AL, Leyva R, Kellstein D. Ibuprofen sodium is absorbed faster than standard Ibuprofen tablets: Results of two open-label, randomized, crossover pharmacokinetic studies. Drugs R. D. 2014; 14: 283-290.

94. Kubitza D, Becka M, Zuehlsdorf M, Mueck W. Effect of food, an antacid, and the H2 antagonist ranitidine on the absorption of BAY 59-7939 (rivaroxaban), an oral,

direct Factor Xa inhibitor, in healthy subjects. J Clin Pharmacol. 2006; 46: 549-558.

95. Kubitza D, Becka M, Voith B, Zuehlsdorf M, Wensing G. Safety, pharmacodynamics, and pharmacokinetics of single doses of BAY 59-7939, an oral, direct factor Xa inhibitor. Clin Pharmacol Ther. 2005; 78: 412-421.

96. ASHP. Drugs.com. [Online]. [cited 2021 10 09. Available from: https://www.drugs.com/monograph/aspirin.html.

97. MPA. Public Assessment Report Scientific discussion. Acetylsalicylic acid Krka (acetylsalicylic acid). SE/H/1604/01-. 2016;: 1-8.

98. MPA. Public Assessment Report Scientific discussion. Peneprin (acetylsalicylic acid). SE/H/1021/002005/DC. 2011.

99. MPA. Public Assessment Report Scientific discussion. Acetylsalicylsyra Teva (acetylsalicylic acid). SE/H/1593/01-03/. 2016.

100. Russell TL, Berardi LL, Barnett JL, Dermentzoglou LC, Jarvenpaa KM, Schmaltz SP. Upper gastrointestinal pH in seventy-nine healthy, elderly, north american men and women. Pharm Res. 1993; 10: 187-96.

101. Al-Gousous J, Amidon GL, Langguth P. Toward Biopredictive Dissolution for Enteric Coated Dosage Forms. Mol Pharm. 2016; 13(6): 1927-36.

102. Becker D, Zhang J, Heimbach T, Penland RC, Wanke C, Shimizu J, et al. Novel orally swallowable IntelliCap® device to quantify regional drug absorption in human GI tract using diltiazem as model drug. Ageing Int. 2014; 15: 1490-7.

103. Advil Package Insert. [Online]. [cited 2023 01 15. Available from: https://www.medicines.org.uk/emc/files/pil.11165.pdf.

104. Laska EM, Sunshine A, Marrero I, Olson N, Siegel C, McCormick N. The correlation between blood levels of ibuprofen and clinical analgesic response. Clin Pharmacol. 1986; 40: 1-7.

105. Brain P, Leyva R, Doyle G, Kellstein D. Onset of analgesia and efficacy of ibuprofen sodium in postsurgical dental pain: Randomized, placebo-controlled study versus standard ibuprofen. Clin J Pain. 2015; 31: 444-450.

106. Schettler T, Paris S, Pellett M, Kidner S, Wilkinson D. Comparative pharmacokinetics of two fast-dissolving oral ibuprofen formulations and a regular-release ibuprofen tablet in healthy volunteers. Clin Drug Investig. 2001; 21: 73-78.

107. Völgyi G, Baka E, Box KJ, Comer JEA, Takács-Novák K. Study of pH-dependent solubility of organic bases. Revisit of Henderson-Hasselbalch relationship. Anal Chim Acta. 2010; 673: 40-46.

108. Kumar R, Thakur AK, Chaudhari P, Banerjee N. Particle Size Reduction Techniques of Pharmaceutical Compounds for the Enhancement of Their Dissolution Rate and Bioavailability. J Pharm Innov. 2022; 17: 333-352.

109. Avdeef A. Solubility. In Absorption and Drug Development. Hoboken, NJ, USA: John Wiley & Sons; 2012. p. 252-308.

110. Takács-Novák K, Szőke K, Völgyi G, Horváth P, Ambrus R, Szabó-Révész P. Biorelevant solubility of poorly soluble drugs: Rivaroxaban, furosemide, papaverine and niflumic acid. J Pharm Biomed Anal. 2013; 83: 279-285.

9 BIBLIOGRAPHY OF THE CANDIDATE'S PUBLICATIONS

9.1 Publication relevant to the dissertation

I. Katona MT, Kakuk M, Szabó R, Tonka-Nagy P, Takács-Novák K, Borbás E. Towards a better understanding of the post-gastric behavior of enteric-coated formulations. Pharm. Res. 2022; 39: 201-211.

II. Katona MT, Nagy-Katona L, Szabó R, Borbás E, Tonka-Nagy P, Takács-Novák K. Multi-compartmental dissolution method, an efficient tool for the development of enhanced bioavailability formulations containing poorly soluble acidic drugs. Pharmaceutics. 2023; 15: 753.

III. Kushwah V, Arora S, Katona MT, Modhave D, Fröhlich E, Paudel A. On absorption modelling and food effect prediction of rivaroxaban, a BCS II drug orally administered as an immediate-release tablet. Pharmaceutics. 2021; 13: 283.

9.2 Other, not related publications

IV. Detrich Á, Dömötör KJ, Katona MT, Markovits I, Vargáné Láng J. Polymorphic forms of bisoprolol fumarate. J Therm Anal Cal. 2019; 135: 3043-3055.

10 ACKNOWLEDGEMENTS

First of all, I am extremely grateful to Krisztina Takács-Novák, who accompanied my studies with patience and enthusiasm. Besides her great experience, her endless respect for teaching and science will always serve as an example for me throughout my professional life. I am thankful to Enikő Jaksáné Borbás for her useful advices and for the projects that we worked on together over the years. I would like to thank Peter Tonka-Nagy for always supporting my personal development and for creating an environment where scientific challenges felt more like play than work. I am especially thankful to Rozália Vanyúr for starting me on my professional journey and always supporting me selflessly. Without her encouragement, I probably would never have started my PhD studies. I'm also grateful to Imre Szentpéteri for his mentorship and for inspiring me with his vast knowledge. “We all came out of his overcoat.” Special thanks to my former graduates Melinda Kakuk, Szabina Kádár, Réka Szabó and Lili Nagy-Katona for the conscientious work they put into our research. I would like to thank my family, especially my parents for their unconditional love and support which made my childhood carefree and provided a calm background for my studies. Last but not least, thank you to my wonderful wife, Adrienn and my rogue son, Vince for brightening my life and making everything meaningful.

Pharm Res (2022) 39:201–211
https://doi.org/10.1007/s11095-021-03163-0

RESEARCH PAPER

Towards a Better Understanding of the Post-Gastric Behavior of Enteric-Coated Formulations

Miklós Tamás Katona[1,2] · Melinda Kakuk[3] · Réka Szabó[2] · Péter Tonka-Nagy[2] · Krisztina Takács-Novák[1] · Enikő Borbás[4]

Received: 25 October 2021 / Accepted: 29 December 2021 / Published online: 18 January 2022

ABSTRACT

Purpose The aim of our work was to develop a biorelevant dissolution method for a better understanding of the *in vivo* performance of delayed-release tablet formulations.

Methods The typical pH profile and residence times in the stomach and small intestine were determined in fasted conditions based on the published results of swallowable monitoring devices. Then, a multi-stage pH shift dissolution method was developed by adding different amounts of phosphate-based buffer solutions to the initial hydrochloric acid solution. Because of the highly variable *in vivo* residence times in the stomach, two alternatives of the method were applied, modeling rapid and slow gastric emptying as well. This approach provided an opportunity to study the effect of the acidic treatment on post gastric release. Six enteric-coated low-dose acetylsalicylic acid (ASA) formulations including the reference Aspirin Protect were tested as a model compound. Moreover, the thickness of the coating of each formulation was investigated by scanning electron microscope.

Results Comparing the *in vitro* results to the known properties of the formulations, the new method was found to be more discriminative than the USP dissolution method. Ingredients affecting the *in vitro* dissolution, and thus probably the *in vivo* performance, were identified in both the tablet core and the coating of the tested formulations. The limited available *in vivo* data also indicated an increased predictivity.

Conclusion Overall, the presented method may be an efficient tool to support the development of enteric coated generic formulations.

KEY WORDS acetylsalicylic acid · biorelevant dissolution · enteric coating · gastric residence time · gastrointestinal pH

ABBREVIATIONS

ACN	Acetonitrile
ASA	Acetylsalicylic acid
API	Active Pharmaceutical Ingredient
BA	Bioavailability
BE	Bioequivalence
CI	Confidence interval
EC	Enteric coating
EMA	European Medicines Agency
GI	Gastrointestinal
HPLC	High Performance Liquid Chromatography
MMC	Migrating motor complex
NSAID	Nonsteroidal anti-inflammatory drug
PVAP	Polyvinyl acetate-phthalate
QC	Quality control
RGE	Rapid gastric emptying
SGE	Slow gastric emptying
AUC	The area under the plot of plasma concentration of a drug *versus* time after dosage
C_{max}	The maximum concentration that a drug achieves in a specified compartment of the body after administration
t_{max}	The time it takes a drug to reach the maximum concentration in plasma

✉ Miklós Tamás Katona
katona.miklos@egis.hu

✉ Enikő Borbás
eniko.jaksaneborbas@edu.bme.hu

1 Department of Pharmaceutical Chemistry, Semmelweis University, 7 Hőgyes Endre Street, Budapest H-1092, Hungary

2 Egis Pharmaceuticals PLC, 116-120 Bökényföldi Street, Budapest H-1165, Hungary

3 Department of Pharmaceutics, Semmelweis University, 9 Hőgyes Endre Street, Budapest H-1092, Hungary

4 Department of Organic Chemistry and Technology, Budapest University of Technology and Economics, 3 Műegyetem rakpart, Budapest H-1111, Hungary

USP United States Pharmacopoeia
FDA U.S. Food and Drug Administration

INTRODUCTION

The reliable prediction of *in vivo* performance of generic formulation candidates is a continuous challenge in drug development. In cases where solubility or the dissolution of the API is the rate limiting factor of absorption, the *in vitro* dissolution test is the primary tool for the prediction of bioavailability (1). However, conventionally used apparatuses and buffer compositions are usually not suitable to model the complex atmosphere of the gastrointestinal system. The lack of predictive *in vitro* dissolution methods is particularly common in formulations such as enteric-coated(EC) products, which was underlined by Al-Gousous *et al.* (2).

The dissolution testing of delayed-release products for quality control (QC) purposes is specified by various Pharmacopoeias. In order to demonstrate the resistance of the coating to the gastric fluid, both EMA and FDA prescribes the testing of the product in an acidic medium (e.g. 0.1 M hydrochloric acid) for 1 to 2 h, which is followed by testing in a buffer solution of pH 6.8 to model the small intestinal environment (3, 4). As evident from the prescriptions of the Pharmacopoeias, these methods apply only one pH to model the small intestine, which is not sufficient to determine the exact site of disintegration and absorption. In general, dissolution methods for QC purposes need to be robust and simple to implement, which limits the *in vivo* predictability of the method. However, in case the aim is to support the formulation development, dissolution methods should be as biorelevant as possible in order to design the formulation able to behave *in vivo* as intended.

The aim of the application of enteric coating is to delay the release of the drug substance until it is emptied from the stomach. Thereafter, the site of drug release is affected by several factors, such as the structure of the employed film former, the thickness of the applied film, and the nature and quantities of the additives used together with it (5). In general, enteric coatings are weakly acidic polymers that are insoluble at gastric pH but ionize and dissolve under intestinal conditions. Different polymers have different pH thresholds, which is an important property when targeting the site of disintegration (2). Due to the acidic nature of coatings, the accumulation of protons on the surface of such formulations in the stomach may also affect their post-gastric release. Based on this, the residence time in the stomach also plays an important role in the subsequent absorption of the drug substance (6). Physiologically, the gastric emptying is related to the migrating motor complex (MMC) of the stomach, which is a ~2 h long cycle that consists of four phases. Phase I is a period of motor quiescence lasting 40–60% of the cycle. Phase II, accounting for 20–30% of the cycle, exhibits irregular phasic contractions. Phase III is a 5- to 10-min period of lumenally occlusive, rhythmic contractions occurring at the slow-wave frequency. Phase IV is a transitional period of irregular contractions between phase III and phase I (7). Non-disintegrating solid dosage forms administered in the fasted state are mainly emptied during the intense contractions of phase III, also known as the 'housekeeper wave' (8, 9). However, Kaniwaka *et al.* found significant correlation between the gastric emptying rates and the size of enteric-coated tablets as well (10).

To develop a predictive *in vitro* dissolution method, the appropriate characterization of the pH conditions and the residence times in each relevant part of the gastrointestinal (GI) system is essential. Some studies focused on the evaluation of gastrointestinal pH conditions using ingestible radiotelemetry capsules as early as the late 1980s (11, 12). To date, a number of similar, new devices have become available (e.g. Bravo capsule, IntelliCap, SmartPill) which help in the precise characterization of GI pH values (13–17). Previously, the determination of residence times in the GI tract was carried out using formulations labeled with radionucleotides (18). However, with the advance of radiotelemetry capsules, a suitable alternative is provided for this purpose as well (12, 15).

The gastrointestinal environment is strongly affected by the food and liquid intake, therefore the *in vivo* bioavailability (BA) studies are conducted under standardized conditions. According to the EMA's guideline, in general, a bioequivalence (BE) study should be conducted under fasting conditions, as this is considered to be the most sensitive condition to detect a potential difference between formulations (19). In order to prove bioequivalence, performing a study in fasted state is prescribed by the FDA as well (20). In general, subjects are fasting for 8 h prior to administration, then test and reference products are administered with a standardized amount of water (at least 150 mL). No food intake is allowed for at least 4 h post-dose. As prescribed by the EMA, the sampling schedule of a bioequivalence study should include frequent sampling around the predicted t_{max} to provide a reliable estimation of peak exposure (19). However, for enteric-coated formulations, the high variability of gastric emptying rate results in high variability of t_{max} value, thus adequately describing their plasma concentration-time profile is challenging. This occurs especially when the plasma half-life of the investigated drug substance is short. The difficulty of *in vivo* testing of EC formulations also confirms the importance of proper *in vitro* characterization.

Acetylsalicylic acid (ASA) is a nonsteroidal anti-inflammatory drug (NSAID) which is commonly used to reduce pain, fever or inflammation (21). ASA irreversibly inhibits platelet aggregation by inhibiting thromboxane A_2 (TxA_2) synthesis, therefore it is also recommended in single and dual antiplatelet therapy. It has been shown that the use

of ASA increases the risk of gastrointestinal bleeding especially when used long-term (22). The adverse effect is dose-related therefore in the antiplatelet indication it is typically given in low-dose (50–100 mg/day) (23). In order to avoid the irritation of the stomach, ASA is available as enteric-coated dosage form as well. Since there have been several reported attempts that failed to demonstrate BE in case of generic enteric-coated ASA formulations this substance was chosen as a model compound in our study (24–26).

According to Garbacz *et al.*, the bicarbonate buffer can be considered as the most biorelevant buffer system for the simulation of intestinal conditions. However, the disadvantage of such buffer solutions is their thermodynamic instability, which requires the control of the pH during dissolution testing (27). Despite their complicated implementation, there are a number of examples of using bicarbonate buffers for the testing of enteric-coated formulations as well (28–30). Alternatively, Al-Gousous*et al.* have successfully developed a dissolution method using phosphate-based surrogate buffer and found good correlation between *in vitro* and *in vivo* properties of Aspirin Protect 300 mg and Walgreens Aspirin 325 mg formulations. The published dissolution method considers the pH change after emptying the stomach and applies two different phosphate buffers to model the pH and buffer molarity gradient along the small intestine (31). However, the referred methods pay less attention to the effect of gastric emptying time on the performance of enteric coatings. In addition, the results of the advanced radiotelemetry capsules allow a more accurate simulation of the characteristic pH profile and residence times of the small intestine, giving a new opportunity to predict the site of disintegration and absorption.

The aim of our work was to develop a new biorelevant *in vitro* dissolution method for enteric-coated formulations considering the physiological conditions of the stomach and the small intestine, such as typical pH profile, residence times and biofluid volume. The accurate modeling of these parameters is expected to provide us with a better understanding of the site of disintegration and the rate of absorption of enteric-coated formulations. However, due to the complex composition of biofluids (enzymes, bile acids, etc.), some simplifications had to be made, to get a better applicable method.

Two alternatives of the new method, modeling rapid and slow gastric emptying, and the USP method were used to test different enteric-coated, low-dose ASA formulations. The tested formulations included the reference product as well as the commercially available generic alternatives in Hungary. Since the comparison of different enteric coatings was also aimed and each of the latter formulations contained the same type of coating polymer, Walgreens Aspirin 81 mg marketed in the USA was also tested despite having a different strength. The coatings of each formulation were examined with scanning electron microscope (SEM). The thickness and the composition of the coatings as well as the composition of the tablet cores were studied to interpret the obtained *in vitro* dissolution results. In case published *in vivo* results were available, the IVIV relationship between the dissolution profiles and the corresponding pharmacokinetic parameters was also investigated. For other formulations, the possible *in vivo* effects of the *in vitro* dissolution results were discussed.

MATERIALS AND METHODS

Materials

Six commercially available enteric-coated ASA-containing products were tested: Walgreens Aspirin 81 mg (LNK, USA; Lot: P106919), Aspirin Protect 100 mg (Bayer AG, Germany; Lot: BTAH3CO), Asatrin-Teva Protect 100 mg (Teva Pharmaceutical Industries Zrt., Hungary; Lot: R43739), ASA Krka 100 mg (KRKA, Slovenia; Lot: D66849), Asactal 100 mg (Actavis Group PTCehf., Iceland; Lot: 037018) and ASA Protect Pharmavit 100 mg (PharmaSwiss Ceska Republika, Chech Republic; Lot: 7E126A). Walgreens Aspirin was purchased in the USA, while other products were purchased from pharmacies in Hungary. All formulations were white colored, round, cylindrical biconvex tablets with slight differences in the sizes: the height and the diameter of the formulations varied between 3 and 4 mm and 6.5–8 mm. The tested products and the inactive ingredients of the tablet cores and the applied coating materials are summarized in Table I.

All chemicals used were of analytical grade. Sodium dihydrogen phosphate monohydrate; trisodium phosphate; acetonitrile; hydrochloric acid; (Molar Chemicals Ltd., Budapest), disodium hydrogen phosphate dihydrate; (Thomasker, Budapest), phosphoric acid; (Emsure ACS. Reag. Ph. Eur., Budapest).

Methods

Dissolution Testing

The dissolution tests were carried out using an Agilent 708 DS dissolution apparatus (Agilent Technologies, Inc., Santa Clara, California, USA). The media were thermostated at 37 ± 0.5°C. Each formulation in each method was tested on six parallel samples.

USP Dissolution Method (32). The samples were first placed into USP I baskets and stirred at 100 rpm in 1000 mL of 0.1 M HCl solution for 120 min, then the medium was replaced by 900 mL of pH 6.8 ± 0.5 phosphate buffer and the test was continued for an additional 60 min at constant stirring rate. The buffer solution was prepared by mixing 0.1 M HCl with 0.2 M tribasic sodium phosphate (3:1). In case it was

Table I Dose and Qualitative Ingredients of the Tested Products

Product	Dose (mg)	Core	Coating
Aspirin Protect	100	Microcrystalline cellulose, corn starch	Methacrylic acid– ethyl acrylate 1:1 copolymer, polysorbate 80, sodium lauryl sulfate, triethyl citrate, talc
Asatrin- Teva Protect	100	Microcrystalline cellulose, potato starch, silica colloidal anhydrous, lactose monohydrate	Methacrylic acid– ethyl acrylate 1:1 copolymer, triacetin, talc
ASA Krka	100	Microcrystalline cellulose, potato starch, silica colloidal anhydrous, lactose monohydrate	Methacrylic acid– ethyl acrylate 1:1 copolymer, polysorbate 80, sodium lauryl sulfate, triacetin, talc
Asactal	100	Microcrystalline cellulose, corn starch, silica colloidal anhydrous, stearic acid	Methacrylic acid– ethyl acrylate 1:1 copolymer, polysorbate 80, sodium lauryl sulfate, triethyl citrate, talc
ASA Protect Pharmavit	100	Microcrystalline cellulose, potato starch, silica colloidal anhydrous, lactose monohydrate,	Methacrylic acid– ethyl acrylate 1:1 copolymer, triacetin, talc
Walgreens Aspirin	81	Microcrystalline cellulose, corn starch, silica colloidal anhydrous, polydextrose, sodium bicarbonate	Hypromellose, methacrylic acid, shellac wax, sodium lauryl sulfate, polyethylene glycol, simecthicone, triacetin, triethyl citrate, talc, titanium dioxide

necessary, the pH was adjusted with 2 M hydrochloric acid or 2 M sodium hydroxide. Samples at each sampling time point were taken into HPLC vials via autosampling. The sampling cannulas were equipped with 10 µm PVDF, full-flow filter tips (Agilent Technologies, Inc., Santa Clara, California, USA). The applied sampling schedule is shown in Table II.

Biorelevant Dissolution Method. The dissolution apparatus was equipped with 250 mL small volume vessels and rotating paddles according to Chinese Pharmacopoeia. The media were stirred at 50 rpm. The initial dissolution medium was 160 mL of 0.01 M HCl solution, which was modified in three steps through the addition of different amounts of Na_2HPO_4 buffer in order to simulate the conditions of the stomach and different parts of the small intestine. The addition of the buffer solution was performed using Cole Parmer 74,900 infusion pumps (Cole Parmer, Vernon Hills, Illinois, USA), the pH of the media was measured by an Inolab-type pH meter (WTW GmbH, Weilheim, Germany). Due to the highly variable *in vivo* residence times in the stomach, two variants of the method were applied which differed only in the length of the acidic treatment. The conditions of the method modeling *rapid* gastric emptying (RGE) and *slow* gastric emptying (SGE) are summarized in Table III.

Samples at each time point were taken manually using equivalent filtration to that of the USP method. The volume of the samples was 1 mL in all cases. Table IV shows the sampling schedule of the biorelevant methods.

Table II Sampling Time Points of USP Method

Medium	Sampling time (min)
0.1 M HCl	60, 120
pH 6.8 phosphate buffer	5, 15, 30, 45, 60

Onset of the dissolution was determined by 5% of dissolved drug substance. The f_2 statistic was calculated based on the EMA guideline on the Investigation of Bioquivalence (33).

Determination of Dissolved Drug Content by High Performance Liquid Chromatography

A Waters Acquity UPLC device (Waters, Milford, Massachusetts, USA) was used to determine the amount of dissolved drug in the solutions. For this purpose, YMC-Pack Pro C18 RS S-5 µm, 8 nm 150 × 4.6 mm I.D type HPLC column was used. The mobile phase was ACN:H_2O:cc.H_3PO_4 = 400:600:1 and the flow rate was 1.0 mL/min. The mode of separation was isocratic. External calibration was applied by five consecutive injections of the standard solution containing the concentration of API corresponding to the approximated concentration of 100% dissolution. The calibration was controlled by the injection of the standard control solution containing the same nominal concentration, then followed by the injection of the sample solutions. The absorbance was detected at 237 nm. For standard preparations, accurate measurements were achieved using a Mettler Toledo XP26 microanalytical balance (Mettler Toledo, Columbus, Ohio, USA). The sample concentrations in mg/L were calculated using the dilution of the standard solution and the sample solution and the peak areas of the sample solutions. The chromatographic conditions for each test preparation were the same as well as the column used for the measurement.

Examination of Coatings by Scanning Electron Microscope

Before the test, the samples were fixed with double-sided carbon glue to copper stumps, then gilded with a JEOL 1200 type device (JEOL, Akishima, Tokyo, Japan). Images were taken from the samples in tablet form using a JEOL JSM-6380LA scanning electron microscope (JEOL, Akishima,

Table III Applied Conditions of Dissolution Method with RGE and SGE

			Method with RGE	Method with SGE
	Medium	pH	Residence time (min)	
Gastric phase	160 mL, 0.01 M HCl solution	2.0	**20**	**120**
pH change 1.	*Addition of 20 mL, 135 mM Na_2HPO_4 buffer*		*10*	*10*
Duodenal phase	180 mL, 15 mM phosphate buffer	6.5	30	30
pH change 2.	*Addition of 10 mL, 100 mM Na_2HPO_4 buffer*		*20*	*20*
Jejunal phase	190 mL, 19.5 mM phosphate buffer	6.8	70	70
pH change 3.	*Addition of 20 mL, 100 mM Na_2HPO_4 buffer*		*10*	*10*
Ileal phase	210 mL, 27.1 mM phosphate buffer	7.2	45	45

The main difference between the two method was highlighted with bold entries

Tokyo, Japan) applying 15 kV accelerating voltage and 10 mm sample distance under high vacuum.

RESULTS AND DISCUSSION

Dissolution Results Obtained by USP Method

A comparative dissolution study of the selected formulations was performed according to the pharmacopoeial prescriptions (32). As evident from Fig. 1, no dissolution was observed during the 2-h treatment in 0.1 M HCl solution. After the replacement of the dissolution medium by pH 6.8 phosphate buffer, each formulation started to dissolve immediately, and a measurable concentration of ASA was observed at the 5-min sampling point in all cases. The post-acidic dissolution of all formulations except Asactal was rapid (≥85% for the mean percent dissolved in ≤30 min). Walgreens Aspirin and Asatrin Teva Protect even met the criterion of very rapid dissolution (≥85% for the mean percent dissolved in ≤15 min in this medium) (34). The dissolution rate of Asactal was significantly lower as its mean dissolution exceeded 85% only after 45 min residence in pH 6.8 buffer.

These results are in agreement with the expectation for delayed release formulations that are designed to release the active substance after the dosage form has reached the small intestine, therefore do not dissolve in acidic media. As the dosage form is placed in the higher-pH environment, the polymer coating dissolves, and the tablet core behaves similarly to immediate-release formulations. Based on the results of the acid phase, the gastro resistance of the enteric coating of each formulation was found to be appropriate. As the pH 6.8 used after the pH change is typical for the *jejunum* in fasted state, the formulations are expected to dissolve in this intestinal tract at the latest. However, in the absence of a medium modeling the duodenal pH, the results do not provide information about the exact site of the onset of the drug release.

According to the individual USP monograph of Aspirin Delayed-Release Tablets not more than 10% of the labeled amount of aspirin is allowed to dissolve in the acidic stage while the dissolution in the buffer stage must exceed 75% in 45 min (35). These criteria are consistent with both USP and Ph. Eur general prescriptions for delayed-release formulations (36, 37). Based on Fig. 1, it can be determined that all formulations met the acceptance criteria. However, the *in vivo* studies performed did not demonstrate bioequivalence for either ASA Krka or Asactal formulations (24, 25). The latter also points out the importance of an appropriate biorelevant dissolution method during generic formulation development phase.

Development of a Biorelevant Dissolution Method

The development of the method was focused on modeling the gastrointestinal conditions in fasted state. The applied pH conditions and residence times were determined based on published experimental results of ingestible pH monitoring capsules (11, 12, 14–18, 38). In case of such devices, gastric residence and small intestinal transit times are determined based on characteristic pH changes. As the capsule passes through the *pylorus*, the acidic environment of the fasted stomach is rapidly and sustainly replaced by an almost neutral pH of the *duodenum*. The small intestinal residence ends with the passage through the *ileocecal* valve, which is indicated by a > 0.5 decrease of pH as a result of bacterial digestion products in the colon. According to the published data, the mean pH of the stomach was found to be around 2.0, which is resulted by the dilution of the initial gastric acid with the liquid intake

Table IV Sampling Time Points of Biorelevant Methods

Method	Sampling time (min)
RGE	20, 30, 60, 70, 80, 90, 100, 110, 120, 135, 150, 160, 175, 190, 205
SGE	120, 130, 160, 170, 180, 190, 200, 210, 220, 235, 250, 260, 275, 290, 305

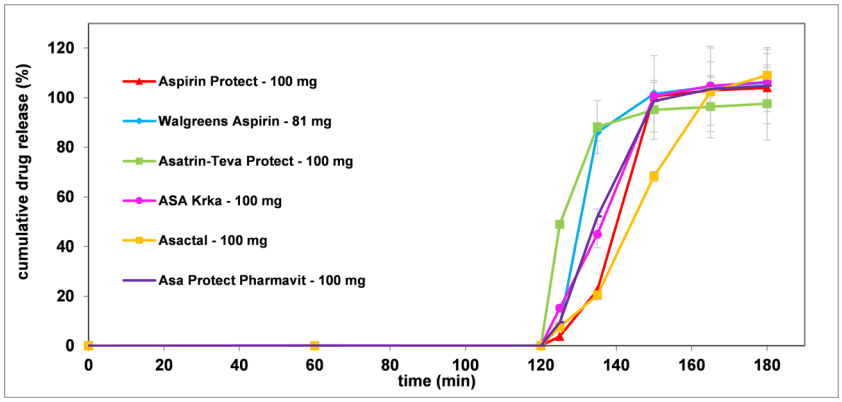

Fig. 1 Dissolution results obtained by USP method.

following the administration of the drug product. The residence time in the stomach is reported to be typically between 20 and 120 min with high variability. Since the time spent in the acidic medium may affect the physicochemical properties of the weakly acidic film formers, instead of specifying the average residence time, two versions of the method were tested, one with 20 min and one with 120 min acidic treatment, to model both faster and slower gastric emptying. The pH conditions modeling the small intestinal tracts were set to pH 6.5 (proximal phase), pH 6.8 (middle phase) and pH 7.2 (distal phase), respectively. The time spent at each pH was 30 min (proximal phase), 70 min (middle phase), and 45 min (distal phase), excluding the time of the pH changes. According to the results of radiotelemetry capsules, the pH change between each tract is rather gradual than momentary (13). To model this phenomenon, the buffer solutions were administered using an infusion pump. The experimental pH *vs* time profile of the developed method with rapid gastric emptying is shown in Fig. 2.

The composition of the gastric buffer was 0.01 M HCl solution, while the appropriate pH changes were achieved by the addition of different amounts of Na_2HPO_4 solutions with different molarities. The molarity of the phosphate-based buffer solutions was set based on the results of Al-Gousou*set al.*, who elaborated a simplified alternative to unstable bicarbonate buffer systems (34). The volume of the dissolution media varied from 160 mL to 210 mL, which better suits the amount of fluid in the stomach after the intake of drugs with a glass of water.

Dissolution Results Obtained by Biorelevant Method with Rapid Gastric Emptying (RGE)

Figure 3 shows the results of the dissolution method modeling rapid gastric emptying. According to the results none of the products releases the API in the gastric or proximal small intestinal phase (0–60 min). In case of Walgreens Aspirin, Asatrin-Teva Protect, ASA Krka and ASA Protect Pharmavit the mean onset of dissolution ranged from 78.3 ± 4.1 to 80.0 ± 6.3 min, which belongs to the pH change between the proximal and middle small intestinal phase. The dissolution profiles of the latter formulations except Walgreens Aspirin were found to be similar, as the calculated similarity factors (f_2) were ≥ 50 ($f_{2,\text{Asatrin-Teva Protect } vs.\text{ ASA Protect Pharmavit}} = 50$; $f_{2,\text{ASA Krka } vs.\text{ ASA Protect Pharmavit}} = 58$). Aspirin Protect and Asactal started to dissolve at the pH of the middle small intestinal phase (pH 6.8; 80–150 min), however, the dissolution rate of Asactal is significantly slower compared to Aspirin Protect ($f_2 = 21$). The dissolution of the products except

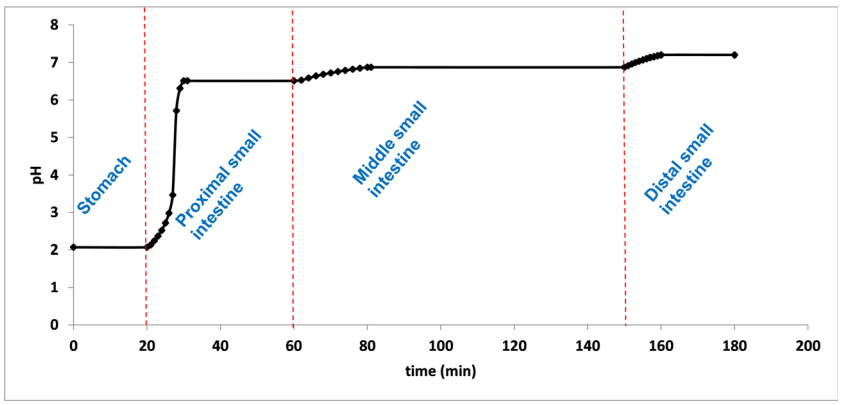

Fig. 2 Experimental pH profile of biorelevant dissolution method with RGE.

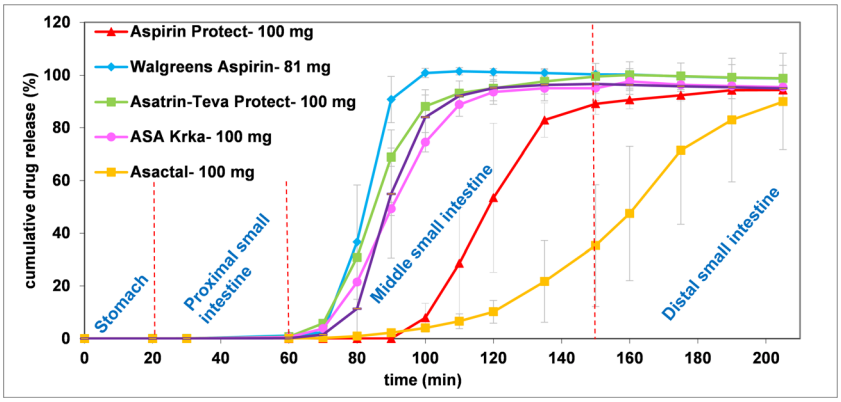

Fig. 3 Dissolution results obtained by biorelevant dissolution method with RGE.

Asactal is completed or almost completed in the 80–150-min interval, while Asactal releases its API mostly in the distal small intestine.

The examined products except Walgreens Aspirin are coated with methacrylic acid − ethyl acrylate 1:1 copolymer, with a dissolution pH threshold of 5.5, which is considered to target the onset of release to the *duodenum*(2). Interestingly, the results showed that the release of the drug substance is more typical in the later small intestinal phases. The dissolution profiles of the generic formulations were different ($f_2 < 50$) from that of the reference Aspirin Protect despite the same coating material, which indicated that other properties of the coating or the composition of the tablet core may also affect the release of the drug substance.

Dissolution Results Obtained by Biorelevant Method with Slow Gastric Emptying (SGE)

Figure 4 shows the results of the dissolution method modeling slow gastric emptying. Similar to the RGE method, there was no dissolution observed in the gastric and proximal small intestinal periods (from 0 to 160 min on Fig. 4). The dissolution of the formulations except Asatrin Teva Protect and Walgreens Aspirin started at the pH 6.8 period (180–250 min). In case of Asatrin Teva Protect and Walgreens Aspirin, a certain amount of API has already been released at the pH change between the proximal and middle small intestinal phases (160–180 min), however it was also less than that of the RGE method. It is also evident from Fig. 4 that, compared to other formulations, the longer gastric residence time had a greater effect on the shape of the dissolution profile of Walgreens Aspirin and resulted in longer saturation time. The mean post-gastric onset of ASA Krka dissolution was delayed by 20.0 min, while other formulations changed slightly by 3.7 to 8.3 min. Similar to the RGE method, the dissolution of Asactal is significantly slower than the reference formulation ($f_{2,\text{Asactal } vs. \text{ Aspirin Protect}} = 26$) and most of the API release occurs in the simulated distal small intestine.

The observed delay in the disintegration of all formulations compared to the RGE method is most probably due to the additional accumulation of protons on the surface of enteric coatings during the longer acidic treatment. The unexpected performance of ASA Krka compared to other formulations with the same coating material requires further investigation. The results suggest that the coating material of Walgreens Aspirin is more sensitive for the longer gastric residence than methacrylic acid−ethyl acrylate 1:1 copolymer.

Scanning Electron Microscopic Images

The structure and thickness of the coatings surrounding the tablet cores are shown in Fig. 5.

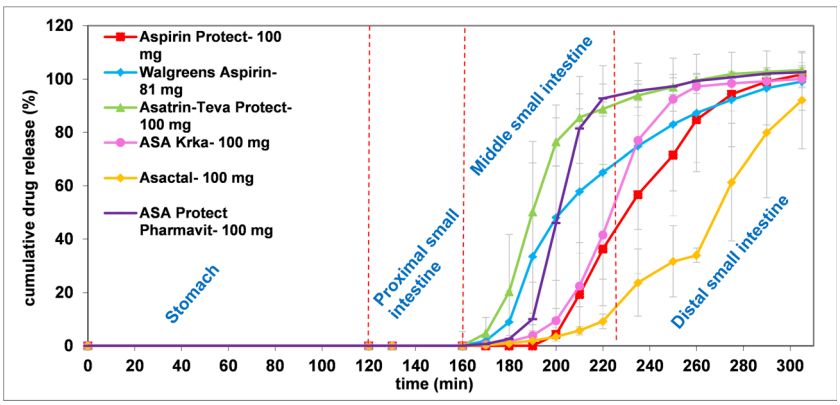

Fig. 4 Dissolution results obtained by biorelevant dissolution method with SGE.

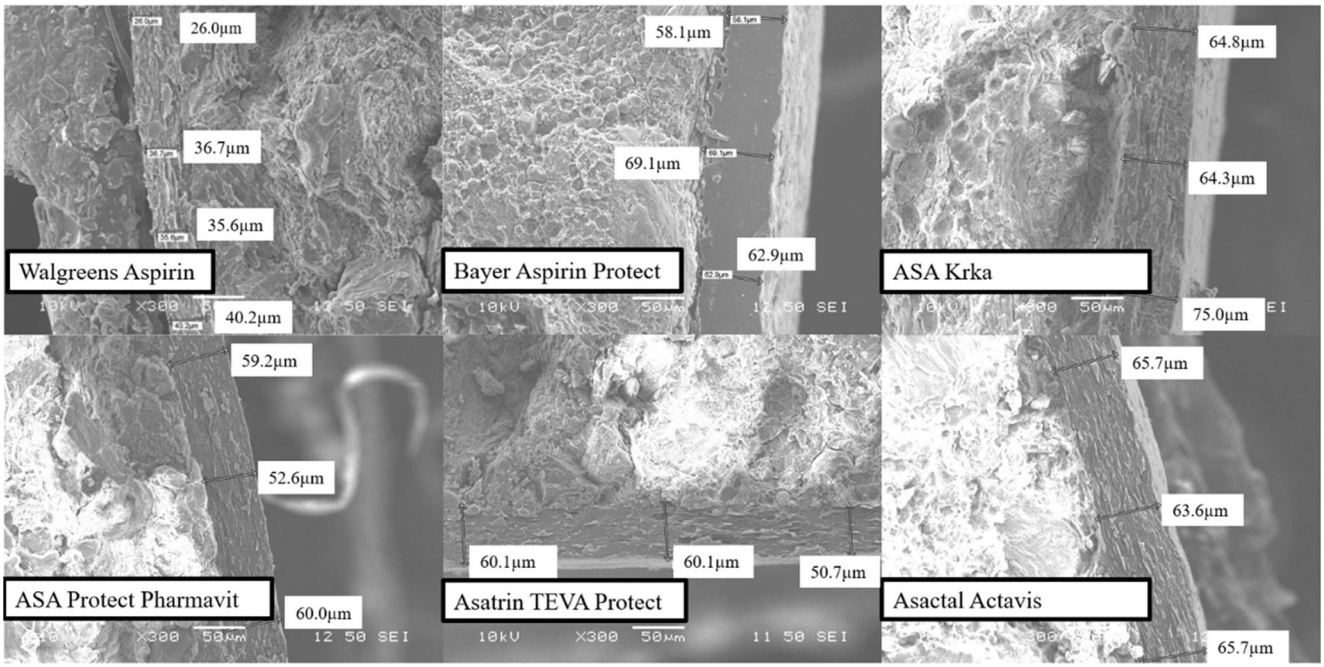

Fig. 5 SEM pictures of enteric coated ASA formulations.

The coatings were found to be evenly distributed around the cores in all cases. Comparing the structure of the coating around Walgreens Aspirin with other formulations coated with methacrylic acid-ethyl acrylate, it can be said that methacrylic acid-ethyl acrylate is more concise, especially in the case of Bayer Aspirin Protect.

As evident from Table V, the coating of Walgreens Aspirin is thinner than that of other formulations. This observation is in accordance with the dissolution results of the RGE method (Fig. 3), where Walgreens Aspirin showed the highest dissolution rate.

In case of all five methacrylic acid-ethyl acrylate coated formulations, the thickness of coating is between 50 and 75 µm which indicates that the differences in their dissolution profiles are most probably due to other factors than the thickness of the coating.

Relationship Between the Composition and *In Vitro*/*In Vivo* Performance

Among the tested formulations the manufacturer of ASA Krka and Asactal submitted BE study results to support the application for marketing authorization (MPA, 2016a; MPA, 2011). Other applicants, such as Teva, referred to the well-established clinical use and provided only an overview of literature references (26). A summary of the available clinical results is presented in Table VI.

Actavis has performed three *in vivo* studies under fasted state to compare Asactal and Aspirin Protect, each of which failed to demonstrate bioequivalence (25). Differences of C_{max} and AUC values were observed in both directions, most probably due to the high variability of the *in vivo* results. Comparing the *in vitro* dissolutions, Asactal dissolved more slowly than all other formulations, which can be seen also with the USP method, but even more typical with the two alternatives of the new method. In case of both RGE and SGE, the onset of dissolution was similar to that of the reference Aspirin Protect formulation, which meets the expectations based on the qualitatively equivalent composition (see Table I.) and similar thickness (see Table V.) of the coatings. The slower rate of dissolution may be explained by the different performance of the tablet cores. As evident from Table I, Asactal contains hydrophobic stearic acid, which may reduce the wettability of the tablet core compared to other formulations. Overall, based on the *in vitro* results, a lower bioavailability compared to the reference product is expected.

In case of ASA Krka, bioequivalence could not be demonstrated in the fasted state. The study showed 16% increase for both AUC and C_{max} compared to the reference product

Table V Thickness of the Coating of ASA Formulations

Product	Thickness of the coating (µm)
Walgreens Aspirin	26.0–40.2
ASA Protect Pharmavit	52.6–60.0
Bayer Aspirin Protect	58.1–69.1
Asatrin- Teva Protect	50.7–60.1
ASA Krka	64.3–75.0
Asactal Actavis	63.6–65.7

Table VI *In Vivo* Results of Available Clinical Studies in Fasting Conditions

Test formulation	Reference formulation	Study ID	PK parameter	Test/ref ratio
ASA Krka 100 mg	Aspirin Protect 100 mg	091B13	C_{max}	1.16 (CI 0.92–1.48)
			AUC	1.16
Asactal 100 mg	Aspirin Protect 100 mg	1267/07	C_{max}	1.22 (CI 1.03–1.43)
			AUC	1.18 (CI 1.05–1.33)
		1321/07	C_{max}	0.76 (CI 0.65–0.89)
			AUC	0.98 (CI 0.88–1.10)
		1747/08	C_{max}	1.24 (CI 1.04–1.47)
			AUC	1.12 (CI 0.97–1.29)

which is consistent with the results of the RGE method, which predicts an earlier release of the ASA Krka formulation compared to Aspirin Protect. The onset of release of ASA Krka obtained from the SGE method is similar to that of Aspirin Protect. However, the slope of its dissolution curve is slightly higher, which generally predicts a higher C_{max} value as well. Based on Table I, the applied plasticizer in the coating of this formulation is triacetin, while the reference product is formulated with triethyl citrate, which may explain the different onset of drug release observed with the RGE method. The slightly higher dissolution rate is probably related to the hydrophilic lactose monohydrate in the tablet core.

In case of Asatrin Teva Protect and ASA Protect Pharmavit there were no clinical data available, thus it was not possible to make *in vitro – in vivo* comparisons. The qualitative compositions of these formulations are equivalent to that of ASA Krka. Accordingly, their dissolution profiles were also similar with the RGE method. Moreover, the onset of their drug release was less affected by the longer acidic pretreatment used in the SGE method. Based on this, both formulations are expected to have higher bioavailability compared to the reference product.

The results also demonstrate the importance of the plasticizer type in the onset of release and the wettability of the tablet core in the rate of dissolution of the tested formulations.

Walgreens Aspirin differs from other formulations tested in the type and thickness of coating, composition of the tablet core, and even in the labeled drug content. This difference occurs especially in case of the SGE method, which indicates that the applied coating material is more sensitive for the longer acidic treatment compared to methacrylic acid−ethyl acrylate 1:1 copolymer. The experienced reduction in the dissolution may be a risk of lower bioavailability in case of subjects with longer gastric residence times.

CONCLUSIONS

Two alternatives of a biorelevant dissolution method – differing in the length of acidic treatment – were successfully developed, modeling the conditions of the stomach and the small intestine in fasted state. Biorelevant molarity and volume of dissolution medium as well as gradual pH change between each tract, were also considered. Six commercially available low-dose enteric coated ASA formulations were tested with the USP method and the two versions of the novel dissolution method.

Despite of the difficulties of demonstrating bioequivalence, all formulations met the acceptance criteria specified in the individual USP monograph of Aspirin Delayed-Release Tablets, which pointed out the importance of an appropriate biorelevant dissolution method. Comparing the compositions of the formulations with the *in vitro* results, the new method, especially with rapid gastric emptying proved to be discriminative. The different plasticizers applied in the coating process appeared to affect the onset of dissolution, while the hydrophilicity of the inactive ingredients affected the dissolution rate by altering the wettability of the tablet cores.

Applying the new method with longer acidic treatment resulted in later onset and slower rate of post-gastric drug release for all formulations. Considering the high variability of *in vivo* gastric residence times, performing the dissolution with both alternatives of the new method may be necessary to lower the risk of bioinequivalence of similar generic drug candidates.

Based on the relationship between the *in vitro* dissolution and the limited available bioequivalence data, and the increased discriminating power of the new dissolution method, an enhanced *in vivo* predictivity can also be assumed.

Overall, we conclude that the new method can be a good alternative for reaching a better understanding of the post-gastric behavior of enteric-coated formulations which is essential to get appropriate information on intestinal release and bioavailability.

ACKNOWLEDGMENTS AND DISCLOSURES

The authors declare that they have no known competing financial interests or personal relationships that could have appeared to influence the work reported in this paper.

FUNDING

Open access funding provided by Budapest University of Technology and Economics. This study was supported by the Department of Pharmaceutical Chemistry, Semmelweis University, Budapest, Hungary and the ÚNKP-21-4 New National Excellence program of the Ministry for Innovation and Technology from the source of the National Research, Development and Innovation Fund.

REFERENCES

1. Amidon GL. A theorical basis for a biopharmaceutic drug classification: the correlation of in vitro drug product dissolution and in vivo bioavailability. Pharm Res. 1995;12:923–9.
2. Al-Gousous J, Tsume Y, Fu M, Salem II, Langguth P. Unpredictable performance of pH-dependent coatings accentuates the need for improved predictive in vitro test systems. Mol Pharm. 2017;14:4209–19.
3. FDA. The United States Pharmacopeia and National Formulary USP 29- NF24, Inc. Rockville: The United States Pharmacopeial Convention; 2011.
4. Council of Europe: European Pharmacopoeia Commission 2.9.3 Dissolution test for solid dosage forms. Eur Pharmacopoeia. 2010;264–88.
5. Agylirah GA, Banker GS. Polymers for enteric coating applications. In: Polymers for controlled drug delivery. Boca Raton: CRC Press; 1991. p. 39–66.
6. Kambayashi A, Blume H, Dressman J. Understanding the in vivo performance of enteric coated tablets using an in vitro-in silico-in vivo approach: case example diclofenac. Eur J Pharm Biopharm. 2013;85:1337–47.
7. Hasler WL. Duodenal Motility. In Johnson LR, editor. Encyclopedia of Gastroenterology, Academic Press, 2003. p. 636–41
8. Locatelli I, Nagelj Kovai N, Mrhar A, Bogataj M. Gastric emptying of non-disintegrating solid drug delivery systems in fasted state: relevance to drug dissolution. Expert Opin Drug Deliv. 2010;7:967–76.
9. Minami H, Mccallum RW. The physiology and pathophysiology of gastric emptying in humans. Gastroenterology. 1984;86:1592–610.
10. Kaniwaka N, Aoyagi N, Ogata H, Ejima A, Motoyama H, Yasumi H. Gastric emptying rates of drug preparations. II. Effects of size and density of enteric-coated drug preparations and food on gastric emptying rates in humans. J Pharmacobiodyn. 1988;40:1569–72.
11. Evans DF, Pye G, Bramley R, Clark AG, Dyson TJ, Hardcastle JD. Measurement of gastrointestinal pH profiles in normal ambulant human subjects. Gut. 1988;29:1035–41.
12. Fallingborg J, Christensen LA, Ingeman-Nielsen M, Jacobsen BA, Abildgaard K, Rasmussen HH. pH-profile and regional transit times of the normal gut measured by a radiotelemetry device. Aliment Pharmacol Ther. 1989;3:605–14.
13. Becker D, Zhang J, Heimbach T, Penland RC, Wanke C, Shimizu J, Kulmatycki K. Novel orally swallowable IntelliCap® device to quantify regional drug absorption in human GI tract using diltiazem as model drug. Ageing Int. 2014;15:1490–7.
14. Ibekwe VC, Fadda HM, McConnell EL, Khela MK, Evans DF, Basit AW. Interplay between intestinal pH, transit time and feed status on the in vivo performance of pH responsive ileo-colonic release systems. Pharm Res. 2008;25:1828–35.
15. Koziolek M, Grimm M, Becker D, Iordanov V, Zou H, Shimizu J, Wanke C, Garbacz G, Weitschies W. Investigation of pH and temperature profiles in the GI tract of fasted human subjects using the Intellicap® system. J Pharm Sci. 2015;104:2855–63.
16. Maurer JM, Schellekens RCA, Van Rieke HM, Wanke C, Iordanov V, Stellaard F, et al. Gastrointestinal pH and transit time profiling in healthy volunteers using the IntelliCap system confirms ileo-colonic release of ColoPulse tablets. PLoS ONE. 2015;10:e0129076.
17. Schneider F, Grimm M, Koziolek M, Modeß C, Dokter A, Roustom T, Siegmund W, Weitschies W. Resolving the physiological conditions in bioavailability and bioequivalence studies: comparison of fasted and fed state. Eur J Pharm Biopharm. 2016;108:214–9.
18. Davis SS, Hardy JG, Fara JW. Transit of pharmaceutical dosage forms through the small intestine. Int J Pharm. 1986;27:886–92.
19. Committee for Medicinal Products for Human use, EMA Guideline on the investigation of bioequivalence, 2010
20. FDA. Bioequivalence studies with pharmacokinetic endpoints for drugs submitted under an ANDA. 2013.
21. Drugs.com. American Society of Health-System Pharmacists, Available: https://www.drugs.com/monograph/aspirin.html. 2016. Accessed 09/10/2021
22. Sørensen HT, Mellemkjær L, Blot WJ, Nielsen GL, Steffensen FH, McLaughlin JK, et al. Risk of upper gastrointestinal bleeding associated with use of low-dose aspirin. Am J Gastroenterol. 2000;95:2218–24.
23. Patrono C, Rodrogez LG, Landolfi R, Baigent C. Low-dose aspirin for the prevention of preeclampsia. N Engl J Med. 2005;3532:2373–83.
24. MPA. Public Assessment Report Scientific discussion. Acetylsalicylic acid Krka (acetylsalicylic acid). SE/H/1604/01-03/DC. 2016;1–8.
25. MPA. Public Assessment Report Scientific discussion. Peneprin (acetylsalicylic acid). SE/H/1021/002005/DC. 2011.

26. MPA. Public Assessment Report Scientific discussion. Acetylsalicylsyra Teva (acetylsalicylic acid). SE/H/1593/01-03/DC. 2016.
27. Garbacz G, Kołodziej B, Koziolek M, Weitschies W, Klein S. An automated system for monitoring and regulating the pH of bicarbonate buffers. AAPS PharmSciTech. 2013;14:517–22.
28. Liu F, Merchant HA, Kulkarni RP, Alkademi M, Basit AW. Evolution of a physiological pH 6.8 bicarbonate buffer system: application to the dissolution testing of enteric coated products. Eur J Pharm Biopharm. 2011;78:151–7.
29. Merchant HA, Goyanes A, Parashar N, Basit AW. Predicting the gastrointestinal behaviour of modified-release products: Utility of a novel dynamic dissolution test apparatus involving the use of bicarbonate buffers. Int J Pharm. 2014;475:585–91.
30. Shibata H, Yoshida H, Izutsu KI, Goda Y. Use of bicarbonate buffer systems for dissolution characterization of enteric-coated proton pump inhibitor tablets. J Pharm Pharmacol. 2016;68:467–74.
31. Al-Gousous J, Amidon GL, Langguth P. Toward biopredictive dissolution for enteric coated dosage forms. Mol Pharm. 2016;13:1927–36.
32. USP. Chapter 724-drug release - delayed-release (enteric-coated)articles-general drug release standard. 2012.
33. Committe for Medicinal Products for Human Use. Guideline on the investigation of bioequivalence [Internet]. 1997 [cited 2021 Dec 8]. Available from: http://www.ema.europa.eu.
34. EMA. ICH guideline M9 on biopharmaceutics classification system based biowaivers. 2018.
35. Interim Revision Announcement. Aspirin Delayed-Release Tablets. 2017;1–2.
36. USP. Chapter 711 - Dissolution. 2011.
37. European Pharmacopoeia. 2.9.3. Dissolution test for solid dosage forms. Eur Pharmacopoeia. 2010;10:326–33.
38. Russell TL, Berardi RR, Barnett JL, Dermentzoglou LC, Jarvenpaa KM, Schmaltz SP, et al. Upper gastrointestinal pH in seventy-nine healthy, elderly, north american men and women. Pharm Res. 1993;10:187–96 Available from: https://pubmed.ncbi.nlm.nih.gov/8456064/.

pharmaceutics

MDPI

Article

Multi-Compartmental Dissolution Method, an Efficient Tool for the Development of Enhanced Bioavailability Formulations Containing Poorly Soluble Acidic Drugs

Miklós Tamás Katona [1,2,*], Lili Nagy-Katona [3], Réka Szabó [2], Enikő Borbás [3], Péter Tonka-Nagy [2] and Krisztina Takács-Novák [1,*]

[1] Department of Pharmaceutical Chemistry, Semmelweis University, 7 Hőgyes Endre Street, H-1092 Budapest, Hungary
[2] Egis Pharmaceuticals PLC, 116-120 Bökényföldi Street, H-1165 Budapest, Hungary
[3] Department of Organic Chemistry and Technology, Budapest University of Technology and Economics, 3 Műegyetem rakpart, H-1111 Budapest, Hungary
* Correspondence: katona.miklos@egis.hu (M.T.K.); novak.krisztina@pharma.semmelweis-univ.hu (K.T.-N.)

Abstract: The purpose of this study was to investigate the applicability of the Gastrointestinal Simulator (GIS), a multi-compartmental dissolution model, to predict the in vivo performance of Biopharmaceutics Classification System (BCS) Class IIa compounds. As the bioavailability enhancement of poorly soluble drugs requires a thorough understanding of the desired formulation, the appropriate in vitro modelling of the absorption mechanism is essential. Four immediate release ibuprofen 200 mg formulations were tested in the GIS using fasted biorelevant media. In addition to the free acid form, ibuprofen was present as sodium and lysine salts in tablets and as a solution in soft-gelatin capsules. In the case of rapid-dissolving formulations, the dissolution results indicated supersaturation in the gastric compartment, which affected the resulting concentrations in the duodenum and the jejunum as well. In addition, a Level A in vitro–in vivo correlation (IVIVC) model was established using published in vivo data, and then the plasma concentration profiles of each formulation were simulated. The predicted pharmacokinetic parameters were consistent with the statistical output of the published clinical study. In conclusion, the GIS method was found to be superior compared to the traditional USP method. In the future, the method can be useful for formulation technologists to find the optimal technique to enhance the bioavailability of poorly soluble acidic drugs.

Keywords: multi-compartmental dissolution; solubility; supersaturation; IVIVC; ibuprofen; BCS Class IIa

Citation: Katona, M.T.; Nagy-Katona, L.; Szabó, R.; Borbás, E.; Tonka-Nagy, P.; Takács-Novák, K. Multi-Compartmental Dissolution Method, an Efficient Tool for the Development of Enhanced Bioavailability Formulations Containing Poorly Soluble Acidic Drugs. *Pharmaceutics* **2023**, *15*, 753. https://doi.org/10.3390/pharmaceutics15030753

Academic Editors: Anne Marie Healy and Dimitrios G. Fatouros

Received: 17 January 2023
Revised: 10 February 2023
Accepted: 22 February 2023
Published: 24 February 2023

1. Introduction

The formulation of poorly soluble drug substances into dosage forms with proper pharmacokinetics is a challenge for both original drug discovery and generic/value-added generic drug development. As the number of drug candidates is shifting towards high lipophilicity and poor water solubility, the importance of formulation strategies to enhance bioavailability is increasing [1]. In the case of BCS Class II (low solubility and high permeability) drugs, improved absorption can be achieved by increasing the dissolution rate of the formulation [2,3]. For this purpose, salt formation with the drug substance is perhaps the most common approach; however, pre-dissolving the drug in a lipid-based formulation, applying amorphous structures, or reducing particle size are also well-known techniques [4–6].

The in vitro dissolution testing is an important tool for characterizing the biopharmaceutical properties of a drug product at different stages throughout its life cycle. Compliance with the dissolution requirements ensures that the finished drug product is consistent with

the release rates of the active pharmaceutical ingredient (API) as determined in bioavailability studies during the clinical trials [7]. The results obtained need to be independent of the testing laboratory, therefore, reproducible methods in standardized equipment are to be used. Immediate-release drug products are generally tested in apparatus I and apparatus II, specified by the United States Pharmacopoeia (USP) [8]. However, such methods are usually not sufficient to represent the complex physiology of the gastrointestinal system. If the aim is to support pharmaceutical development by understanding the in vivo effect of different formulation techniques, the usage of advanced in vitro biopharmaceutics models may be necessary.

In order to achieve better predictivity, pharmaceutical scientists made great efforts to develop dynamic multi-compartmental dissolution systems [9]. A two-compartmental artificial stomach duodenal model (ASD) was published by Vatier et al. for the evaluation of the effect of antacids [10]. The ASD has also been used to aid formulation development and crystal form selection [11,12]. To date, several more complex systems have been reported in the literature, such as TNO gastro-Intestinal Model (TIM) [13], Dynamic Gastric Model (DGM) [14], and Human Gastric Simulator (HGM) [15]. Based on the ASD system, Takeuchi et al. developed the Gastrointestinal Simulator (GIS), which is a three-compartmental model consisting of a gastric, a duodenal, and a jejunal chamber connected by peristaltic pumps. The transfer rates (representing the gastric-emptying rate) were determined using propranolol and metoprolol model compounds by comparing the dissolution results with clinical data [16]. The GIS was successfully applied in several studies to predict the in vivo performance of drugs, investigate the supersaturation phenomena, or evaluate the possible drug-drug interaction with acid-reducing agents [17–21]. In order to achieve better in vitro–in vivo correlation (IVIVC), some of the models are combined with in silico simulations. The published studies focused primarily on BCS Class IIb (and BCS Class IIc) compounds. Despite the promising results achieved with the GIS system, to the best of our knowledge, poorly soluble acidic drugs (BCS Class IIa) have not yet been studied.

Non-Steroidal Anti-Inflammatory Drugs (NSAIDs) are well-known for their anti-inflammatory activities and analgesic, antipyretic effects [22]. In the case of analgesic indication, the patient's interest is to achieve the onset of pain relief as fast as possible [23], which is reported to be in direct correlation with the serum concentration of the active substance [24]. In general, the majority of NSAIDs have an acidic moiety (carboxylic acid, enol), with pK_a in the 3–5 range, attached to a planar, aromatic/heteroaromatic functionality [25]. The most widely used NSAIDs, such as diclofenac, ibuprofen, and naproxen, are classified as BCS Class IIa drugs [26–28]. These compounds are typically poorly soluble in the acidic gastric media, where the molecules are mostly present in an unionized free acid form. However, due to the ionization, they dissolve at the higher pH of the small intestinal fluids, which, together with high permeability, results in complete or almost complete absorption [26]. Ibuprofen is one of the most common analgesic/antipyretic agents. It is available in over-the-counter (OTC) strengths (100 mg and 200 mg) and prescription strengths (400 mg, 600 mg and 800 mg) as well. In case of OTC dosing, adults and children over 12 years old are advised to take 1 to 2 tablets (i.e., 200 mg to 400 mg) by mouth every 4 to 6 h while symptoms last; the maximum daily dose should not exceed six tablets (1200 mg) in 24 h [29]. In addition to the conventional tablet form, ibuprofen is marketed as different rapid-dissolving formulations (e.g., soft-gelatin capsules and tablets containing sodium or lysinate salts of the API). The rapid onset of the analgesic effect as well as the higher absorption rate of rapid-dissolving formulations, is discussed by several in vivo studies [24,30,31]. Legg et al. published the results of a five-period, crossover pharmacokinetic study in which fasted subjects received five different 400 mg ibuprofen dose equivalent formulations (as 2 × 200 mg tablets/capsules). According to the statistical analysis, ibuprofen-sodium and ibuprofen-lysinate, as well as Advil soft-gelatin capsules, were absorbed significantly faster but to a similar extent to standard ibuprofen formulations [23]. In a recent study, Cámara-Martinez et al. tested two different formulations containing ibuprofen in USP II dissolution apparatus. The tests were carried out using

different phosphate and maleate buffers with and without acidic pre-treatment of the tablets. Based on the results, they found the acidic pre-treatment to be important to find proper correlation with in vivo results [32].

The aim of this study was to investigate the applicability of multi-compartmental dissolution methods to predict the in vivo performance of BCS Class IIa compounds. For this purpose, different conventional and rapid-dissolving ibuprofen 200 mg formulations were tested using the GIS system with biorelevant dissolution media. The formulations were also dissolved with the quality control method of ibuprofen tablets according to USP [33], and the predictivity of each method was evaluated. To better understand the dissolution results, the pH-dependent equilibrium solubility of the API in Britton-Robinson (BR) buffers and the equilibrium solubility in biorelevant media were also determined using the saturation shake-flask method. Moreover, a Level A IVIVC model was established based on the GIS dissolution profiles and the clinical data published by Legg et al. [23].

2. Materials and Methods

2.1. Materials

Four commercially available immediate release ibuprofen-containing products were investigated. The formulations were purchased from pharmacies in the United States and Hungary. The tested products and their active ingredients are listed in Table 1.

Table 1. Dosage form and active ingredients of the tested products.

Product	Manufacturer	API Form	Abbreviation
Advil 200 mg coated tablets	Pfizer Consumer Healthcare, Madison, NJ, USA	ibuprofen free acid	IBU
Advil 256 mg film-coated tablets	Pfizer Consumer Healthcare, Madison, NJ, USA	ibuprofen sodium	IBU-Na
Dolowill RAPID 342 mg film-coated tablets	Goodwill Pharma, Szeged, Hungary	ibuprofen lysinate	IBU-Lys
Advil ULTRA 200 mg soft-gelatin capsules	Pfizer Consumer Healthcare, Madison, NJ, USA	Ibuprofen in solution	IBU-lq

Ibuprofen drug substance was purchased from Sigma–Aldrich (Burlington, VT, USA). All chemicals used were of analytical grade. The following chemicals were used: sodium-hydroxide; sodium-chloride; sodium dihydrogen phosphate monohydrate; hydrochloric acid; (Molar Chemicals Kft., Budapest, Hungary); acetonitrile (PanReac AppliChem, Darmstadt, Germany); phosphoric acid; (Emsure ACS. Reag. Ph. Eur., Budapest, Hungary); SIF powder (Biorelevant^{TM}, London, UK); and Pepsin (Sigma–Aldrich, Burlington, VT, USA).

2.2. Equilibrium Solubility Measurements

The saturation shake–flask method was used to determine the equilibrium solubility of the API [34,35]. The measurements were carried out at 37 ± 0.1 °C. Ibuprofen was added in an excess amount (100–600 mg) to 3–5 mL solvent in a stoppered flask. In case it was necessary, the pH was adjusted to the initial value with 1M NaOH solution after 1 h. The flasks were then placed in a GFL 1092 type shaking water bath (GFL GmbH, Burgwedel, Germany) and shaken at 150 rpm for 6 h. The agitation phase was followed by 18 h sedimentation at controlled temperature. A total of 3 aliquot (10–100 µL) samples were then taken from the saturated solution and diluted to the required extent (2–250x) with the tested medium. The concentration was measured by UV spectroscopy at λ_{max}: 264 nm. The UV detection was chosen because of its simplicity, taking into account the literature recommendations [35]. In each medium, the solubility experiments were performed in triplicate. The pH dependence of solubility was determined in BR buffers (a mixture of 0.04 M boric acid, 0.04 M phosphoric acid, and 0.04 M acetic acid titrated to the desired pH with 0.2 M sodium-hydroxide) in the pH range 2–8 (pH = 2.0; 4.0; 6.0; 7.0; 8.0) and in 1 M

NaOH (pH = 14). The equilibrium solubility was also investigated in biorelevant media modelling gastric and small intestinal fluid in a fasted and fed state with and without solubilizing agents (pepsin or lecithin and bile acid salts). The tested biorelevant media were Blank FaSSGF, FaSSGF, Blank FaSSIF, FaSSIF, FeSSGF-acetate (without milk), Blank FeSSIF, and FeSSIF. The solutions were prepared according to the media preparation tool of biorelevant.com [36].

2.3. Dissolution Testing

The dissolution tests were carried out using an Agilent 708 DS dissolution apparatus (Agilent Technologies, Inc., Santa Clara, CA, USA). The media were thermostated at 37 ± 0.5 °C. Each formulation in each method was tested on six parallel samples.

2.3.1. USP Dissolution Method

The tests were performed in a USP II (paddle) apparatus. The dissolution medium was pH 7.2 ± 0.5 phosphate buffer solution prepared by dissolving 6.89 g $NaH_2PO_4.H_2O$ in 1 L distilled water, and the pH was adjusted with 3 M NaOH solution. The samples were placed into a 900 mL medium and stirred at 50 rpm. Samples at 5, 15, 30, 45, and 60 min were taken into HPLC vials via autosampling. The volume of each sample was ~1.2 mL. The sampling cannulas were equipped with 10 µm PVDF full-flow filter tips (Agilent Technologies, Inc., Santa Clara, CA, USA).

2.3.2. GIS Dissolution Method

The GIS was implemented in a dissolution apparatus equipped with 250 mL small-volume vessels, according to Chinese Pharmacopoeia [37]. The system consisted of three main compartments (250 mL vessels) modelling the stomach, duodenum, and jejunum. The vessels were connected to each other by Gilson Minipuls 3-type peristaltic pumps (Gilson Inc., Middleton, WI, USA). At the beginning of the test, 50 mL pH1.6 gastric fluid and 250 mL water were poured into the stomach, 50 mL pH 6.5 intestinal fluid into the duodenum, and the jejunal chamber was left empty. Two additional vessels were used to model the inner fluid secretion into the stomach (pH 1.6 gastric fluid) and the duodenum (pH 6.5 intestinal fluid concentrate), both the stomach and duodenum had a flow rate of 1 mL/min. The biorelevant dissolution media were prepared, and the tests were conducted with and without biomolecules (pepsin, SIF powder). The composition of the applied buffer solutions is summarized in Table 2.

Table 2. Preparation of 1 L buffer solutions for GIS dissolution.

	Blank Biorelevant Media			**Biorelevant Media**		
	Blank FaSSGF	**Blank FaSSIF**	**Blank FaSSIF conc.**	**Full FaSSGF**	**Full FaSSIF**	**Full FaSSIF conc.**
NaCl	2.00 g	6.19 g	40.24 g	2.00 g	6.19 g	40.24 g
NaOH	-	0.40 g	2.60 g	-	0.40 g	2.60 g
$NaH_2PO_4.H_2O$	-	3.96 g	25.74 g	-	3.96 g	25.74 g
SIF powder	-	-	-	0.06 g	2.25 g	14.63 g
Pepsin	-	-	-	0.10 g	-	-
pH adjustment	cc. HCl:purified water = 1:1	1M NaOH	-	cc. HCl:purified water = 1:1	1M NaOH	-

The tested formulation was dropped into the gastric chamber, and the media were stirred at 50 rpm using rotating paddles. The applied flow rates were 5.5 mL/min from the gastric to the duodenal and 6.5 mL/min from the duodenal to the jejunal chamber, as suggested by Takeuchi et al. [16]. Samples from the compartments were taken manually every 5 min during the 45-min duration of the tests. The duration was limited by the initial

fluid volume and the gastric emptying rate. Each sample was filtered through Acrodisc® syringe filters (d = 13mm) with 0.45 µm GHP membrane (Pall Co., Port Washington, NY, USA). The volume of each sample was ~0.5 mL. The schematic diagram of the GIS system is shown in Figure 1.

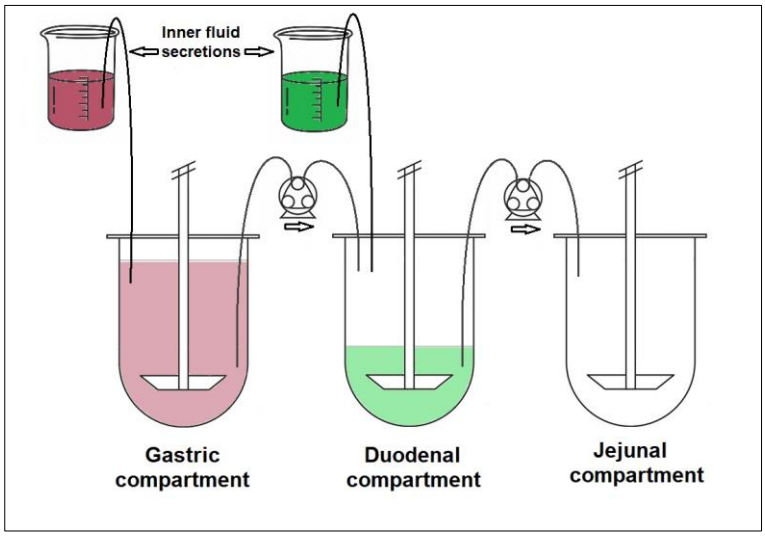

Figure 1. Gastrointestinal Simulator [16].

2.4. Determination of Dissolved Drug Content by High-Performance Liquid Chromatography (HPLC)

Waters Acquity-type UPLC device (Waters, Milford, MA, USA) was used to determine the amount of dissolved drug in the solutions. For this purpose, Waters Acquity BEH C18 1.7 µm (2.1 × 50 mm)-type UPLC column was used. The mobile phase was acetonitrile:H_2O:cc.H_3PO_4 = 450:550:1, and the flow rate was 0.7 mL/min. The mode of separation was isocratic. External calibration by five consecutive injections of a standard solution containing the concentration of API corresponding to the approximated concentration of 100% dissolution was applied. The calibration was controlled by the injection of the control standard solution containing the same nominal concentration, followed by the injection of the sample solutions. The absorbance was detected at 214 nm. For standard preparations, accurate measurements were achieved using a Mettler Toledo XP 26 microanalytical balance (Mettler Toledo, Columbus, OH, USA). The sample concentrations in mg/L were calculated using the dilution factor of the standard and the sample solutions and the peak areas of the sample solutions. The chromatographic conditions for each test preparation were the same as the column used for the measurement.

2.5. In Vitro In Vivo Correlation (IVIVC)

A Level A IVIVC model was developed using the IVIVC Toolkit 8.3. of Phoenix WinNonlin 8.3.4.295 for Windows (Certara, St. Louis, MO, USA). In vivo data were obtained by digitizing the mean plasma concentration profiles of four different ibuprofen formulations from a fasted state crossover pharmacokinetic study published by Legg et al. [23]. The administered formulations were identical to that of Table 1, except for IBU-Lys. In the case of IBU-Lys, Nurofen Express 342 mg caplets (Reckitt Benckiser, Slough, Berkshire, UK) were administered, the manufacturer of which differed from the formulation used in the in vitro studies. However, the salt form of the active ingredient was the same. A two-compartmental pk model (model 14 of pK tab) was then fitted to the data of each formulation. The gained parameters of Advil 200 mg tablets were implemented to the unit impulse response (UIR) function, and the fitted plasma concentration curve was deconvolved, resulting in the calculated fraction absorbed profile. The cumulative dissolution data of the duodenal and jejunal compartments of the GIS measured in blank biorelevant

media were fitted with the Weibull equation. The in vitro fraction dissolved and in vivo fraction absorbed of Advil 200 mg tablets were correlated using the Levy plot. Based on the calculated correlation and UIR function, the plasma concentration profile of each formulation was simulated from the fitted dissolution profiles. Finally, the plasma concentrations predicted from the model and the observed data were compared.

3. Results and Discussion

3.1. Thermodynamic Equilibrium Solubility Measurements

3.1.1. pH-Dependent Solubility

The pH-dependent solubility (S_{pH}) of ibuprofen was tested at 5 different pH values in the pH 2–8 range using BR buffer solutions. Additionally, the solubility of the fully ionized form was determined in 1M NaOH solution. The results obtained are summarized in Table 3, and the solubility/pH profile is shown in Figure 2.

Table 3. The pH-dependent equilibrium solubility of ibuprofen at 37 °C.

pH	S_{pH} ± SD (μg/mL) [1]	$\log S_{pH}$ (mol/L)
1.92	70.8 ± 3.0	−3.46
3.96	124 ± 13	−3.22
5.95	1910 ± 70	−2.03
7.17	32,033 ± 4135	−0.81
8.02	300,000 ± 6500	0.16
14	734,000 ± 30,500	0.55

[1] the results at each pH are the mean of 3 parallel measurements.

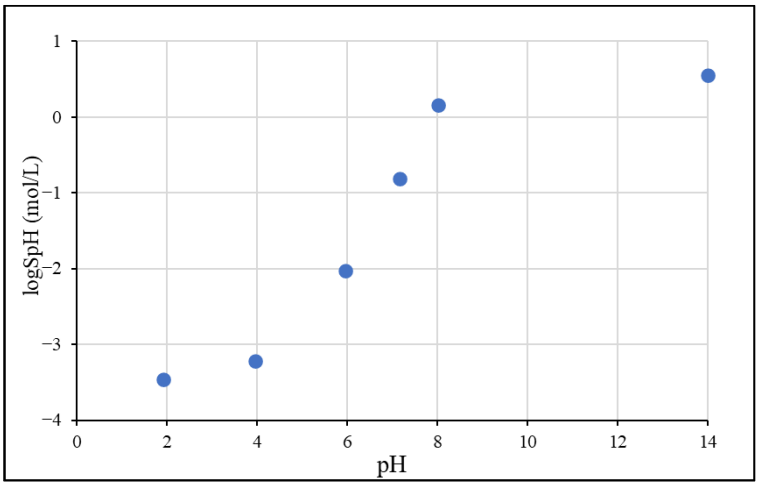

Figure 2. The solubility-pH profile of ibuprofen in Britton–Robinson buffers.

As expected from a weak acid compound with pK_a: 4.45, the solubility of ibuprofen is increasing according to the Henderson–Hasselbalch relationship in the pH 2–8 range and reaches a plateau at a higher pH due to the salt formation [38]. Below pH 5, the solubility is low, therefore, it can be assumed that from the formulations, the API can only partially dissolve in acidic gastric media. The measured equilibrium solubility in pH 2.0 BR buffer (logS = −3.46 mol/L) is consistent with the literature intrinsic solubility data ($\log S_0$ = −3.62) [39]. The small difference might be explained by the fact that the literature data were measured at 25 °C and that at pH 2.0, the molecules are mostly—but not totally—unionized; thus, a slightly higher value is expected compared to the intrinsic solubility.

3.1.2. Solubility in Biorelevant Media

The equilibrium solubility values in biorelevant media are listed in Table 4.

Table 4. Equilibrium solubility of ibuprofen in biorelevant media at 37 °C.

Solvent	$S_{pH} \pm SD$ (μg/mL) [1]
FaSSGF blank, pH 1.6	56.3 ± 0.6
FaSSGF, pH 1.6	56.0 ± 0.5
FeSSGF-acetate, pH 4.5	194 ± 2
FeSSIF blank, pH 5.0	416 ± 12
FeSSIF, pH 5.0	2103 ± 56
FaSSIF blank, pH 6.5	2513 ± 15
FaSSIF, pH 6.5	3160 ± 31

[1] the results at each pH are the mean of 3 parallel measurements.

Solubility data in biorelevant media are in accordance with results measured in BR buffers, showing that the pH significantly affects the solubility of ibuprofen. Changing the pH from 1.6 to 4.5, 5.0, and 6.5 results in a 3.4-fold, 7.4-fold, and 44.6-fold increase in solubility, respectively. Pepsin has no effect on solubility at gastric pH. However, the solubilizing effect of natural surfactants of the small intestine further increases the solubility: FaSSIF/FaSSIF blank 1.3-fold; and FeSSIF/FeSSIF blank 5-fold. In the case of FeSSIF, a greater solubilizing effect was observed, which can be explained by the higher concentration of taurocholate and lecithin.

3.2. Dissolution Results Obtained by the USP Method

The USP individual monograph of ibuprofen tablets suggests the dissolution of the formulations at pH 7.2 using USP II (Paddle) apparatus with 50 rpm [33]. The average dissolution profiles of each formulation (1 × 200 mg dosage unit per vessel) are presented in Figure 3.

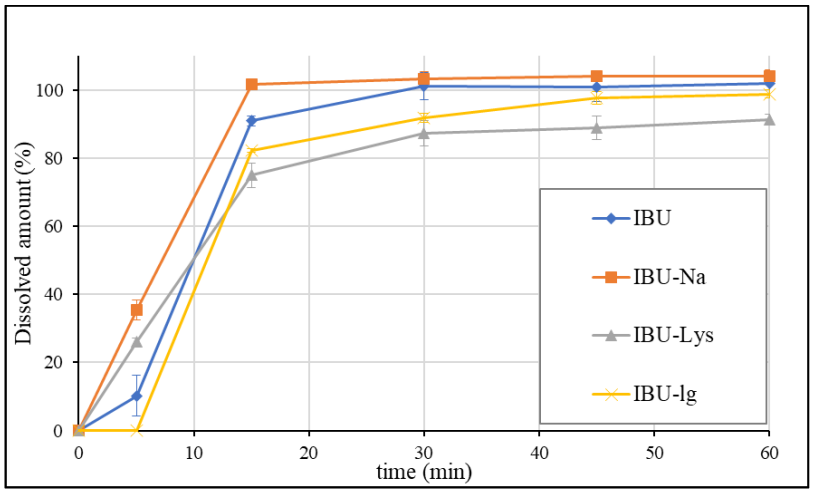

Figure 3. Dissolution results of ibuprofen formulations obtained by USP method.

According to the USP method, IBU and IBU-Na dissolved rapidly, as more than 85% of the drug substance dissolved in 15 min. The mean dissolved amount of IBU-lq was less than 85% in 15 min, however, its dissolution profile can be considered statistically similar to IBU based on the calculated similarity factor (f2 = 55). The dissolution rate of IBU-Lys was found to be significantly slower than that of IBU (f2 = 37). Overall, the USP method was unable to discriminate between rapid-release and standard ibuprofen formulations.

3.3. Dissolution Results Obtained by GIS Method

Since it is advised to take 1 to 2 tablets of the 200 mg dose strength formulations, 400 mg dose equivalents were administered in the published pharmacokinetic study, and the in vitro dissolution of IBU 1 × 200 mg tablets vs. 2 × 200 mg tablets was compared in blank biorelevant media. The average dissolution profiles in each compartment are presented in Figure 4.

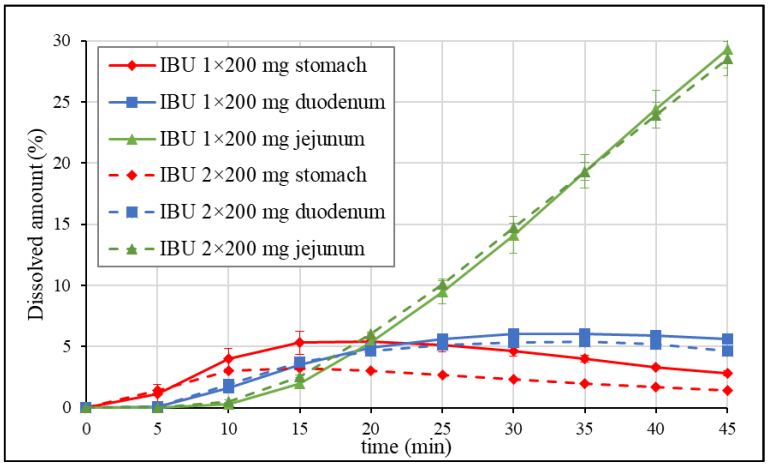

Figure 4. GIS dissolution results of IBU 1 × 200 mg vs. 2 × 200 mg tablets in blank biorelevant media.

Figure 4 shows that only a small amount of the API was dissolved in the stomach. Both dissolution profiles reached a maximum after 15 min, then a slow decrease was observed. The maximum of the curve represents the time when the gastric emptying rate of the API equals the dissolution rate. The difference in the percentage dissolved in the later stage of the test can be explained by reaching the equilibrium solubility limit (the different percentages belong to similar concentrations). The dissolution in the duodenum is determined by the composition of the suspension (dissolved API and suspended solid particles) entering the gastric chamber. Due to the higher equilibrium solubility in pH 6.5 blank FaSSIF (~2.5 mg/mL), the transferred solid particles are expected to dissolve. A dose-proportional dissolution profile was observed in this compartment and the jejunum. Since most of the absorption takes place in the upper small intestine, linear pharmacokinetics may be assumed based on the dissolution results.

The GIS dissolutions in blank biorelevant media were also performed with the other formulations. Figure 5 shows the obtained concentration profiles in the gastric compartment.

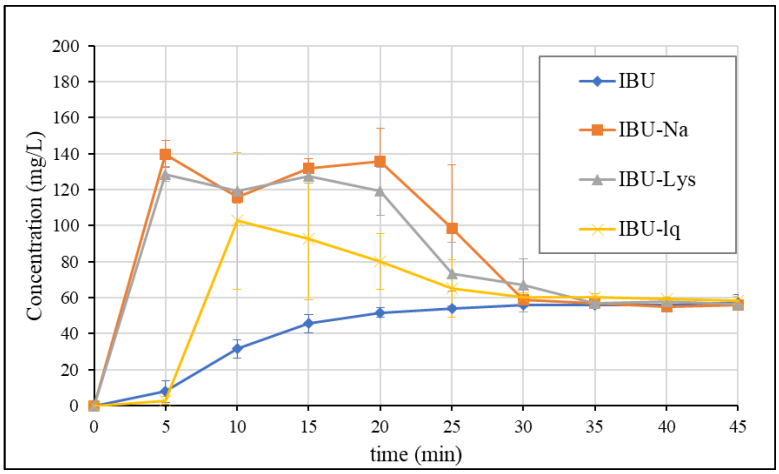

Figure 5. Gastric concentration profiles of ibuprofen formulations (1 × 200 mg) in blank biorelevant media.

The results show that rapid-release products form supersaturated solutions that precipitate over time. By the end of the measurement, the concentration of the API approaches the equilibrium solubility ($S_{BlankFaSSGF}$ = 56.3 mg/L) for all formulations. The degree of supersaturation is similar in the case of salt forms (IBU-Na: ~2.5× and IBU-Lys: ~2.3×) and somewhat less in the case of soft-gelatin capsules (IBU-lq: ~1.8×). The onset of release is delayed by ~5 min for IBU-lq, which is due to the disintegration of the capsule shell based on visual observation. The lack of supersaturation of IBU (free acid in conventional tablets) suggests that the obtained result of rapid-release products is a consequence of the applied formulation techniques (salt formation or pre-dissolved API).

Figure 6 shows the dissolution curves in the duodenal chamber (a) compared to the first 45 min of the published clinical results (b) [23].

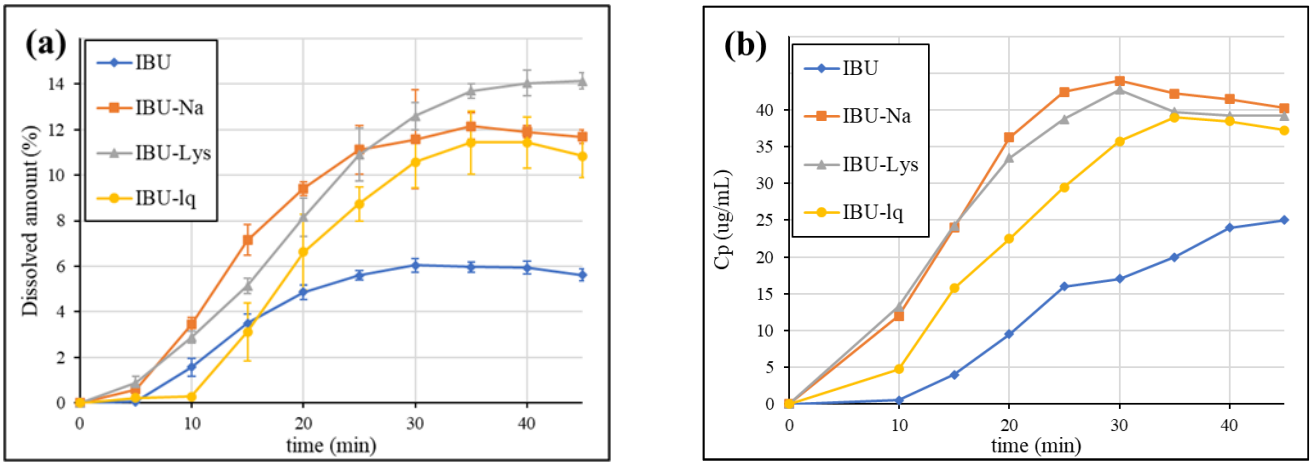

Figure 6. GIS duodenal dissolution in blank biorelevant media (**a**) vs. fasting BA study results (**b**) [23].

Based on the dissolution profiles of Figure 6a, the effect of gastric supersaturation results in a higher dissolved amount in the duodenum as well. All three rapid-release products reach a higher maximum concentration compared to the standard IBU formulation, which is consistent with the in vivo results. The plateau of IBU-Lys is slightly higher than that of IBU-Na and IBU-lq, which, however, was not experienced in vivo. It should be noted, though, that the formulations containing ibuprofen-lysinate salt tested in the in vitro and in vivo studies came from different manufacturers. In the case of IBU-lq, the delay in the onset of dissolution experienced in the gastric chamber persists in the duodenum and also appears in vivo.

The absorption of the API is expected in the entire upper small intestine, therefore, the sum of dissolution in the duodenum and jejunum compartments may correlate with the in vivo performance of the formulations. Thus, the results were also evaluated in this way. In addition to the GIS dissolutions in blank biorelevant media, the tests were also carried out in biorelevant media containing biomolecules. The obtained results are compared in Figure 7. The dissolution in the jejunum itself showed a very similar tendency to that of the sum of the two chambers. The results are shown in Figure S1 in the Supplementary Materials.

According to Figure 7, regardless of the addition of biomolecules, the dissolution rate of rapid-release formulations is higher than that of IBU (conventional tablet). The applied natural surfactants have only a small effect on the dissolution, which indicates that the increase in solubility (owing to the ionization caused by the pH shift between the stomach and the duodenum) is sufficient to dissolve the entering suspension. In general, the small intestinal dissolution of BCS Class IIa drugs in fasted conditions is expected to be much more influenced by the pH change (i.e., ionization) than by the presence of biomolecules (solubilizing effect). These findings are in agreement with previous study results [40]. The

simplification of biorelevant buffers by omitting the addition of biomolecules may be a cost-effective way of the GIS analysis without affecting the predictivity of the method.

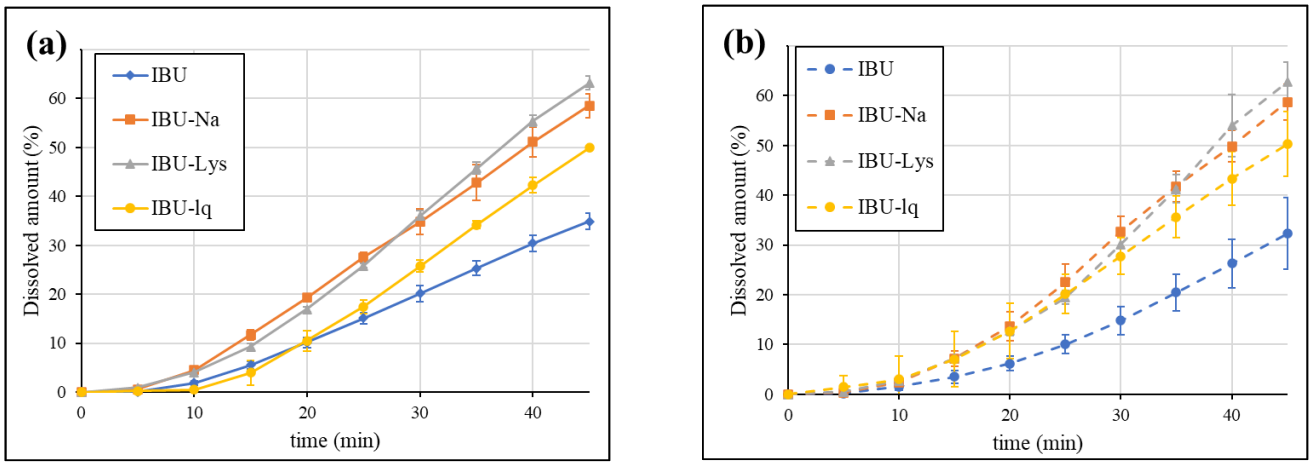

Figure 7. GIS sum of the amount dissolved in the duodenum and jejunum in blank biorelevant media (**a**) and biorelevant media (**b**).

Overall, the GIS results highlighted a complex process leading to enhanced absorption of rapid-dissolving ibuprofen formulations: The initial supersaturation is followed by precipitation in the acidic stomach; however, the continuous emptying of the supersaturated suspension resulted in a higher dissolution rate at the higher pH of the duodenum and the jejunum. The multi-compartmental design, as well as the appropriate modelling of the gastrointestinal pH conditions and fluid volumes, were essential to achieve the desired predictivity. In contrast, the USP dissolution method using a high volume of pH 7.2 phosphate buffer to ensure sink condition was unable to differentiate between conventional and enhanced bioavailability formulations.

3.4. Establishment of the IVIVC Model

IVIVC is a predictive mathematical model describing the relationship between an in vitro property and a relevant in vivo response. Level A correlation, which represents a point-to-point relationship, is considered to be the most informative and is recommended by the authorities whenever possible [41]. The IVIVC model was established to justify the predictivity of the GIS method. The correlation was built on the in vitro and in vivo data of IBU (internal batch), and then the plasma profiles of the other formulations were simulated based on the dissolution results (external batches).

3.4.1. Analysis of In Vivo Data

The mean plasma concentrations of the fasting crossover pharmacokinetic study published by Legg et al. [23]. were first digitized and then fitted using the pK module (Model 14: two-compartmental pK model) of the WinNonLin IVIVC Toolkit. The in vivo profiles are presented in Figure 8.

The estimated parameters of the model describing the plasma profile of IBU were applied as input parameters to calculate the UIR function. The estimated parameters were A1 = 50.32, A2 = 0.007514, alpha1 = 0.004773, and alpha2 = 0.004006. The UIR function enabled the deconvolution of plasma concentration profiles, resulting in the fraction absorbed curves, which are shown in Figure 9.

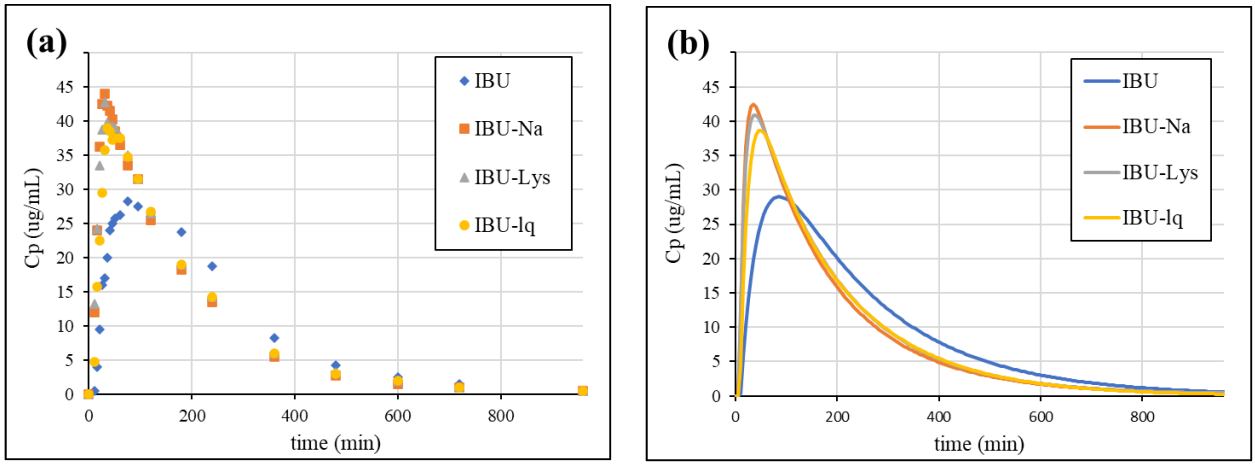

Figure 8. Published plasma concentration profiles (**a**) [23] vs. fitted curves (**b**).

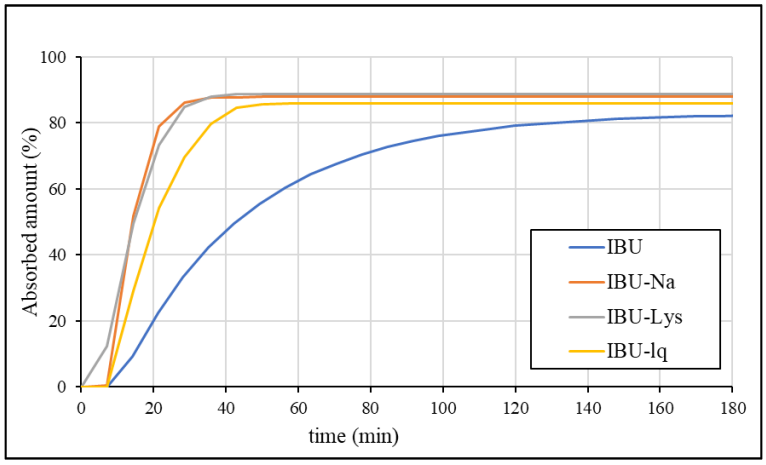

Figure 9. Absorption profiles obtained by deconvolution of clinical data [23].

3.4.2. Fitting of In Vitro Dissolution Data

The sum of the amount of dissolved curves in the duodenum and jejunum chambers of the GIS using blank biorelevant media was fitted with the Weibull function. The estimated parameters of the functions are listed in Table 5.

Table 5. Estimated parameters of the Weibull functions.

Formulation	B	MDT (min)
IBU	1.759	71.55
IBU-Na	1.786	48.23
IBU-Lys	2.087	44.55
IBU-lq	2.274	52.18

The calculated dissolution profiles fitted to the average data are shown in Figure 10.

Based on Figure 10, the calculated curves fit the experimental data well, however, extrapolation is required to describe the whole dissolution profile. Therefore, this phase of the profiles has a greater uncertainty. Comparing the in vitro (Figure 10) and the in vivo (Figure 9) data, it appears that there is a slightly greater difference in the absorption rate between IBU and the rapid-release formulations than in the observed dissolution rate.

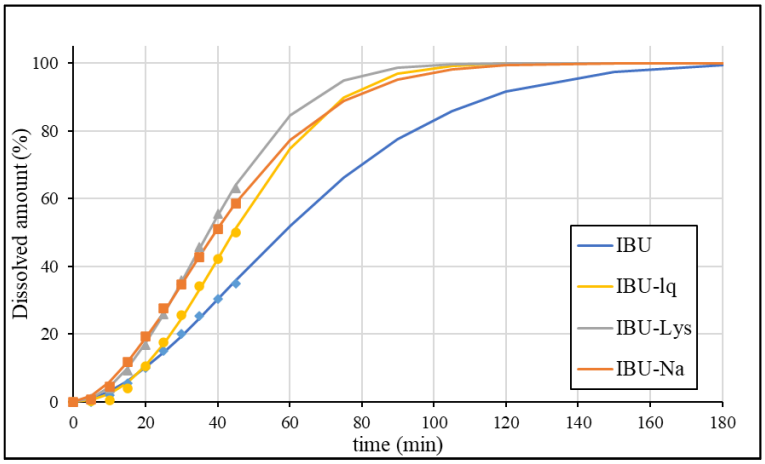

Figure 10. Fitted dissolution data using the Weibull function.

3.4.3. Correlation

The in vitro dissolution (from Weibull fitting) and the in vivo absorption (from deconvolution) of IBU were correlated using the Levy plot. The times corresponding to nominally the same dissolution (t_{Vitro}) and absorption (t_{Vivo}) were plotted, and the relationship was estimated using linear regression. The Levy plot is presented in Figure 11.

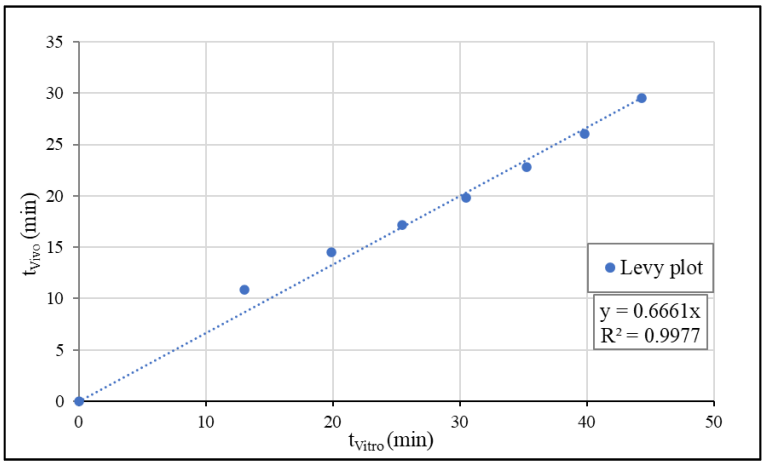

Figure 11. The Levy plot of IBU.

3.4.4. Simulation of Plasma Concentration Profiles

Based on the estimated correlation, we calculated the absorption curves from the dissolution of the formulations and then convolved using the UIR function, which resulted in the plasma concentration profiles. The simulated profiles are shown in Figure 12.

The Cmax values and their ratio compared to IBU from the statistical analysis of the individual plasma concentration profiles, the mean curves, and the IVIVC prediction is summarized in Table 6.

According to the summarized Cmax values, the ratios predicted based on IVIVC correlate more with the statistical analysis of the individual profiles than with the ratio of the mean profiles. The statistical output of a clinical study provides the most relevant description of the differences between the formulations of interest, however, mean profiles are usually used for modelling purposes in the absence of published individual data. The simulation of the plasma concentration profiles using the established IVIVC model was able to predict the enhanced absorption rate of the rapid-dissolving ibuprofen formulations. Higher Cmax and lower tmax values were obtained compared to IBU. For both parameters,

the differences were slightly underestimated. The rapid-release formulations were found to be similar to each other, which is also consistent with the in vivo data.

Table 6. Observed [23] vs. predicted pharmacokinetic data of ibuprofen formulations.

	Clinical Data Statistical Analysis of Individual Profiles			Clinical Data Mean Plasma conc. Profiles		IVIVC Prediction from GIS Dissolution		
Formulation	**Cmax**	**Ratio**	**tmax**	**Cmax**	**Ratio**	**Cmax**	**Ratio**	**tmax**
IBU	37.70	N/A	82.1	28.25	N/A	37.80	N/A	81.7
IBU-Na	47.00	1.25	35.2	44.00	1.56	41.00	1.09	60.5
IBU-Lys	49.90	1.32	35.1	42.75	1.51	42.40	1.12	61.4
IBU-lq	46.80	1.24	40.0	39.00	1.38	42.20	1.12	60.5

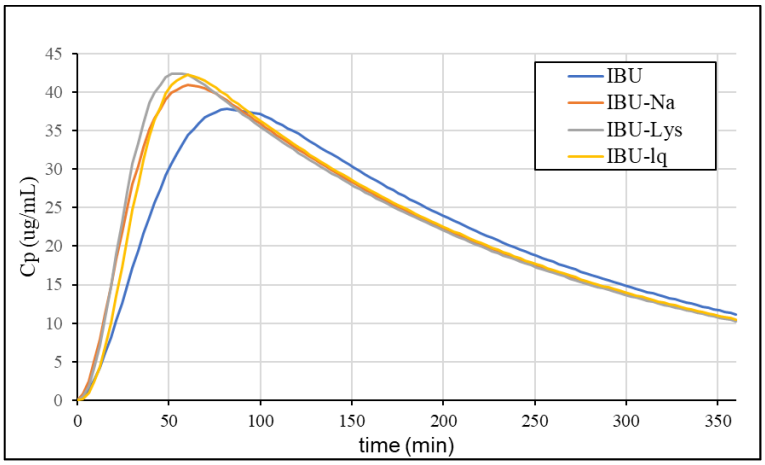

Figure 12. The simulated plasma concentration profiles of ibuprofen formulations.

4. Conclusions

The advanced in vivo predictivity of the GIS system for BCS Class IIb and Class IIc compounds has previously been studied in the literature. In the present paper, the better in vivo predictivity of the method was also demonstrated for immediate release formulations containing BCS Class IIa compounds, to which less attention was paid before. The key factors resulting in the superiority of the GIS compared to the USP method were the multi-compartmental design, the biorelevant fluid volumes and the pH change, which enabled the modelling of the complex mechanism behind the advanced absorption of rapid-dissolving ibuprofen formulations. It was found that pre-dissolving or salt formation of poorly soluble acidic compounds leads to temporary supersaturation in an acidic medium, which, thanks to the continuous gastric emptying, affects the resulting concentration in the upper small intestine as well. Both dissolution and solubility results indicated that the role of gastrointestinal pH conditions in the in vivo dissolution of poorly soluble, acidic drug substances is more significant compared to the solubilizing effect of biomolecules. In conclusion, the multi-compartmental GIS model using blank biorelevant media was found efficient in predicting the in vivo performance of ibuprofen formulations. Predicting the in vivo behaviour and providing a better understanding of the absorption process can both contribute to the successful development of enhanced bioavailability formulations containing BCS Class IIa drugs.

Supplementary Materials: The following supporting information can be downloaded at: https://www.mdpi.com/article/10.3390/pharmaceutics15030753/s1, Figure S1: GIS jejunal dissolution in blank biorelevant media.

Author Contributions: Conceptualization, M.T.K., K.T.-N., P.T.-N. and E.B.; methodology, M.T.K., K.T.-N., P.T.-N. and E.B.; software, M.T.K.; formal analysis, R.S., L.N.-K., M.T.K. and K.T.-N.; data curation, M.T.K.; writing—original draft preparation, M.T.K.; writing—review and editing, M.T.K. and K.T.-N.; visualization, L.N.-K. and M.T.K.; supervision, K.T.-N. All authors have read and agreed to the published version of the manuscript.

Funding: This research received no external funding.

Institutional Review Board Statement: Not applicable.

Informed Consent Statement: Not applicable.

Data Availability Statement: Not applicable.

Conflicts of Interest: The authors declare no conflict of interest.

Abbreviations

API	Active pharmaceutical ingredient
ASD	Artificial stomach duodenal model
BCS	Biopharmaceutics Classification System
BR	Britton–Robinson
DGM	Dynamic Gastric Model
GIS	Gastrointestinal Simulator
HPLC	High-Performance Liquid Chromatography
HGM	Human Gastric Simulator
IVIVC	In vitro–In vivo correlation
NSAID	Non-Steroidal Anti-Inflammatory Drug
S_{pH}	PH-dependent solubility
TIM	TNO gastro-Intestinal Model
UIR	Unit impulse response
USP	United States Pharmacopoeia

References

1. Stegemann, S.; Leveiller, F.; Franchi, D.; de Jong, H.; Linden, H. When poor solubility becomes an issue: From early stage to proof of concept. *Eur. J. Pharm. Sci.* **2007**, *31*, 249–261. [CrossRef] [PubMed]
2. Amidon, G.L.; Lennernäs, H.; Shah, V.P.; Crison, J.R. A Theorical Basis for a Biopharmaceutic Drug Classification: The Correlation of In Vitro Drug Product Dissolution and In Vivo Bioavailability. *Pharm. Res.* **1995**, *12*, 413–420. [CrossRef] [PubMed]
3. Dahlgren, D.; Sjögren, E.; Lennernäs, H. Intestinal absorption of BCS class II drugs administered as nanoparticles: A review based on in vivo data from intestinal perfusion models. *ADMET DMPK* **2020**, *8*, 375–390. [CrossRef] [PubMed]
4. Serajuddin, A.T.M. Salt formation to improve drug solubility. *Adv. Drug Deliv. Rev.* **2007**, *59*, 603–616. [CrossRef] [PubMed]
5. Kanaujia, P.; Poovizhi, P.; Ng, W.K.; Tan, R.B.H. Amorphous formulations for dissolution and bioavailability enhancement of poorly soluble APIs. *Powder Technol.* **2015**, *285*, 2–15. [CrossRef]
6. Kumar, R.; Thakur, A.K.; Chaudhari, P.; Banerjee, N. Particle Size Reduction Techniques of Pharmaceutical Compounds for the Enhancement of Their Dissolution Rate and Bioavailability. *J. Pharm. Innov.* **2022**, *17*, 333–352. [CrossRef]
7. Agilent Dissolution Seminar Series. Available online: https://www.agilent.com/cs/library/flyers/Public/Dissolution_Seminar_Series.pdf (accessed on 10 January 2023).
8. USP Chapter 711—Dissolution. Available online: https://www.usp.org/sites/default/files/usp/document/harmonization/gen-method/stage_6_monograph_25_feb_2011.pdf (accessed on 9 February 2023).
9. Kostewicz, E.S.; Abrahamsson, B.; Brewster, M.; Brouwers, J.; Butler, J.; Carlert, S.; Dickinson, P.A.; Dressman, J.; Holm, R.; Klein, S.; et al. In vitro models for the prediction of in vivo performance of oral dosage forms. *Eur. J. Pharm. Sci.* **2014**, *57*, 342–366. [CrossRef]
10. Vatier, J.; Malikova-Sekera, E.; Vitre, M.T.; Mignon, M. An artificial stomach-duodenum model for the in-vitro evaluation of antacids. *Aliment. Pharmacol. Ther.* **1992**, *6*, 447–458. [CrossRef]
11. Carino, S.R.; Sperry, D.C.; Hawley, M. Relative bioavailability estimation of carbamazepine crystal forms using an artificial stomach-duodenum model. *J. Pharm. Sci.* **2006**, *95*, 116–125. [CrossRef]
12. Bhattachar, S.N.; Perkins, E.J.; Tan, J.S.; Burns, L.J. Effect of gastric pH on the pharmacokinetics of a BCS Class II compound in dogs: Utilization of an artificial stomach and duodenum dissolution model and GastroPlus,™ simulations to predict absorption. *J. Pharm. Sci.* **2011**, *100*, 4756–4765. [CrossRef]

13. Minekus, M.; Smeets-Peeters, M.; Havenaar, R.; Bernalier, A.; Fonty, G.; Marol-Bonnin, S.; Alric, M.; Marteau, P.; Huis In't Veld, J.H.J. A computer-controlled system to simulate conditions of the large intestine with peristaltic mixing, water absorption and absorption of fermentation products. *Appl. Microbiol. Biotechnol.* **1999**, *53*, 108–114. [CrossRef] [PubMed]
14. Wickham, M.J.S.; Faulks, R.M.; Mann, J.; Mandalari, G. The design, operation, and application of a dynamic gastric model. *Dissolution Technol.* **2012**, *19*, 15–22. [CrossRef]
15. Kong, F.; Singh, R.P. A Human Gastric Simulator (HGS) to Study Food Digestion in Human Stomach. *J. Food Sci.* **2010**, *75*, E627–E635. [CrossRef] [PubMed]
16. Takeuchi, S.; Tsume, Y.; Amidon, G.E.; Amidon, G.L. Evaluation of a three compartment in Vitro gastrointestinal simulator dissolution apparatus to predict in Vivo dissolution. *J. Pharm. Sci.* **2014**, *103*, 3416–3422. [CrossRef] [PubMed]
17. Tsume, Y.; Takeuchi, S.; Matsui, K.; Amidon, G.E.; Amidon, G.L. In vitro dissolution methodology, mini-Gastrointestinal Simulator (mGIS), predicts better in vivo dissolution of a weak base drug, dasatinib. *Eur. J. Pharm. Sci.* **2015**, *76*, 203–212. [CrossRef]
18. Tsume, Y.; Matsui, K.; Searls, A.L.; Takeuchi, S.; Amidon, G.E.; Sun, D.; Amidon, G.L. The impact of supersaturation level for oral absorption of BCS class IIb drugs, dipyridamole and ketoconazole, using in vivo predictive dissolution system: Gastrointestinal Simulator (GIS). *Eur. J. Pharm. Sci.* **2017**, *102*, 126–139. [CrossRef]
19. Tsume, Y.; Igawa, N.; Drelich, A.J.; Amidon, G.E.; Amidon, G.L. The Combination of GIS and Biphasic to Better Predict In Vivo Dissolution of BCS Class IIb Drugs, Ketoconazole and Raloxifene. *J. Pharm. Sci.* **2018**, *107*, 307–316. [CrossRef]
20. Tsume, Y.; Igawa, N.; Drelich, A.J.; Ruan, H.; Amidon, G.E.; Amidon, G.L. The in vivo predictive dissolution for immediate release dosage of donepezil and danazol, BCS class IIc drugs, with the GIS and the USP II with biphasic dissolution apparatus. *J. Drug Deliv. Sci. Technol.* **2020**, *56*, 1–9. [CrossRef]
21. Hens, B.; Bermejo, M.; Tsume, Y.; Gonzalez-Alvarez, I.; Ruan, H.; Matsui, K.; Amidon, G.E.; Cavanagh, K.L.; Kuminek, G.; Benninghoff, G.; et al. Evaluation and optimized selection of supersaturating drug delivery systems of posaconazole (BCS class 2b) in the gastrointestinal simulator (GIS): An in vitro-in silico-in vivo approach. *Eur. J. Pharm. Sci.* **2018**, *115*, 258–269. [CrossRef]
22. Day, R.O.; Graham, G.G. NSAIDs and their Indications. In *Encyclopedia of Pain*; Springer: Berlin/Heidelberg, Germany, 2007; pp. 1460–1463.
23. Legg, T.J.; Laurent, A.L.; Leyva, R.; Kellstein, D. Ibuprofen Sodium Is Absorbed Faster than Standard Ibuprofen Tablets: Results of Two Open-Label, Randomized, Crossover Pharmacokinetic Studies. *Drugs R. D* **2014**, *14*, 283–290. [CrossRef]
24. Laska, E.M.; Sunshine, A.; Marrero, I.; Olson, N.; Siegel, C.; McCormick, N. The correlation between blood levels of ibuprofen and clinical analgesic response. *Clin. Pharmacol. Ther.* **1986**, *40*, 1–7. [CrossRef] [PubMed]
25. DeRuiter, J. Non-Steroidal Antiinflammatory Drugs (NSAIDS). 2002. Available online: http://webhome.auburn.edu/~deruija/nsaids_2002.pdf (accessed on 21 February 2023).
26. Van Den Abeele, J.; Brouwers, J.; Mattheus, R.; Tack, J.; Augustijns, P. Gastrointestinal Behavior of Weakly Acidic BCS Class II Drugs in Man—Case Study of Diclofenac Potassium. *J. Pharm. Sci.* **2016**, *105*, 687–696. [CrossRef] [PubMed]
27. Khalid, F.; Farid Hassan, S.M.; Noor, R.; Zaheer, K.; Hassan, F.; Muhammad, I.N. Possibility of extending biopharmaceutics classification system based biowaiver to BCS class IIa drug. *Pak. J. Pharm. Sci.* **2019**, *32*, 2065–2073. [PubMed]
28. Fu, Q.; Lu, H.D.; Xie, Y.F.; Liu, J.Y.; Han, Y.; Gong, N.B.; Guo, F. Salt formation of two BCS II drugs (indomethacin and naproxen) with (1R, 2R)-1,2-diphenylethylenediamine: Crystal structures, solubility and thermodynamics analysis. *J. Mol. Struct.* **2019**, *1185*, 281–289. [CrossRef]
29. Advil Package Insert. Available online: https://www.medicines.org.uk/emc/files/pil.11165.pdf (accessed on 15 January 2023).
30. Brain, P.; Leyva, R.; Doyle, G.; Kellstein, D. Onset of analgesia and efficacy of ibuprofen sodium in postsurgical dental pain: Randomized, placebo-controlled study versus standard ibuprofen. *Clin. J. Pain* **2015**, *31*, 444–450. [CrossRef]
31. Schettler, T.; Paris, S.; Pellett, M.; Kidner, S.; Wilkinson, D. Comparative pharmacokinetics of two fast-dissolving oral ibuprofen formulations and a regular-release ibuprofen tablet in healthy volunteers. *Clin. Drug Investig.* **2001**, *21*, 73–78. [CrossRef]
32. Cámara-Martinez, I.; Blechar, J.A.; Ruiz-Picazo, A.; Garcia-Arieta, A.; Calandria, C.; Merino-Sanjuan, V.; Langguth, P.; Gonzalez-Alvarez, M.; Bermejo, M.; Al-Gousous, J.; et al. Level A IVIVC for immediate release tablets confirms in vivo predictive dissolution testing for ibuprofen. *Int. J. Pharm.* **2022**, *614*, 121415. [CrossRef]
33. USP Monograph-Ibuprofen Tablets. Available online: http://www.pharmacopeia.cn/v29240/usp29nf24s0_m39890.html (accessed on 15 January 2023).
34. Baka, E.; Comer, J.E.A.; Takács-Novák, K. Study of equilibrium solubility measurement by saturation shake-flask method using hydrochlorothiazide as model compound. *J. Pharm. Biomed. Anal.* **2008**, *46*, 335–341. [CrossRef]
35. Avdeef, A.; Fuguet, E.; Llinàs, A.; Ràfols, C.; Bosch, E.; Völgyi, G.; Verbic, T.; Boldyreva, E.; Takács-Novák, K. Equilibrium solubility measurement of ionizable drugs—Consensus recommendations for improving data quality. *ADMET DMPK* **2016**, *4*, 117–178. [CrossRef]
36. Biorelevant Media Preparation Protocol. Available online: https://biorelevant.com/#media_prep_tool_tab (accessed on 15 January 2023).
37. Appendix X—Dissolution Test. In *Chinese Pharmacopoeia*; China Medical Science and Technology Press: Beijing, China, 2010; pp. A105–A107.
38. Völgyi, G.; Baka, E.; Box, K.J.; Comer, J.E.A.; Takács-Novák, K. Study of pH-dependent solubility of organic bases. Revisit of Henderson-Hasselbalch relationship. *Anal. Chim. Acta* **2010**, *673*, 40–46. [CrossRef]

39. Avdeef, A. Solubility. In *Absorption and Drug Development*; John Wiley & Sons: Hoboken, NJ, USA, 2012; pp. 252–308. ISBN 3175723993.
40. Takács-Novák, K.; Szoke, V.; Völgyi, G.; Horváth, P.; Ambrus, R.; Szabó-Révész, P. Biorelevant solubility of poorly soluble drugs: Rivaroxaban, furosemide, papaverine and niflumic acid. *J. Pharm. Biomed. Anal.* **2013**, *83*, 279–285. [CrossRef] [PubMed]
41. FDA Extended Release Oral Dosage Forms: Development, Evaluation, and Application of In Vitro/In Vivo Correlations. Available online: https://www.fda.gov/regulatory-information/search-fda-guidance-documents/extended-release-oral-dosage-forms-development-evaluation-and-application-vitroin-in-vivo-correlations (accessed on 15 January 2023).

pharmaceutics

MDPI

Article

On Absorption Modeling and Food Effect Prediction of Rivaroxaban, a BCS II Drug Orally Administered as an Immediate-Release Tablet

Varun Kushwah [1], Sumit Arora [1,2], Miklós Tamás Katona [3], Dattatray Modhave [1,4], Eleonore Fröhlich [1,5] and Amrit Paudel [1,6,*]

1 Research Center Pharmaceutical Engineering (RCPE) GmbH, Inffeldgasse 13, 8010 Graz, Austria; varun.kushwah@rcpe.at (V.K.); sumit0607@gmail.com (S.A.); datta.niper@gmail.com (D.M.); eleonore.froehlich@medunigraz.at (E.F.)
2 Simcyp Division, Certara UK Limited, Level 2-Acero, Sheffield S1 2BJ, UK
3 Department of Pharmaceutical Chemistry, Semmelweis University, Hőgyes Endre u. 9., H-1092 Budapest, Hungary; Katona.Miklos@egis.hu
4 Galapagos, Analytical Development CMC, Generaal De Wittelaan L11 A3, 2800 Mechelen, Belgium
5 Center for Medical Research, Medical University of Graz, Stiftingtalstr. 24, 8010 Graz, Austria
6 Institute for Process and Particle Engineering, Graz University of Technology, Inffeldgasse 13, 8010 Graz, Austria
* Correspondence: amrit.paudel@tugraz.at; Tel.: +43-316-873-30912

Abstract: The present work evaluates the food effect on the absorption of rivaroxaban (Riva), a BCS II drug, from the orally administered commercial immediate-release tablet (Xarelto IR) using physiologically based pharmacokinetic (PBPK) and conventional in vitro–in vivo correlation (IVIVC) models. The bioavailability of Riva upon oral administration of Xarelto IR tablet is reported to exhibit a positive food effect. The PBPK model for Riva was developed and verified using the previously reported in vivo data for oral solution (5 and 10 mg) and Xarelto IR tablet (5 and 10 mg dose strength). Once the PBPK model was established, the in vivo performance of the tablet formulation with the higher dose strength (Xarelto IR tablet 20 mg in fasted and fed state) was predicted using the experimentally obtained data of in vitro permeability, biorelevant solubility and in vitro dynamic dissolution data using United States Pharmacopeia (USP) IV flow-through cell apparatus. In addition, the mathematical IVIVC model was developed using the in vitro dissolution and in vivo profile of 20 mg strength Xarelto IR tablet in fasted condition. Using the developed IVIVC model, the pharmacokinetic (PK) profile of the Xarelto IR tablet in fed condition was predicted and compared with the PK parameters obtained via the PBPK model. A virtual in vivo PK study was designed using a single-dose, 3-treatment cross-over trial in 50 subjects to predict the PK profile of the Xarelto®IR tablet in the fed state. Overall, the results obtained from the IVIVC model were found to be comparable with those from the PBPK model. The outcome from both models pointed to the positive food effect on the in vivo profile of the Riva. The developed models thus can be effectively extended to establish bioequivalence for the marketed and novel complex formulations of Riva such as amorphous solid dispersions.

Keywords: in vitro–in vivo correlation; physiologically based pharmacokinetic model; BCS Class II; Rivaroxaban; Xarelto; food effect; population kinetics

Citation: Kushwah, V.; Arora, S.; Tamás Katona, M.; Modhave, D.; Fröhlich, E.; Paudel, A. On Absorption Modeling and Food Effect Prediction of Rivaroxaban, a BCS II Drug Orally Administered as an Immediate-Release Tablet. *Pharmaceutics* **2021**, *13*, 283. https://doi.org/10.3390/pharmaceutics13020283

Academic Editor: Luisa Di Marzio
Received: 23 January 2021
Accepted: 12 February 2021
Published: 20 February 2021

1. Introduction

Developing and deploying approaches that enable predicting the in vivo efficacy and safety profile of pharmaceutical drug products enormously expedite the product and process development effort as well as reduce the need for expensive clinical studies. For solid oral dosages, a thorough biopharmaceutical characterization at the in vitro level, such as solubility and dissolution testing using biorelevant media, study of food–formulation

interaction, in vitro membrane permeability and drug transport studies etc., provides the input data for in vivo absorption prediction. In recent years, prominent progress has been made in the in vitro biopharmaceutics profiling as well as in silico modeling for solid drug products [1]. A set of biorelevant and clinically relevant in silico models are expected to account for the critical formulation and physiological factors to facilitate the correlation between in vitro drug dissolution and in vivo pharmacokinetic profiles.

A widely accepted approach to assess the correlation between in vitro dissolution and in vivo bioavailability of an immediate-release (IR) drug product is based on the Biopharmaceutics Classification System (BCS). The BCS categorizes drug substances into one of four classes based on their solubility and permeability. In general, BCS Class I (highly soluble and highly permeable) drugs are well-absorbed. The rate-limiting step to absorption is dissolution or gastric emptying. In vitro–in vivo correlation (IVIVC) is expected if dissolution rate is slower than gastric emptying rate. In the case of IR drug products containing BCS Class II drug substance (dissolution as a rate-limiting step for absorption), conventional IVIVC can be used to establish the (cor)relation between the in vitro drug release and in vivo plasma concentration. Dissolution media and methods that reflect the in vivo controlling process are particularly important in this case if good in vitro–in vivo correlations are to be obtained. For BCS Class III drugs (for which permeability is the rate-limiting step for absorption), limited or no IVIV correlation is expected with the dissolution rate. Drug products containing BCS Class IV drug substance (low solubility and low permeability) has to be evaluated case by case; however, these drugs exhibit poor and variable bioavailability [2,3].

IVIVC is a predictive mathematical model describing the relationship between an in vitro property and a relevant in vivo response. In the case of immediate release dosage forms, the main objective of an IVIVC is to reduce the number of BE studies via supporting the optimization of the drug formulation. A Level A IVIVC is usually established by a two-stage procedure: in vivo absorption is estimated using an appropriate deconvolution technique (e.g., Wagner-Nelson, Loo-Riegelman, numerical deconvolution) followed by the comparison of drug absorbed to the fraction of drug dissolved. Even though the deconvolution method is often applied for regulatory submission, the method is limited to linear pharmacokinetics (PK) regimen [4].

Alternatively, the mechanistic deconvolution using the physiologically based pharmacokinetic (PBPK) modeling popularly known as physiologically based IVIVC (PB-IVIVC) is nowadays extensively utilized for biopharmaceutics modeling [5,6]. Besides its applicability to the nonlinear PK, the PBPK model also considers the different factors governing the drug release and absorption such as particle size of the API, food effect, pH-dependent solubility profile, precipitation, gastric emptying time, drug degradation, drug solubilization in the presence of excess bile acids and permeation across the intestinal membranes [7–10].

In the present work, we established both PB-IVIVC and conventional (numerical) IVIVC models for the immediate release oral tablet (Xarelto) formulations containing Rivaroxaban (Riva), a BCS II anti-coagulant drug. Riva is reported to exhibit dose-dependent food effects. More precisely, while the lower dose (10 mg) can be taken with or without food, the highest dose strength tablet (20 mg) should be taken with food to attain the positive food effect for oral absorption and systemic availability [6]. As per the regulatory requirement, clinical trials are required to establish bioequivalence between the innovator and generic drug products containing the BCS II drug, and especially exhibiting a food effect. As the critical formulation and drug product information of Riva is still covered by patent protection and no biowaiver exists, the design of a generic formulation containing this drug can be a challenge, especially considering the food effect displayed by the highest dose strength [11,12]. Here, we first developed an in silico PBPK model using the fasted conditions and low-dose formulations. On the basis of developed models, the PK profile of Xarelto formulations of the highest dose strength was predicted in fed conditions. The in vitro permeability of Riva as the pure API alone, and in the reference formulations (Xarelto® IR tablet) was determined using Caco-2 cell lines. Using combined

in vitro solubility, dissolution, and permeation data with literature data as the input in the developed PBPK model, the extent of food effect in vivo on the oral absorption of the drug was predicted by mimicking the fed state condition using biorelevant media. In addition, a conventional IVIVC model was established using the two-stage deconvolution method. The dissolution of Xarelto 20 mg IR tablet in USP IV apparatus was determined both in fasted and fed biorelevant media. The correlation was built based on the experimental in vitro dissolution data in fasted media and the mean in vivo plasma concentration profile in the fasted state obtained from the literature. Thereafter, the correlation was used to predict the in vivo profile in the fed state based on the in vitro dissolution in fed biorelevant media. The predicted results of the IVIVC model were compared with the PBPK model. Lastly, a virtual bioequivalence trial was performed to assess the performance of formulation in the fed state taking into consideration the population variability.

2. Materials and Methods

2.1. Chemical and Reagents

The reference formulations (Xarelto^{TM} of 20 mg strength IR tablet) were acquired from the market. Caco-2 cell line was purchased from American Type Culture Collection (ATCC) (Rockville, MD, USA). Minimal Essential Medium (MEM), fetal bovine serum (FBS), L-glutamine, trypsin (0.25%)-EDTA (1 mM), and penicillin-streptomycin mixture were purchased from Sigma (Vienna, Austria). Simulated fluid powders were purchased from Biorelevant.com Ltd, the UK, for the cell culture studies. Whereas for the solubility and dissolution studies, the simulated media were prepared using sodium taurocholate, lecithin and pepsin purchased from Sigma. The milk used for the solubility studies were purchased from the local market with a natural fat content of 3.5% fat. All other chemicals were of analytical reagent grade.

2.2. Software

Simulations were performed using the advanced compartmental absorption and transit model (ACAT) model implemented in the GastroPlus^{TM} (version 9.0., Simulation Plus, Inc., Lancaster, CA, USA). The ACAT model serves as a bridge between the formulation performance and PK parameters of the drug products and hence provides a valuable tool to guide formulation development to achieve the desired quality target product profile. In addition, the simulations from the ACAT models were verified using the conventional IVIVC model developed using the IVIVC Toolkit of Phoenix WinNonlin, Certara, NJ, USA.

2.3. Chromatographic Quantitative Analysis

Ultra-High-Performance Liquid Chromatography (UHPLC) was used to quantify Riva in the samples obtained during in vitro dissolution, solubility, and permeability. A Waters Acquity H-Class instrument (Milford, CT, USA) equipped with a PDA detector (operating at a wavelength value of 248 nm) was used. The column used was Acquity UPLC BEH C18, 1.7 µm, 2.1 mm × 50 mm (Waters), and the mobile phase was 3:7 (*v/v*) mixture of acetonitrile and 0.1M Ammonium-acetate buffer. The analysis was performed applying isocratic elution at the flow rate of 0.5 ml min^{-1}. The injection volume was 2 µL, and the total run time was 5 min. The dissolved amount of Riva was determined based on the area under the appropriate peak and using external standard calibration.

2.4. Biopharmaceutical Properties of Riva

2.4.1. Biorelevant Solubility Determination

Equilibrium solubility of Riva was determined in water, fasted state simulated gastric fluid (FaSSGF), fed state simulated gastric fluid (FeSSGF), fasted state simulated intestinal fluid (FaSSIF), and fed state simulated intestinal fluid (FeSSIF). All the simulated fluids (version 01) were prepared fresh on the day of the experiments conducted. In the case of FaSSIF media, 3 mM and 0.75 mM, and for FeSSIF, 15 mM and 3.75 mM of the sodium taurocholate and lecithin were used, respectively. The FaSSGF media contain 0.08 mM

and 0.02 mM sodium taurocholate and lecithin, whereas the FeSSGF media were prepared using an equivalent amount of milk and monobasic sodium phosphate buffer of pH 5. The concentration of different components of the media in detail is mentioned in Table S1 of the Supplementary Materials.

For the solubility determination, an excess amount of the pure drug was added to 5 mL of different simulated fluids. Thereafter, the sample was incubated at RT for 24 h with gentle shaking at 100 rpm using a rotatory shaker. The samples were then filtered using 0.22 µm syringe filter, and the filtrate was analyzed using UHPLC [13,14]. The solubility results of Riva obtained in different simulated media were incorporated in GastroPlus™.

2.4.2. In vitro Dynamic Biorelevant Dissolution

Dynamic dissolution of Xarelto™ (20 mg) tablets were carried out using USP Apparatus 4 fitted with 12 mm tablet cell using the media mimicking both the fasted and fed gastrointestinal state. In the in vitro fasted state, the tablet was exposed to FaSSGF (pH 1.6) for 0.5 h, followed by exposure of the same tablet to FaSSIF (pH 6.5) for 5.5 h. The dissolution study was evaluated with 12 replicates. During the dissolution test, samples were withdrawn at predetermined time points and then filtered with 0.7 µm GF/F disc filter (Whatman, Maidstone, UK). The in vitro fed state experiments were conducted in a similar manner to that of the fasted state, using FeSSGF and FeSSIF as dissolution media. The dissolution media (FaSSGF, FeSSGF, FaSSIF, FeSSIF) were prepared based on the composition available at https://biorelevant.com/shop/ (accessed on 24 February 2021); however, enzymes were excluded and SIF powder was replaced by surfactants such as tween 80 and sodium lauryl sulfate.

2.4.3. In Vitro Caco-2 Permeability Determination

Caco-2 cells (ATCC) were cultured in Minimal Essential Medium (MEM), 20% fetal bovine serum, 2 mM L-glutamine, and 1% penicillin-streptomycin at 37 °C in humid air atmosphere containing 5% CO_2 in 75 cm^2 cell culture flasks. Freshly prepared FaSSIF was used for the study.

For the transport studies, 0.5×10^6 cells were seeded per 12-well transwell insert (translucent, 0.4 µm pore size, Greiner Bio-one®). Cells were cultured with 500 µL medium in the upper compartment and 1500 µL in the lower compartment. The medium was changed every 2 or 3 days, and transepithelial electrical resistance was measured via EVOM STX-2-electrode (World Precision Instruments, Florida, USA). The cell monolayers were used for the experiments, once the resistance reached a transepithelial electrical resistance (TEER) value of >300 Ω*cm^2 (18–21 days) [15,16].

Thereafter, the medium was removed, and the cells were coated with 90 µL gastric porcine mucin (40 mg/ml in MEM + 10%FBS) for 30 min. A concentration of 10 µM of Riva and Xarelto™ (20 mg) tablets (equivalent to 10 µM of Riva) was used. For the preparation of Xarelto™ (20 mg) samples, the tablets were ground using a mortar, and pestle and the amount of the formulation containing the desired amount of Riva was dispersed in FaSSIF and stirred for 30 min at RT. The respective suspensions (510 µL) were applied to the upper compartment of the transwell and 1500 µL Krebs Ringer buffer added in the lower compartment. Ten microliters were immediately withdrawn from the apical compartment to determine the total amount applied. Plates with transwell were incubated upon agitation for a total of 120 min. One-hundred-microliter samples were taken from the lower compartment at predetermined time points of 0, 30, 60, 90, and 120 min and replaced by pre-warmed Krebs-Ringer buffer. In addition, at the end of the experiment, 10 µL of the upper compartment were collected for the calculation of the recovery rate. TEER values were measured before and after the transport study to identify potential damage to the cell layer. The permeability of sodium fluorescein (10 µg/mL) in the Krebs-Ringer buffer was determined to verify the barrier properties of the Caco-2 monolayer. All samples were stored at −20 °C until further analysis. On the day of analysis, the samples were thawed at room temperature, and the content was measured using UHPLC.

For the determination of the apparent permeability coefficient (P_{app}), the following equation was used, where dQ/dt is the flux across the cell monolayer (ng/s), A the surface of the monolayer (cm^2), and C the initial concentration in the donor compartment (ng/mL):

$$P_{app} = \frac{dQ}{dt \times A \times c} \quad (1)$$

2.4.4. Determination of Systemic Disposition Parameters of Riva

The in vivo PK profile of Riva after intravenous administration was not found in the literature. Therefore, plasma concentration–time profile after 10 mg oral solution administration under the fasted state was used in the PKPlus™ to obtain the systemic clearance, volume of distribution, half-life, and distribution constants between the central and peripheral compartments [17,18]. Models were fitted empirically in the PKPlus™ employing 1-, 2-, and 3- compartment separately. The Hooke & Jeeves pattern search method was used during the fitting and the weighing was equal to $1/Yhat^2$. Akaike information criterion (AIC) and Schwarz criterion (SC) were used to select the best-fitted compartment model. The obtained PK parameters were then fixed and employed in the simulation of solid oral dosage forms.

2.5. Physiologically Based Gastrointestinal Absorption Modeling

2.5.1. Model Compound Parameters

Physiochemical properties of Riva such as molecular weight and lipophilicity were compiled from the literature (Table 1) [19]. Human duodenum effective permeability (P_{eff}) was estimated from in vitro CaCo-2 permeability data using the in-built relation present in the GastroPlus™. The experimentally obtained values of solubility, particle size, and dissolution parameters were used.

Table 1. Input parameters of Riva for building the PBPK model in GastroPlus™.

Physiochemical Parameter	Values
Molecular Weight (g/mol)	435.89
logP	1.36
pKa	strongest acidic: 13.6strongest basic: 1.6
Solubility vs. pH	water solubility (pH = 7) = 10 µg/mL pH 1.2, FaSSGF = 11 µg/mL pH 6.5, FaSSIF = 9.9 µg/ml pH 5.0, FeSSIF =16.8 µg/ml
Particle Size (Radius)	7.5 µm (Xarelto tablet, 20 mg) d_{90} = 9.4 µm; d_{50} =3.8 µm; d_{10} =0.7 µm
Caco-2 Permeability	$2.69 \pm 0.72 \times 10^{-6}$ cm/s (Xarelto)
Dissolution Profiles (USP 4)	Xarelto IR tablet (20 mg)

2.5.2. Development of In-Silico Physiology Based Gastrointestinal Absorption Model

The ACAT model implemented in GastroPlus™ was used for all the simulations in the current study. Input parameters for the ACAT model can be categorized into three classes, i.e., formulation properties (such as particle size distribution, density, and release profiles of drug products), physicochemical properties of drug substances (such as diffusion coefficient, lipophilicity, pKa, solubility, and permeability), and pharmacokinetic parameters (such as clearance, the volume of distribution, and the disposition model). All other parameters were set at default values in GastroPlus™. The simulations were performed using the default "Human Physiological-Fasted" and "Opt LogD Model SA/V6.1", in order to simulate the plasma concentration profiles of Riva following oral administration of tablet dose in fed condition. The Opt. LogD SA/V v6.1 model is one of the ACAT models in GastroPlus software. In the ACAT model, the option "CR Dispersed" was selected using the USP4 profile to model the release of the drug. Once the drug is released, solubility and PSD were used to model dissolution of the drug via the Johnson model.

On the basis of LogD value of the drug molecules, the model can automatically fine-tune the absorption scale factor for the different compartment of the intestine, resulting in improved simulation and thus prediction of the regional absorption of the API.

Model Verification

Initially, the predictive power, robustness, and the effect of Absorption Scale Factor (ASF) optimization on the absorptive phase of Riva were evaluated. To do so, the predicted pharmacokinetic parameters were compared with the in vivo data from literature. The pharmacokinetic model was developed using oral solution doses (5 and 10 mg) as well as for oral IR tablet doses (5 and 10 mg) of Riva under the fasted state and compared with the published data [17,18]. The percent prediction error value was calculated to evaluate the accuracy of the model. The calibrated ACAT model for Riva was then applied to simulate the plasma concentration–time profile of Xarelto tablet (20 mg) in the fed state.

Parameter Sensitivity Analysis (PSA)

PSA was performed for the uncertain and key parameters in formulations such as mean particle radius, dose volume, particle density, effective permeability, precipitation time, and diffusion coefficient for the dosage forms investigated under the fasted and fed tates.

2.6. IVIVC Studies

In addition to the PBPK model, the conventional IVIVC was used to predict the PK profile after oral administration of formulation in the fed state using IVIVC Toolkit 8.0 of Phoenix WinNonlin 8.2.0.4383 for Windows (Pharsight, Certara, USA Inc, St. Louis, MO, USA). The IVIVC model was developed and calibrated using the in vitro dissolution and in vivo profile of 20 mg strength of Xarelto IR tablet in the fasted condition. Thereafter, using the established IVIVC, the PK profile of the Xarelto IR tablet in fed condition was predicted and compared with the simulation results obtained from the PBPK model.

IVIVC was based on a two-step deconvolution method. Initially, the Weibull function was fitted to the in vitro data of the Xarelto IR tablet (20 mg tablet) in the fasted condition. Moreover, the time course of in vivo absorption was derived using deconvolution. The in vivo data of the 10 mg oral solution published by Kubitza were used as a reference for calculating the unit impulse response (UIR) function [17,18]. The in vivo data of the PK profiles of the Xarelto IR tablet (20 mg tablet) were then deconvolved and compared to the in vitro dissolution profiles using the fraction absorbed (F_{abs}) vs. the fraction dissolved F_{diss} plot.

Thereafter, in the second step, a correlation was built between the in vitro drug release and in vivo drug absorption. The IVIVC model was established based on in vitro dissolution profile of the Xarelto IR tablet, and in vivo results were obtained from the literature. As per the condition, the regression slope line most closely aligned with a value of 1.0, whereas the elimination phase of Riva was calculated using the PK profile of 10 mg oral solution.

Thereafter, as the final step, validation of the developed IVIVC model is required, in order to establish quantitative resilience of the predictive capacity of the model. The validation of the model was performed using the results of the in vivo fate of the formulation used to establish the model, known as internal validation, and/or by the application of a different formulation, known as external validation. In the present model development, the internal validation of the IVIVC model was performed by comparing the predicted and observed PK profile of the reference product Xarelto 20 mg tablet in the fasted condition. Thereafter, the predictability of the model was evaluated using the percentage prediction error (%*PE*) from the following equation:

$$\%PE = 100 \times \left(\frac{Predicted\ value - Observed\ value}{Observed\ value} \right) \quad (2)$$

For the development of a robust model, the average absolute *%PE* of ≤10% for the maximum plasma concentration (C_{max}) and area under the curve (AUC) establishes the predictability of the IVIVC. Furthermore, the *%PE* for each formulation should not exceed 15%. If the *%PE* conditions are not met for the internal validation, further validation using the external formulation is required [20,21].

2.7. Food Effect (FE) Studies of Riva in Simulated Healthy Population

Simulations were carried out for 20 mg dose strength using the fed state physiology of GastroPlus™ to evaluate the quantitative prediction of FE based on the measurements of in vitro biorelevant solubility and dissolution. The percentage prediction error for the predicted PK parameters was calculated in comparison with the predicted values Xarelto IR tablet (20 mg tablet).

A single-dose (20 mg), three-period virtual trial in 50 subjects was carried out. Gastro Plus™ randomly generates subjects by varying physiological factors such as gastrointestinal transit times, pH, fluid volumes, PK parameters as well as compound parameters. Three populations, namely A, B, and C, with 50 subjects each (in order to gain a thorough sampling across all the variables) were given the same treatment (20 mg strength of Xarelto IR tablet).

3. Results and Discussion

3.1. Biopharmaceutical Properties of Riva

3.1.1. Equilibrium solubility in simulated media

Table 2 depicts the solubility of the Riva in different biorelevant media. The solubility of the Riva was found to be comparable among different media, i.e., water, FaSSGF (pH 1.6), and FaSSIF (pH 6.5). Whereas in the case of FeSSIF and FeSSGF (pH 5.0), the solubility of the Riva was found to be markedly higher as compared to other simulated biorelevant media. The FeSSIF contains 15 mM sodium taurocholate and 3.75 mM lecithin as compared to 3 mM sodium taurocholate and 0.75 mM lecithin in the case of FaSSIF. Thus, an approx. 2-fold increase in the solubility in the Fed conditions could be attributed to the increase in the lipidic component of the media with a higher fraction solubilized in taurocholate and lecithin micelles. The increased solubility of Riva in the Fed state is in accordance with the literature, demonstrating higher bioavailability of equal of more than 80% when taken with food (for 20 mg dose of Riva) [19,22].

Table 2. Solubility of Riva in biorelevant media.

Solubility in	pH	Values (µg/mL)
Unbuffered water	7.0	10.0
FaSSGF	1.6	11.0
FaSSIF	6.5	9.9
FeSSGF	4.5	24.0
FeSSIF	5.0	16.8

3.1.2. In Vitro Release Profile of Riva in Fasted and Fed Conditions

Figure 1 demonstrates the in vitro release profiles of the Xarelto IR tablet (20 mg) in fasted and fed conditions using the dynamic dissolution method. After 30 min, in vitro release of Xarelto IR tablet in the fed state and fasted simulated gastric fluids were found to be 27.7 and 11.0%.

Thereafter, the fed and fasted simulated gastric fluid was replaced via simulated intestinal fluids without removing the Xarelto IR tablets. The in vitro release, and the time to 80% drug release was found to be the 360 and 210 min in case of fasted and fed state conditions, respectively. Furthermore, the $f1$ (the difference factor) and $f2$ (the similarity factor) were also calculated and found to be 28 and 38, respectively. For bioequivalent in vitro release profile, the values of $f1$ should be between 0 and 15, whereas the value of $f2$ should be between 50 and 100 [23,24]. Thus, the release profile in the case of the fed

condition was found to be significantly higher as compared to the fasted condition. The results demonstrated that the lower solubility in the absence of food components could be the rate-limiting factor for the dose-proportional absorption of Riva from Xarelto IR tablets, independent of the formulation. The significantly higher dissolution in the presence of a food-induced increase in bile salt concentration was found to be in accordance with the solubility study and is the key parameter for the establishment of the PBPK model.

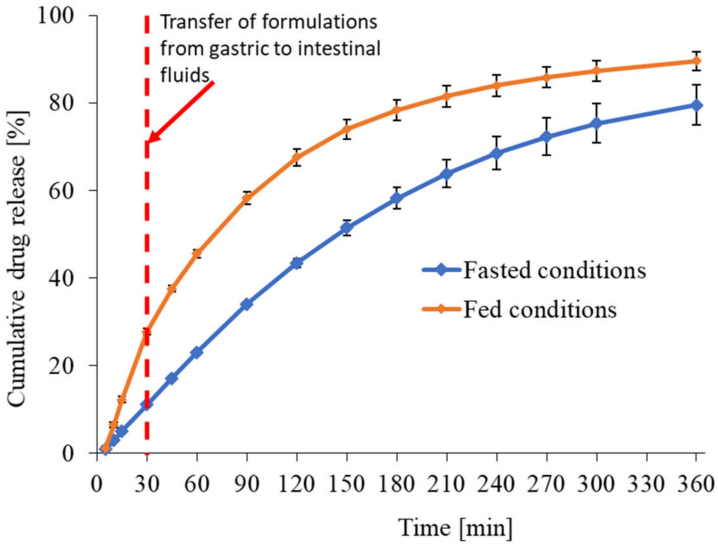

Figure 1. In-vitro release profile of Riva from Xarelto IR tablet (20 mg strength) using USP 4 apparatus. The tablets were transferred from FaSSGF (pH 1.6) and FeSSGF (pH 4.5) media to FaSSIF (pH 6.5) and FeSSIF (pH 5.0) media, respectively, after 30 min.

3.1.3. In Vitro Caco-2 Permeability

Permeation of the marker substance, fluorescein, did not cause any alterations of transepithelial electrical resistance (TEER) values compared to controls (no permeation performed). The API powder and, to a greater extent, the formulations caused a decrease in TEER values (Figure 2A). Despite the decrease in TEER values induced by the formulations, there was no increased transport of Riva across the monolayers. Apparent permeability coefficient (P_{app}) values ($2.69 \pm 0.72 \times 10^{-6}$ cm/s) were not increased in the formulations compared to standard Riva ($3.11 \pm 0.24 \times 10^{-6}$ cm/s, (Figure 2B)). The P_{app} of fluorescein was $0.72 \pm 0.13 \times 10^{-6}$ cm/s, indicating a good barrier function of the Caco-2 monolayer and absence of damage by FaSSIF.

P_{app} and transport rates were identical for formulated products and standard Riva. The decrease in TEER values was slightly higher in the formulations than in the unformulated Riva but was not reflected in changes of the P_{app} values. Excipients in the formulations more likely to decrease the TEER values. However, taking into consideration that there is no difference in the P_{app} of pure Riva in comparison with Xarelto (presence of excipients) despite the change in TEER values of CaCo-2 cells in Xarelto, it can be suggested that passage of Riva is mainly transcellular through the CaCo-2 cells. P_{app} values determined in the study were lower than the values published by Gnoth et al. ($8.0 \pm 0.6 \times 10^{-6}$ cm/s) [25]. The most likely reason for this difference is the lack of mucus production of Caco-2 cells, which can affect permeation. To reproduce the physiological situation, a mucus layer has been added to the Caco-2 monolayer in this study. The effect of mucus on the permeation of active pharmaceutical ingredients (APIs) has been reported controversially [26,27]. The comparison between Caco-2 cells and mucus-producing HT29-MTX did not show prominent differences for many lipophilic and hydrophilic compounds, suggesting that mucus does not represent a strong barrier for the permeation [28]. The exclusive assessment of the role of mucus, however, was not possible because HT29-MTX cells lack P-glycoprotein expression and the lack of reverse transport will increase the measured P_{app} values. Although

the same cell types were used, another study reported that the permeability of drugs with a partition coefficient (logP) > 1 was decreased in the mucus-producing cell lines [28]. The passage of Riva might be hindered by mucus because of its logP value of 1.36 [28]. It can be concluded that Riva formulations reacted very similarly and did not display a permeation-enhancing effect on the permeability of Riva. The results obtained of various physicochemical parameters such as those from the solubility study, Caco-2 permeability, and the published literature were used as the input parameters for the development of the PBPK model. The values of the input parameters used in the PBPK model are mentioned in Table 1 [19,29–33].

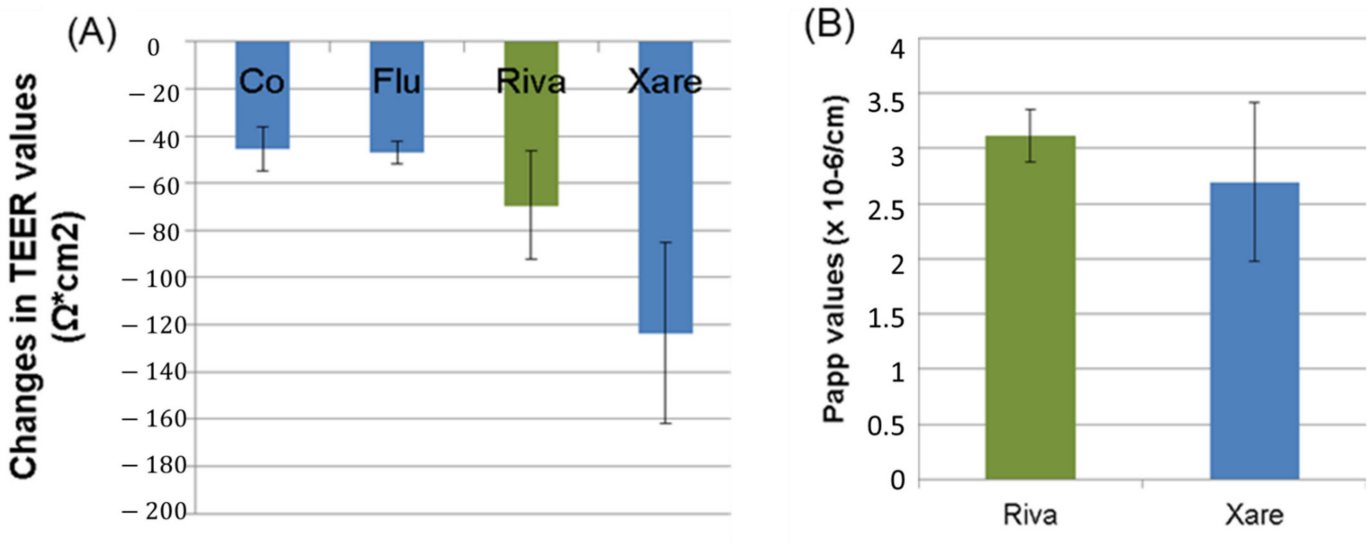

Figure 2. (**A**) Differences in transepithelial electrical resistance (TEER) values between the start value and measurement at the end of the permeation studies. Abbreviations: Control (Co), fluorescein (Flu), rivaroxaban (Riva), Xarelto (Xare). (**B**) Papp values of rivaroxaban (Riva) and Xarelto (Xare).

3.1.4. Systemic Disposition Parameters of Riva

The two-compartment model was found to be the best fit model according to the AIC and SC criteria to describe the Riva pharmacokinetics following the administration of oral solution dose (10 mg) (Figure 3). Values of clearance, the volume of distribution (Vc) and, $T_{1/2}$ were in accordance with the literature values. Other parameters such as the peripheral volume of distribution (V_2), distribution constant from the central to the peripheral compartment (K_{12}), and distribution coefficient from the peripheral to central compartment determined (K_{21}) from the two-compartment model fitting were used for further simulations. Table 3 depicts the mean baseline values used for the simulation of Riva plasma concentration–time profile following the administration of oral solution and IR formulation doses. The value of clearance and elimination half-life obtained through fitting is found to be in accordance with the value reported in the Xarelto product information after intravenous administration of Riva at a dose of 1 mg [34,35].

3.2. Physiology Based Gastrointestinal Absorption Model of Riva Formulation

Prediction of PK Profiles and Optimization of ACAT Model

Taking into consideration the input parameter as mentioned in Table 1 and the pharmacokinetic parameters mentioned in Table 3, the PK profile of the oral solution dose (10 mg) of Riva was simulated using the ACAT model in GastroPlus™ with default fasted human physiology and ASF values (Table 4). Simulation of 10 mg oral dose with the default Gastroplus™ Human Physiology Fasted largely underestimated the absorption phase of Riva, resulting in the poor fitting of the extracted plasma concentration–time profile obtained for 10 mg oral dose (Figure 4A). This observation suggested that the default fasted

human physiology in GastroPlus™ was not able to capture the absorption phase of Riva. Thereafter, the influence of effective permeability (P_{eff}) on the C_{max} and T_{max} predictions under fasted conditions for oral solution dose (10 mg) of Riva were evaluated. The results showed that even though the P_{eff} was increased by 10 folds to 3.1, T_{max} was overpredicted by 5 folds and C_{max} was underpredicted by 1.78 folds compared to the average observed values (Table 5) [18].

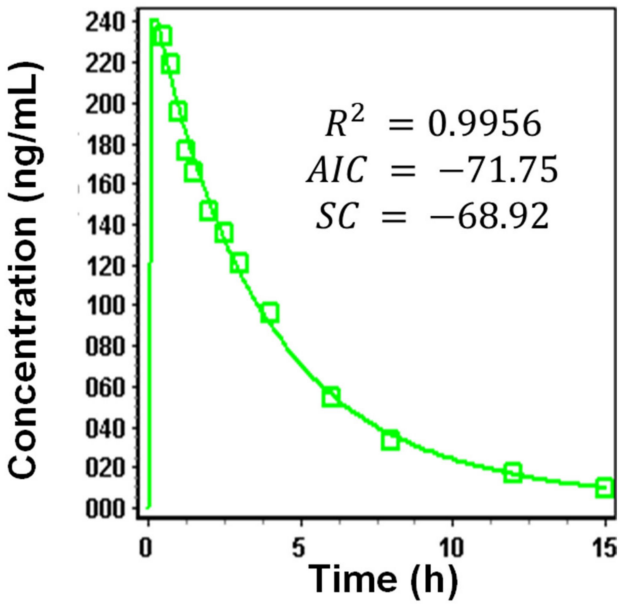

Figure 3. Pharmacokinetic data fitting 2- compartment of oral solution dose (10 mg) of Riva.

Table 3. PK parameters obtained from two-compartment model fitting of oral solution (10 mg) of Riva.

Parameter	Values
Clearance (L/h)	9.43
V_c (L/kg)	0.47
$T_{1/2}$ (h)	4.62
K_{12} (1/h)	0.04
K_{21} (1/h)	0.21
V_2 (L/kg)	0.09

Table 4. ASF values before and after optimization of ACAT model.

Compartment	Default (GastroPlus) ASF	Optimized ASF
Stomach	0	0
Duodenum	2.673	36.44
Jejunum 1	2.658	36.25
Jejunum 2	2.629	35.85
Ileum 1	2.592	35.35
Ileum 2	2.568	35.02
Ileum 3	2.505	34.16
Caecum	0.535	0.535
Asc Colon	1.038	1.038

Furthermore, it is also important to consider the solubility of Riva in gastric medium and concentration of Riva attained with 5 mg and 10 mg of oral solutions. Table 2 reports fasted state gastric solubility of 11 µg/mL (i.e., 0.011 mg/mL) for Riva. Considering 250 mL of dosing volume with instantaneous saturation translates to a solubilization capacity of 2.75 mg in the medium. At a dose of 10 mg, this can generate ~3.6-fold supersaturation,

which can lead to faster absorption as reflected by high C_{max} and lower T_{max} in the observed profile (assuming absence of precipitation from the supersaturated state). As simulations were conducted with solubility values of ~11 µg/mL, this could have led to underpredictions.

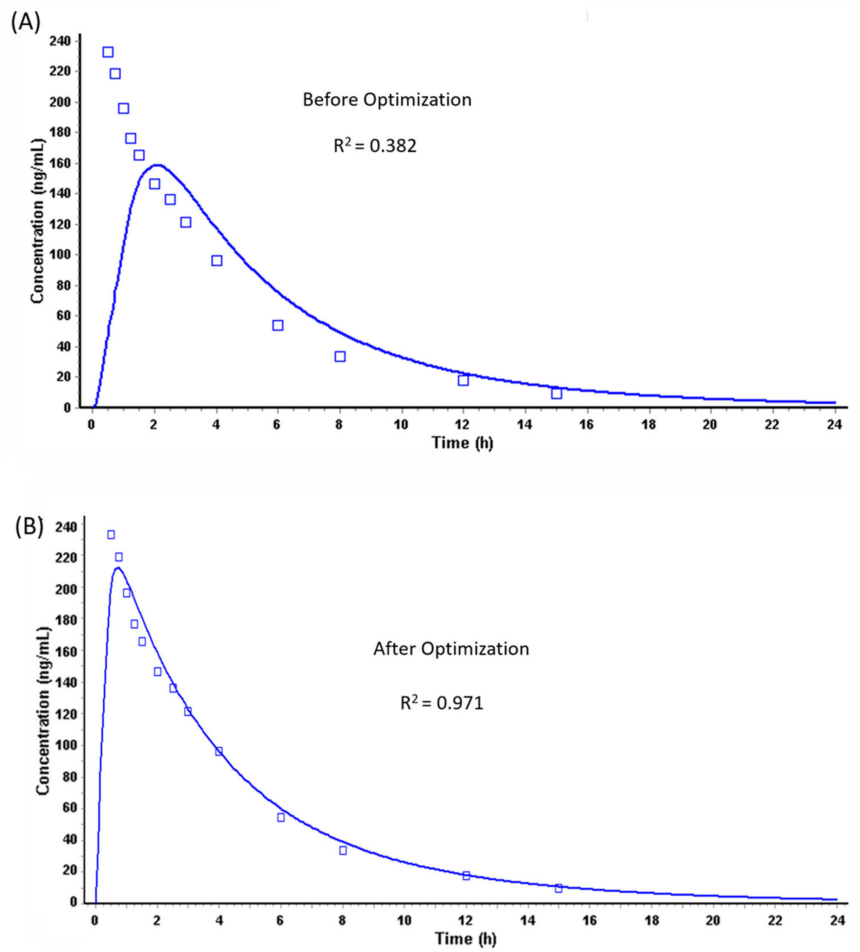

Figure 4. Riva plasma concentration–time profile from solution oral dose (10 mg) (**A**) before and (**B**) after optimization.

Table 5. PK parameters obtained from simulated PK profiles.

Parameter	Actual (Reported) [a]	Predicted (Before Optimization)	Predicted (After Optimization)
PK parameters obtained from simulated PK profile of solution oral dose (10 mg) of Riva before and after optimization			
C_{max} (µg/L)	266/25.1 (187–412)	159.27	212.23
T_{max} (h)	0.50 (0.25–1.00)	1.92	0.72
AUC (µg·h/L)	997/25.1 (613–1383)	1056	1058
F%	>90%	99.54	99.79
Pharmacokinetic parameters for 5 mg oral (solution) dose of Riva in fasted conditions			
C_{max} (µg/L)	119/18.5 (97.2–158)	80.13	107.06
T_{max} (h)	0.63 (0.5–0.75)	1.92	0.66
AUC (µg·h/L)	461/17.2 (348–587)	528.24	529.37
F%	>90%	99.58	99.80

[a]—taken from literature; data are represented as geometric means/percent geometric coefficient of variation and range in case of reported data [18].

As a result, the ASF values were optimized using the optimization module in the GastroPlus™, which could capture the absorption phase of the plasma concentration–time profile of oral solution (10 mg) (Figure 4B). ASFs in GastroPlus™ are a multiplier used to

scale the effective permeability to account for variations in surface-to-volume ratio, pH effects, influx, or efflux transporter differences, and other absorption-rate-determining effects. On the basis of the GI physiology, ASFs are used to scale the effective permeability of the API across the different sections of the GI tract.

The ASFs were optimized using the PK data set of single-dose oral solution (10 mg) in the fasted state changing the C1 and C2 coefficients of Opt logD Model SA/V 6.1, which determines absorption from the small intestinal compartments. However, the C3 and C4 coefficients which determine absorption from the colon were kept at their default values. The optimized ASF were nearly 14 folds higher than the default values, leading to the faster absorption of Riva in the small intestine. In addition, the default value for compartment volume occupation by water in the colon was reduced from 10% to 2% to better account for measured free water content in the colon [8,36]. All other parameters were set at default values in GastroPlus^{TM}; the default and optimized ASF values are mentioned in Table 4.

Table 5 shows the pharmacokinetic parameters obtained from the simulated PK profile of solution oral dose (10 mg) of Riva before and after optimization of ASF and compared with the literature data.

In order to verify that the optimized ASF values for the small intestine can reasonably capture the absorption phase of Riva, simulations of mean plasma concentration–time profile of Riva following administration of oral solution dose (5 mg and 10 mg) and IR tablet formulation (5 mg and 10 mg) under the fasted condition were also carried out. Simulated mean plasma concentration–time profiles of Riva from solution and IR tablet formulation and corresponding pharmacokinetic parameters (C_{max}. T_{max} and $AUC_{0-\infty}$) calculated are demonstrated in Tables 5 and 6. All the predictions of pharmacokinetic parameters for different formulation and doses of Riva were within two folds of the reported values. This fosters our confidence in the predictive ability of the developed ACAT model for Riva.

Table 6. Pharmacokinetic parameters for IR Tablet in fasted conditions.

Parameter	Actual (Reported) [a]	Predicted (Optimized ASF)
Pharmacokinetic parameters for 5 mg oral (IR Tablet) dose of Riva in fasted conditions		
C_{max} (µg/L)	72/19.7 (55–96)	76.13
T_{max} (h)	1.88 (0.5–4.00)	2.1
AUC (µg·h/L)	466/23.0 (348–677)	524.42
F%	80–100%	98.86
Pharmacokinetic parameters for 10 mg oral (IR Tablet) dose of Riva in fasted conditions		
C_{max} (µg/L)	141/15.5 (112–184)	149
T_{max} (h)	2.00 (0.5–2.50)	2.20
AUC (µg·h/L)	1020/14.9 (797–1217)	1037
F%	80–100%	97.75

[a]—taken from literature; data are represented as geometric means/percent geometric coefficient of variation and range in case of reported data [18].

Parameter sensitivity studies were performed investigating the impact of key factors on the bioavailability of Riva. The mean particle size of the API in the IR tablet formulation was found to be the most important factor influencing the bioavailability of Riva (Data not shown) irrespective of fasted and fed state. Other factors such as dose volume, particle density, precipitation time, diffusion coefficient, and P_{eff} seem to have a relatively minor influence on the bioavailability of Riva.

Once the ACAT model was optimized with modified ASF values, pharmacokinetic parameter predictions were carried out for Riva 5 mg oral solution dose (Table 5) and Xarelto IR tablet for 5 mg and 10 mg (Table 6) dose in the fasted condition. The in vitro release profile and the physicochemical parameters of the API was found to be biopredictive and was able to describe the plasma concentration profiles, and the predicted values of C_{max}, AUC, and T_{max} were found to be in agreement with those of the literature, which increased the confidence in the developed ACAT model.

In silico simulation of Xarelto (20 mg dose strength) in fasted and fed state

The developed ACAT model was used to simulate the plasma concentration–time profile of Xarelto (20 mg dose strength) in the fasted and fed state with the dissolution

profiles using the USP 4 flow-through apparatus and biorelevant dissolution medium. It was observed that the inclusion of dissolution profiles of Xarelto IR Tablet (20 mg) during modeling led to an improvement in the simulations with predicted values close to the observed values, as reported in the literature. Table 7 and Figure 5 represent the simulated plasma concentration–time profile and key pharmacokinetic parameters predicted from the simulation of Xarelto (20 mg) IR tablet in the fasted and the fed states.

Table 7. Key pharmacokinetic parameters predicted from the simulation of Xarelto (20 mg) IR tablet in the fasted and fed states.

Parameters	Fasted State		Fed State	
	Actual (Reported) a	Predicted (Optimized ASF)	Actual(Reported) b	Predicted (Optimized ASF)
Cmax (µg/L)	173/35.6 (111–294)	171.15	294.4/15 (225.4–360.6)	236.64
Tmax (h)	1.50 (0.5–4.00)	3	3.00 (0.5–6.00)	2.9
AUC (µg·h/L)	1612/36.1 (859–2193)	1433.8	2294/19 (1464–3227)	1857.3
F%	66%	67.57	80–100%	87.54

a—taken from Reference [18]; b—taken from Reference [17]; data are represented as geometric means/percent geometric coefficient of variation and range in case of reported data.

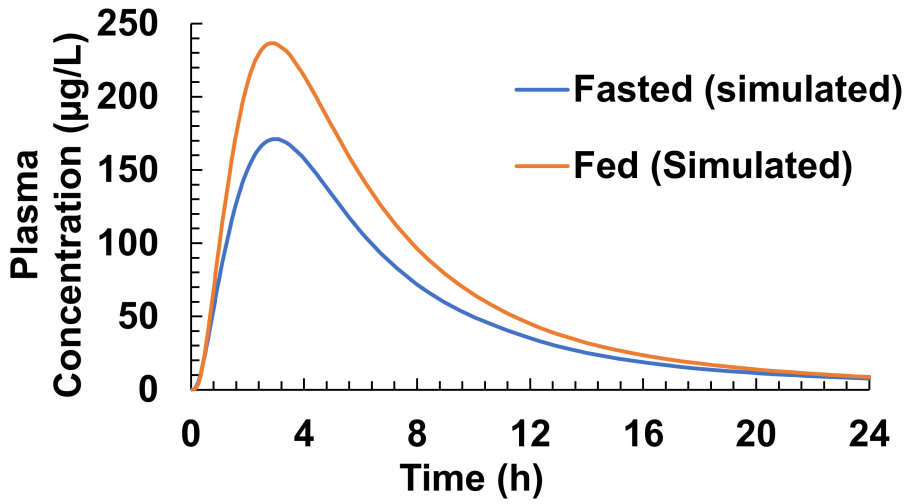

Figure 5. Simulated plasma concentration-time profile of Xarelto (20 mg) in fasted and fed states using GastroPlus™ ACAT model.

The results clearly depict the presence of food effects when Xarelto (20 mg) is administered in the fasted and fed states. However, the food effect was a bit underestimated compared to that reported in the literature.

As evident from Figure 6, the increase in bioavailability of Xarelto during the fed state simulation was found, which could be due to the enhanced dissolution of Riva in the fed state. The increase in solubility in the fed state resulted in a greater fraction of Riva to be absorbed from the duodenum and Jejunum 1 as compared to the fasted state. The simulated results are in accordance with the Xarelto product literature outlining site-specific absorption of Riva [34,35].

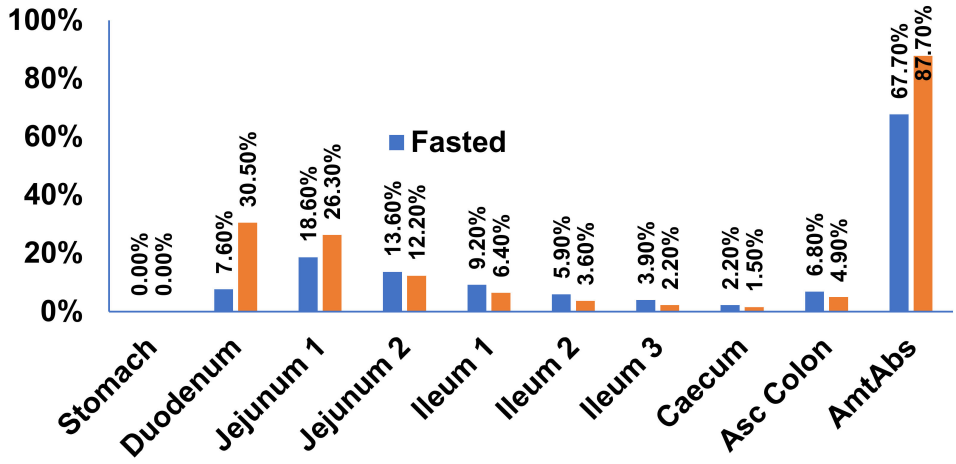

Figure 6. Regional amount absorbed from Xarelto in fasted and fed states in the gastrointestinal tract.

3.3. IVIVC Studies

3.3.1. Modelling

In Vitro and In Vivo Raw Data

The in vitro release profile of Xarelto 20 mg tablet in the fasted state was used for the establishment of the IVIVC model. As evident from the dynamic in vitro dissolution of the Xarelto (Figure 1), after 30 min of incubation in a simulated gastric medium, the simulated gastric medium was replaced by a simulated intestinal medium. Upon incubating the tablets for 5.5 hours, the amount of API release was found to be approx. 80 and 90% in case of fasted and fed conditions, respectively.

The in vivo data of the Xarelto 20 mg tablet and 10 mg oral solution in the fasted condition were obtained by literature published by Kubitza and co-workers [17,18]. The T_{max} in the case of solution and tablet was found to be 0.5 and 3 h, respectively. In addition, the C_{max} was reported to be markedly higher in the case of the solution as compared to the tablet. The observation suggests higher absorption of the Riva in presence of solutions, which is reported to be due to the faster and higher amount of Riva available to be absorbed. Thus, suggesting the absorption of Riva to be not limited by permeability.

Dissolution Curve Fitting

The fasted state in vitro release profile of the Xarelto 20 mg tablet was fitted with the Weibull function. As evident from Figure 7, using the Weibull function, the predicted in vitro release or, more precisely, the fraction of API dissolved was found to be overlapping with the observed in vitro release data as a function of time, suggesting that the Weibull function was suitable to fit the dissolution data.

$$\text{Weibull function, } y(t) = F_{inf}\left[1 - e^{-(t/MDT)^b}\right] \quad (3)$$

where, *y(t)* or *Fdiss(t)* - Fraction of drug dissolved; dependent variable of the function, *t*: time (h); independent variable of the function, F_{inf}: Fraction of drug dissolved at infinity time; parameter of the function, *MDT*: mean dissolution time; parameter of the function, *b*: beta; shape parameter of the function

3.3.2. Calculation of Unit Impulse Response (UIR) Function

To obtain the in vivo data, the pharmacokinetic parameters of 10 mg oral solution was used. Thus, the UIR function was used to calculate the oral pharmacokinetic data. As evident from Figure 8, using the UIR function, the observed pharmacokinetic profile was found to be overlapping with the predicted pharmacokinetic profile and a linear relation was established suggesting the best fit model. The UIR function obtained were then used to

deconvolute the in vivo pharmacokinetic profile of Xarelto 20 mg tablet in fasted condition, for the assessment of in vivo absorption profile (Figure 9).

$$\text{UIR Function, } Cp(t) = A_1 e^{\alpha 1(t\text{-}tlag)} + A_2 e^{\alpha 2(t\text{-}tlag)} + A_3 e^{\alpha 3(t\text{-}tlag)} \quad (4)$$

Where, Cp(t): Concentration of drug in plasma [ng/L]; dependent variable of the function, t: time [h]; independent variable of the function, A (coefficient) and α (exponential); parameter values, tlag: lagtime; parameter value.

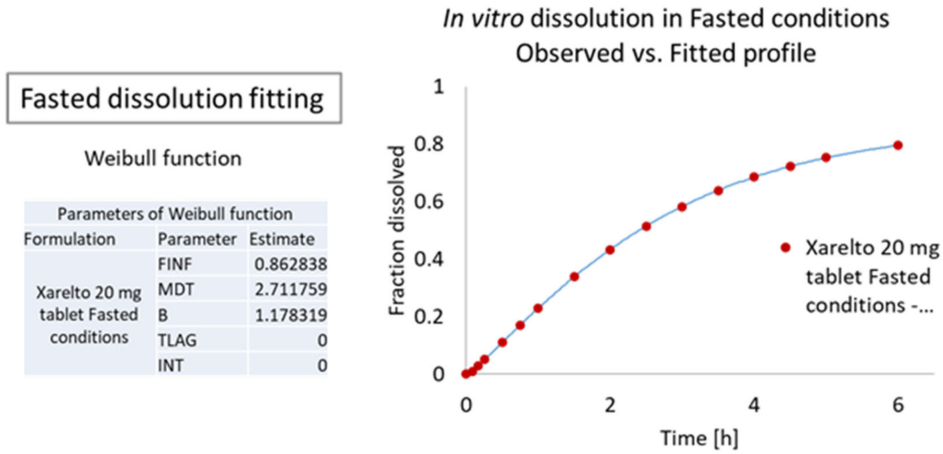

Figure 7. Observed in vitro profile vs. fitted curves of the Xarelto 20 mg tablet.

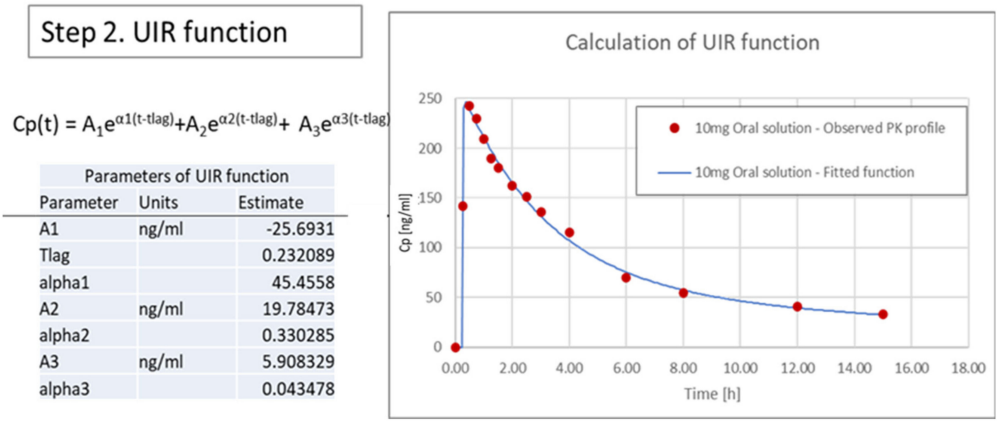

Figure 8. Properties of the unit impulse response (UIR) function.

3.3.3. Correlation

The dissolved API fraction (obtained from the fitting of in vitro release profile) was then related with the absorbed in vivo fractions (obtained from the deconvolution of plasma concentration). As evident from Figure 10, the in vivo fraction absorbed was found to be linearly correlated with the fraction of API dissolved in vitro. The observed relation was found to be aligned with the linear regression analysis. Thus, the slope and regression values of Fabs vs. Fdiss plot suggest the development of a robust mathematical IVIVC model.

$$\text{Correlation equation, } F_{abs} = \text{AbsScalexDiss}(T_{scale} \times T_{vivo} - T_{shift}) \quad (5)$$

where, Fabs: Fraction of drug absorbed; dependent variable of the function, Tvivo: in vivo time (h); independent variable of the function, AbsScale: Absorption scale factor, T_{scale}: Time scaling factor, T_{shift}: Time scale shift, Diss: Internal function that linearly interpolates

the predicted dissolution data, i.e., the predicted data from the dissolution model fitted to the in vitro data.

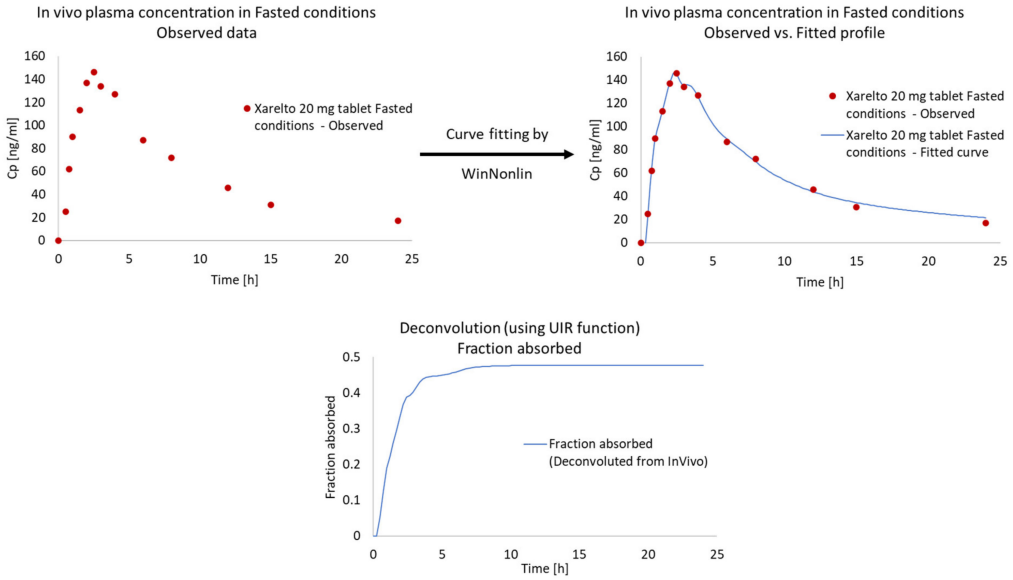

Figure 9. Calculated absorption after deconvolution of Xarelto 20 mg tablet.

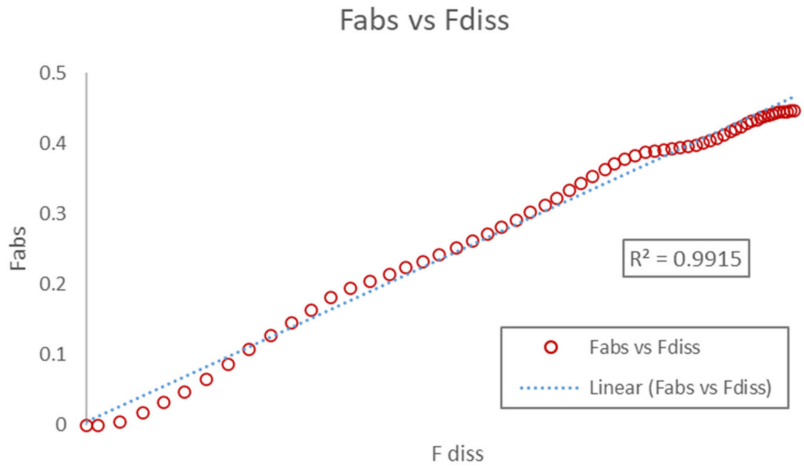

Figure 10. Fraction absorbed in vivo vs. fraction dissolved in vitro for the Xarelto 20 mg tablet in the fasted condition.

The AbsScale, Tscale, and Tshift parameters of the correlation equation were found to be 0.595, 1.494, and 0.188, respectively.

3.3.4. Internal Validation and Prediction

An IVIVC model was established based on the USP IV fasted state dissolution data and using published in vivo data as an internal validation of the reference product Xarelto 20 mg tablet (Figure 11). The result of the internal validation was promising (<2% error).

The IVIVC model was then used for the prediction of in vivo performance of the Xarelto 20 mg tablet in the fed state. As evident from Figure 12 and Table 8, the C_{max} and AUC were found to be distinctly higher, whereas no significant difference in the T_{max} was predicted in the case of the fed state as compared to the fasted condition. The increase in absorption was found to be in accordance with the increase in solubility of Riva in the presence of simulated fed media. Thus, the developed IVIVC was able to adapt the effect of fed media, predicting the in vivo profile in the fed state. The developed IVIVC model

(developed for reference product) can also be used as an effective tool to predict the in vivo fate of formulations with different strength and release profiles, considering an average percentage error of less than 10% and tolerance limit in the range of 0.8–1.25.

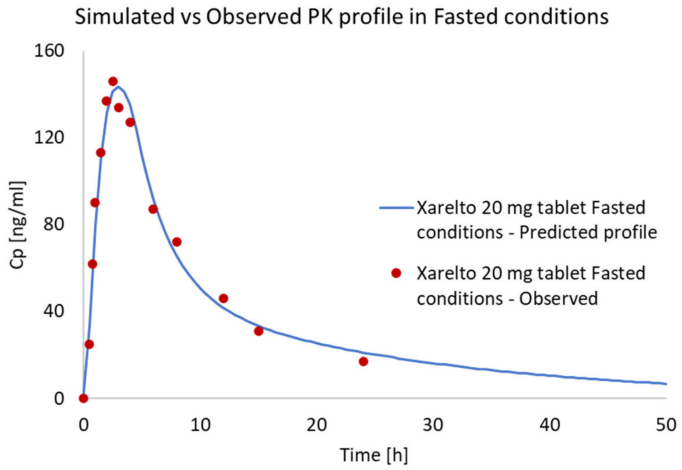

Figure 11. Internal validation (Xarelto 20 mg tablet Fasted condition) of the in vitro–in vivo correlation (IVIVC) model.

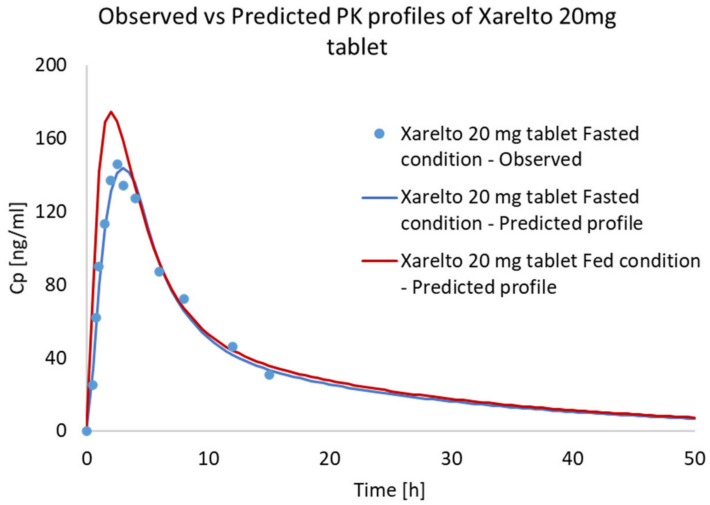

Figure 12. Predicted mean in vivo profiles of Xarelto 20 mg tablet using IVIVC model.

In the present report, both PBPK absorption and IVIVC model were developed to predict the food effect on the in vivo fate of the Riva released from Xarelto 20 mg tablet. Both models predicted a higher amount of Riva absorption in case of fed conditions, which could be due to higher solubility and release profile in simulated fed media [17]. The findings are in accordance with the literature, which reported an increase in Riva AUC and the mean C_{max} by 39% and 76%, respectively, when the 20 mg tablet was orally administered with food [37]. Interestingly, both 10 and 20 mg strength of the marketed formulation contain sodium lauryl sulfate (SLS) in order to increase the solubility of the API in the in vivo conditions. However, as evident from the lower bioavailability, the solubilization efficiency of SLS in increasing the solubility of Riva in the 20 mg tablet was found to be less as compared to the Riva in 10 mg tablet [37]. This decrease in solubilization efficiency in the fasted state could be due to a higher amount of API above the saturation solubility in the case of 20 mg Riva, as the volume of the in vivo fluid remains the same, potentially resulting in local precipitation and thus reduced bioavailability. Now in the case of the fed state, the excess of API higher than the saturation solubility could dissolve in lipidic components of the food and thus resulted in higher AUC and mean C_{max}. On further

increasing the dose to supra-therapeutic levels of 50 mg of Riva, no further increase in the AUC and mean C_{max} values was observed even in the presence of fed conditions [33,37]. The ceiling effect observed in the case of 50 mg of Riva dosing could be due to attainment of maximum solubility in fed conditions, assuming the volume of food is nearly alike.

Table 8. Observed and predicted values of the internal validation (Xarelto 20 mg tablet fasted condition) and predicted values of theXarelto 20 mg tablet fed condition.

Formulation	Parameter	Predicted	Observed [a]	%PE	Ratio
Xarelto 20 mg tablet Fasted condition	AUClast (µg·h/L)	1381.946	1361.125	1.52966	1.015297
Xarelto 20 mg tablet Fasted condition	Cmax (µg/L)	143.567	146.000	−1.66657	0.983334
Xarelto 20 mg tablet Fasted condition	Tmax (h)	3.0	1.5	N/A	N/A
Xarelto 20 mg tablet Fed condition	AUClast (µg·h/L)	1543.120	1750.175	13.41790	1.134179
Xarelto 20 mg tablet Fed condition	Cmax (µg/L)	174.566	241.000	38.05670	1.380567
Xarelto 20 mg tablet Fed condition	Tmax (h)	2.0	3.0	N/A	N/A

[a]—taken from References [17,18].

The C_{max} and AUC values predicted by the PBPK and IVIVC model were found to be comparable. However, the C_{max} and AUC values in the case of the PBPK model were slightly higher compared to the IVIVC model. The increase in C_{max} and AUC values in the case of the PBPK model could be due to the incorporation of different physicochemical and formulation properties, for the development of the model, whereas the IVIVC model lacks integration of such parameters. In the present case, as evident from the parameter sensitivity studies, the particle size of the API was found to be a critical factor affecting the release profile and thus the bioavailability of the Riva. The impact of particle size on the bioavailability was found to be in accordance with the product filling, as the reference formulation was developed using the micronized Riva in order to improve oral bioavailability via increasing solubility [37]. Thus, the development/optimization of the PBPK model using the particle size distribution of API could be responsible for the slight difference in the predicted C_{max} and AUC values compared to the IVIVC model. Thus, the developed model can further be used to develop and optimize the formulation parameters, mainly in the early stage development phase, reducing preclinical and clinical time and cost.

3.4. Food Effect (FE) Studies of Riva in Simulated Healthy Subjects

A virtual trial is a stochastic simulation that randomly samples parameters from predefined distributions. In order to take into account the effect of population variability on the plasma concentration profile of Riva following administration of Xarelto, a single dose (20 mg) 3-period virtual study design was carried out in the fed state. Three virtual populations of 30-year American Male/Female A, B, and C, each of 50 subjects, were created and subjected to Xarelto IR tablet (20 mg tablet). GastroPlus™ randomly generates subjects by varying the physiological factors such as gastrointestinal transit times, pHs, fluid volumes, and pharmacokinetics parameters, as well as compound parameters [38]. Table 9 and Figure 13 provides a summary of in silico investigation of food effect variability across virtual populations.

Table 9. Summary in vivo pharmacokinetic profile of Xarelto IR tablet (20 mg Strength) for Populations A, B, and C in fed conditions.

Parameters	Population A	Population B	Population C
C_{max} (ng/mL)	238	236	237
$AUC_{0-\infty}$ (ng·h/mL)	1856	1888	1988

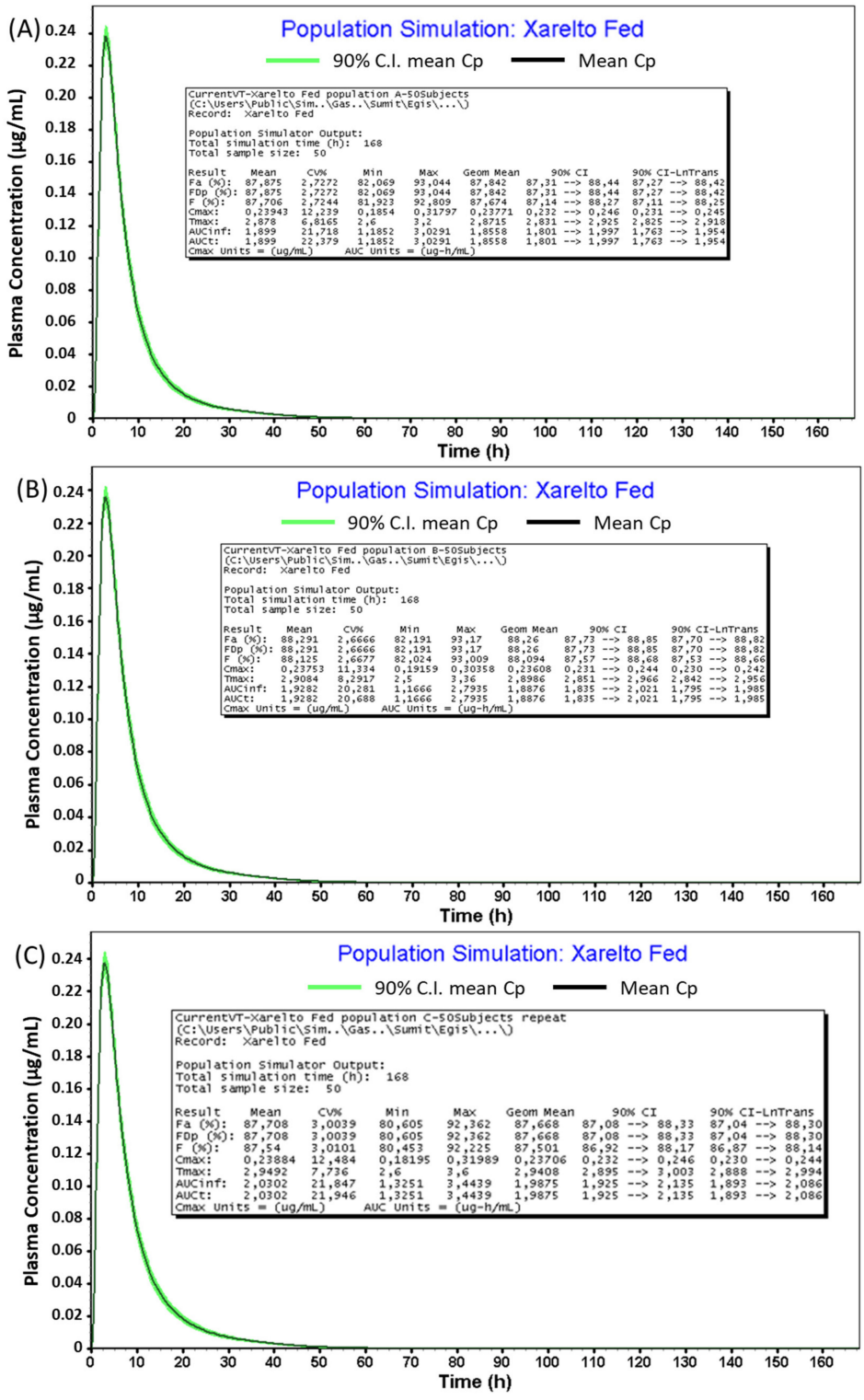

Figure 13. Virtual in vivo pharmacokinetic profile of Xarelto IR tablet (20 mg Strength) for Populations (**A**–**C**) in fed conditions.

The predicted population in vivo pharmacokinetic profile of Xarelto IR tablet (20 mg strength) in the fed condition was found to be comparable in populations A, B, and C in the conditions, i.e., the average value of population geometric means were found to be within the range of 80–125% compared to the mean predicted in vivo profile mentioned in in Table 7, Figure 5 (C_{max} and $AUC_{0-\infty}$ value of 236.64 and 1857.3, respectively). However,

marked difference (>80–125%) was observed in case of fasted conditions (C_{max} and $AUC_{0-\infty}$ value of 171.15 and 1433.8, respectively), as compared to the predicted in vivo population pharmacokinetics of Xarelto IR tablet (20 mg strength) in fed conditions.

During the virtual simulations, the physiological and pharmacokinetic parameters of the same subjects were identical for reference formulations. However, in reality, physiological and pharmacokinetic parameters could fluctuate within the same subjects if they were given different formulations on different occasions. Thus, by incorporating this intra-subject variability, it is possible that in vivo profile of Xarelto IR tablet in the fasted condition might be bioequivalent to the population kinetics of Xarelto IR tablet (Fed) in population A since its 80% confidence interval for the AUC value (77%) is close to the edge of the BE limits.

4. Conclusions

In the present manuscript, a mechanistic physiology-based model for the Xarelto IR tablet was developed considering different physicochemical and pharmacokinetic parameters. In addition, a conventional IVIVC model was also developed in order to verify the in vivo profile obtained via the PBPK model. The validation results demonstrated the development of successful models, and the predicted in vivo profiles from both models were found to be comparable. The results demonstrated a significant food effect increasing the C_{max} of the Riva, which could be due to higher solubility in Fed conditions. The developed model strategy can be effectively adopted to increase the confidence of the model. Furthermore, the PBPK model can also lead to the establishment of the biased dissolution methods crucial for the generic company to establish bioequivalence mainly focusing on new formulations with a similar drug release mechanism using external validation.

Supplementary Materials: The following are available online at https://www.mdpi.com/1999-4923/13/2/283/s1, Table S1: Concentration of different components of the simulated media used in the solubility and dissolution studies, Figure S1: Predicted combined effect of Riva particle size and dose on the bioavailability.

Author Contributions: Conceptualization, A.P., S.A.; methodology, S.A., D.M., and E.F.; Software, S.A. and M.T.K.; Formal analysis, V.K., S.A., D.M. and M.T.K.; Data curation, V.K. and S.A.;Writing—original draft preparation, V.K.; Writing—review and editing, V.K., M.T.K. and A.P.; supervision, A.P.; project administration, A.P. All authors have read and agreed to the published version of the manuscript.

Funding: This research was funded by Egis Pharmaceuticals.

Institutional Review Board Statement: Not applicate.

Informed Consent Statement: Not applicate.

Data Availability Statement: The data presented in this study are available in the research article and supplementary material here.

Acknowledgments: Miklós Katona would like to thank Krisztina Takács-Novák (Department of Pharmaceutical Chemistry, Semmelweis University) for her useful suggestions.

Conflicts of Interest: The authors declare no conflict of interest.

Abbreviations

Absorption Scale Factors	ASF
Active pharmaceutical ingredients	APIs
Advanced compartmental absorption and transit	ACAT
Akaike information criterion	AIC
Apparent permeability coefficient	Papp
American Type Culture Collection	ATCC

Bioavailability	BA
Bioequivalence	BE
Biopharmaceutical Classification System	BCS
Immediate release	IR
In vitro–in vivo correlation	IVIVC
Minimal Essential Medium	MEM
Fasted state simulated gastric fluid	FaSSGF
Fasted state simulated intestinal fluid	FaSSIF
Fed state simulated gastric fluid	FeSSGF
Fed state simulated intestinal fluid	FeSSIF
Fetal bovine serum	FBS
Parameter Sensitivity Analysis	PSA
Pharmacokinetics	PK
Physiologically based pharmacokinetic	PBPK
Rivaroxaban	Riva
Schwarz criterion	SC
Sodium lauryl sulfate	SLS
Transepithelial electrical resistance	TEER
Ultra-High-Performance Liquid Chromatography	UHPLC
Unit impulse response	UIR
United States Pharmacopeia	USP

References

1. Jamei, M.; Abrahamsson, B.; Brown, J.; Bevernage, J.; Bolger, M.B.; Heimbach, T.; Karlsson, E.; Kotzagiorgis, E.; Lindahl, A.; McAllister, M. Current status and future opportunities for incorporation of dissolution data in PBPK modeling for pharmaceutical development and regulatory applications: OrBiTo consortium commentary. *Eur. J. Pharm. Biopharm.* **2020**, *155*, 55–68. [CrossRef]
2. European Medicines Agency. ICH M9 on biopharmaceutics classification system based biowaivers. Available online: https://www.ema.europa.eu/en/ich-m9-biopharmaceutics-classification-system-based-biowaivers#current-version-section (accessed on 18 January 2021).
3. Amidon, G.L.; Lennernäs, H.; Shah, V.P.; Crison, J.R. A Theoretical Basis for a Biopharmaceutic Drug Classification: The Correlation of in vitro Drug Product Dissolution and in vivo Bioavailability. *Pharm. Res. An Off. J. Am. Assoc. Pharm. Sci.* **1995**, *12*, 413–420. [CrossRef]
4. FDA. Extended Release Oral Dosage Forms: Development, Evaluation, and Application of In vitro/In vivo Correlations. Available online: https://www.fda.gov/regulatory-information/search-fda-guidance-documents/extended-release-oral-dosage-forms-development-evaluation-and-application-vitroin-vivo-correlations (accessed on 18 January 2021).
5. Stillhart, C.; Pepin, X.; Tistaert, C.; Good, D.; Bergh, A.; Van Den Parrott, N.; Kesisoglou, F. PBPK Absorption Modeling: Establishing the In vitro–In vivo Link—Industry Perspective. *AAPS J.* **2019**, *21*, 1–13. [CrossRef]
6. Kesisoglou, F.; Xia, B.; Agrawal, N.G.B. Comparison of Deconvolution-Based and Absorption Modeling IVIVC for Extended Release Formulations of a BCS III Drug Development Candidate. *AAPS J.* **2015**, *17*, 1492–1500. [CrossRef]
7. Kaur, N.; Narang, A.; Bansal, A.K. Use of biorelevant dissolution and PBPK modeling to predict oral drug absorption. *Eur. J. Pharm. Biopharm.* **2018**, *129*, 222–246. [CrossRef]
8. Pepin, X.J.H.; Flanagan, T.R.; Holt, D.J.; Eidelman, A.; Treacy, D.; Rowlings, C.E. Justification of drug product dissolution rate and drug substance particle size specifications based on absorption PBPK modeling for lesinurad immediate release tablets. *Mol. Pharm.* **2016**, *13*, 3256–3269. [CrossRef] [PubMed]
9. Willmann, S.; Thelen, K.; Becker, C.; Dressman, J.B.; Lippert, J. Mechanism-based prediction of particle size-dependent dissolution and absorption: Cilostazol pharmacokinetics in dogs. *Eur. J. Pharm. Biopharm.* **2010**, *76*, 83–94. [CrossRef]
10. Pepin, X.J.H.; Huckle, J.E.; Alluri, R.V.; Basu, S.; Dodd, S.; Parrott, N.; Emami Riedmaier, A. Understanding Mechanisms of Food Effect and Developing Reliable PBPK Models Using a Middle-out Approach. *AAPS J.* **2021**, *23*, 1–14. [CrossRef] [PubMed]
11. Davit, B.M.; Kanfer, I.; Tsang, Y.C.; Cardot, J.M. BCS biowaivers: Similarities and differences among EMA, FDA, and WHO requirements. *AAPS J.* **2016**, *18*, 612–618. [CrossRef] [PubMed]
12. Services, H. Vladimir Nikolaevich Chernigovski. *Acta Physiol. Pharmacol. Bulg.* **1977**, *3*, 3–5.
13. Jain, S.; Jain, R.; Das, M.; Agrawal, A.K.; Thanki, K.; Kushwah, V. Combinatorial bio-conjugation of gemcitabine and curcumin enables dual drug delivery with synergistic anticancer efficacy and reduced toxicity. *RSC Adv.* **2014**, *4*, 29193–29201. [CrossRef]
14. Arora, R.; Katiyar, S.S.; Kushwah, V.; Jain, S. Solid lipid nanoparticles and nanostructured lipid carrier-based nanotherapeutics in treatment of psoriasis: A comparative study. *Expert Opin. Drug Deliv.* **2017**, *14*, 165–177. [CrossRef]
15. Shilpi, D.; Kushwah, V.; Agrawal, A.K.; Jain, S. Improved Stability and Enhanced Oral Bioavailability of Atorvastatin Loaded Stearic Acid Modified Gelatin Nanoparticles. *Pharm. Res.* **2017**, *34*, 1505–1516. [CrossRef]
16. Tripathi, S.; Kushwah, V.; Thanki, K.; Jain, S. Triple antioxidant SNEDDS formulation with enhanced oral bioavailability: Implication of chemoprevention of breast cancer. *Nanomed. Nanotechnol. Biol. Med.* **2016**, *12*, 1431–1443. [CrossRef]

17. Kubitza, D.; Becka, M.; Zuehlsdorf, M.; Mueck, W. Effect of food, an antacid, and the H2 antagonist ranitidine on the absorption of BAY 59-7939 (rivaroxaban), an oral, direct Factor Xa inhibitor, in healthy subjects. *J. Clin. Pharmacol.* **2006**, *46*, 549–558. [CrossRef] [PubMed]
18. Kubitza, D.; Becka, M.; Voith, B.; Zuehlsdorf, M.; Wensing, G. Safety, pharmacodynamics, and pharmacokinetics of single doses of BAY 59-7939, an oral, direct factor Xa inhibitor. *Clin. Pharmacol. Ther.* **2005**, *78*, 412–421. [CrossRef]
19. Takács-Novák, K.; Szőke, V.; Völgyi, G.; Horváth, P.; Ambrus, R.; Szabó-Révész, P. Biorelevant solubility of poorly soluble drugs: Rivaroxaban, furosemide, papaverine and niflumic acid. *J. Pharm. Biomed. Anal.* **2013**, *83*, 279–285. [CrossRef]
20. EMEA. Note for Guidance on Quality of Modified Release Products: A: Oral Dosage Forms B: Transdermal Dosage Forms Section I (Quality). *Guidance* **1999**, *96*, 6–7.
21. Malinowski, H.; Marroum, P.; Uppoor, V.R.; Gillespie, W.; Ahn, H.Y.; Lockwood, P.; Henderson, J.; Baweja, R.; Hossain, M.; Fleischer, N.; et al. FDA guidance for industry extended release solid oral dosage forms: Development, evaluation, and application of *in vitro/in vivo* correlations. *Dissolution Technol.* **1997**, *4*, 23–32. [CrossRef]
22. Stampfuss, J.; Kubitza, D.; Becka, M.; Mueck, W. The effect of food on the absorption and pharmacokinetics of rivaroxaban. *Int. J. Clin. Pharmacol. Ther.* **2013**, *51*, 549–561. [CrossRef]
23. EMA, C. Guideline on the conduct of bioequivalence studies for veterinary medicinal products. **2010**, *44*, 1–25.
24. Shah, V.P.; Lesko, L.J.; Fan, J.; Fleischer, N.; Handerson, J.; Malinowski, H.; Makary, M.; Ouderkirk, L.; Bay, S.; Sathe, P.; et al. FDA guidance for industry 1 dissolution testing of immediate release solid oral dosage forms. *Dissolution Technol.* **1997**, *4*, 15–22. [CrossRef]
25. Gnoth, M.J.; Buetehorn, U.; Muenster, U.; Schwarz, T.; Sandmann, S. In vitro and in vivo P-glycoprotein transport characteristics of rivaroxaban. *J. Pharmacol. Exp. Ther.* **2011**, *338*, 372–380. [CrossRef]
26. Thanki, K.; Kushwah, V.; Jain, S. *Recent Advances in Tumor Targeting Approaches*; Springer: Cham, Germany, 2015; pp. 41–112.
27. Wilcox, M.D.; Van Rooij, L.K.; Chater, P.I.; Pereira De Sousa, I.; Pearson, J.P. The effect of nanoparticle permeation on the bulk rheological properties of mucus from the small intestine. *Eur. J. Pharm. Biopharm.* **2015**, *96*, 484–487. [CrossRef] [PubMed]
28. Pontier, C.; Pachot, J.; Botham, R.; Lenfant, B.; Arnaud, P. HT29-MTX and Caco-2/TC7 monolayers as predictive models for human intestinal absorption: Role of the mucus layer. *J. Pharm. Sci.* **2001**, *90*, 1608–1619. [CrossRef]
29. Wharf, C.; Kingdom, U. Keppra CHMP Assessment Report for Paediatric Use Studies Submitted According to Article 46 of the RegulationEC No. 1901/. **2006**, *2013*, 44.
30. Weinz, C.; Schwarz, T.; Kubitza, D.; Mueck, W.; Lang, D. Metabolism and excretion of rivaroxaban, an oral, direct factor Xa inhibitor, in rats, dogs, and humans. *Drug Metab. Dispos.* **2009**, *37*, 1056–1064. [CrossRef]
31. Michailidou, A.; Trenz, H.-J.; de Wilde, P.; Annex, I. The Internet and European Integration. *JSTOR* **2019**, 167–172. [CrossRef]
32. Mueck, W.; Schwers, S.; Stampfuss, J. Rivaroxaban and other novel oral anticoagulants: Pharmacokinetics in healthy subjects, specific patient populations and relevance of coagulation monitoring. *Thromb. J.* **2013**, *11*, 10. [CrossRef]
33. European Medicines Agency (EMA) Assessment report Xarelto (Rivaroxaban) Procedure No. EMEA/H/C/000944/X/0017. 2013; 44, 1–75.
34. Available online: https://www.accessdata.fda.gov/drugsatfda_docs/label/2018/022406s028lbl.pdf (accessed on 15 February 2021).
35. Available online: https://www.ema.europa.eu/en/documents/product-information/rivaroxaban-accord-epar-product-information_en.pdf (accessed on 15 February 2021).
36. Pepin, X.J.H.; Moir, A.J.; Mann, J.C.; Sanderson, N.J.; Barker, R.; Meehan, E.; Plumb, A.P.; Bailey, G.R.; Murphy, D.S.; Krejsa, C.M.; et al. Bridging in vitro dissolution and in vivo exposure for acalabrutinib. Part II. A mechanistic PBPK model for IR formulation comparison, proton pump inhibitor drug interactions, and administration with acidic juices. *Eur. J. Pharm. Biopharm.* **2019**, *142*, 435–448. [CrossRef] [PubMed]
37. Committee for Medicinal Products for Human Use (CHMP) Assessment report: Xarelto; EMA/CHMP/301607/2011. 2011; 44.
38. Parrott, N.; Lukacova, V.; Fraczkiewicz, G.; Bolger, M.B. Predicting pharmacokinetics of drugs using physiologically based modeling—application to food effects. *AAPS J.* **2009**, *11*, 45–53. [CrossRef]